MATHEMATICAL PROGRAMMING APPROACHES FOR TWO PROBLEMS IN ENERGY SYSTEMS

by
BAHAR CENNET OKUMUŞOĞLU

Submitted to the Graduate School of Natural Sciences
in partial fulfilment of
the requirements for the degree of Master of Science

Sabancı University
June 2022

MATHEMATICAL PROGRAMMING APPROACHES FOR TWO PROBLEMS IN ENERGY SYSTEMS

Approved by:

Asst. Prof. BURAK KOCUK .....
(Thesis Supervisor)

Asst. Prof. BESTE BAŞÇİFTCİ .....
(Thesis Co-Supervisor)

Prof. TONGUÇ ÜNLÜYURT .....

Asst. Prof. ESRA KOCA .....

Assoc. Prof. AYŞE SELİN KOCAMAN .....

Date of Approval: June 27, 2022

ABSTRACT

MATHEMATICAL PROGRAMMING APPROACHES FOR TWO PROBLEMS IN ENERGY SYSTEMS

BAHAR CENNET OKUMUŞOĞLU

INDUSTRIAL ENGINEERING M.S. THESIS, JUNE 2022

Thesis Supervisor: Asst. Prof. BURAK KOCUK
Thesis Co-Supervisor: Asst. Prof. BESTE BAŞÇİFTCİ

Keywords: Joint chance-constrained stochastic programming, condition-based maintenance, power systems, mixed-integer nonlinear programming, mixed-integer second-order cone programming, natural gas networks.

A wide variety of problems in energy systems can be formulated as mathematical programs. In the first part of this thesis, we focus on the integrated maintenance and operations planning problem in power systems, which is formulated as a mixed-integer joint-chance constrained stochastic program. Due to the intractability of the joint chance-constraint, we propose a cutting-plane method to obtain its exact reformulation and derive its second-order cone programming based safe approximation. To solve this program, we propose a decomposition algorithm by exploiting the features of the integer L-shaped method and introduce various algorithmic enhancements. We design an extensive computational study and demonstrate the performance of the proposed approach with reliable and cost-effective maintenance and operational schedules. In the second part of this thesis, we focus on the multi-period natural gas storage optimization problem by considering the important aspects of gas physics and switching status of active elements. Under steady-state conditions, we formulate this problem as a nonconvex mixed-integer nonlinear program. We propose mixed-integer linear and second-order cone programming relaxations of this complex problem to obtain tight dual bounds. We design a computational study to compare these formulations on different instances from the literature. Our results demonstrate the computational efficiency of our approach and its ability to obtain (near) globally optimal solutions in comparison with a global optimization solver.

ÖZET

ENERJI SISTEMLERINDEN IKI PROBLEM IÇIN MATEMATIKSEL PROGRAMLAMA YAKLAŞIMLARI

BAHAR CENNET OKUMUŞOĞLU

ENDÜSTRİ MÜHENDİSLİĞİ YÜKSEK LİSANS TEZİ, HAZİRAN 2022

Tez Danışmanı: Dr. BURAK KOCUK
Eş Tez Danışmanı: Dr. BESTE BAŞÇİFTCİ

Anahtar Kelimeler: ortak şans kısıtlı rassal programlama, durum tabanlı bakım, güç sistemleri, karma tamsayılı doğrusal olmayan programlama, karma tamsayılı ikinci dereceden konik programlama, doğal gaz ağları.

Enerji sistemlerindeki birçok problem matematiksel programlama kullanılarak modellenebilir. Bu tezin ilk bölümünde, karma tamsayılı ortak şans kısıtlı rassal program olarak modellenen güç sistemlerinde entegre bakım ve operasyon planlama problemine odaklanılmıştır. Ortak şans kısıtının zorluğu nedeniyle, kesin gösterimi elde etmek için kesen düzlem algoritması ve ikinci dereceden konik programlama temelli güvenli yaklaşıklaması sunulmuştur. Bu programı çözmek için, tamsayı L-Şekil yönteminin özelliklerinden yararlanarak bir ayrıştırma algoritması önerilmiş ve çeşitli algoritmik iyileştirmeler sunulmuştur. Önerilen yaklaşımların başarımı ve etkinlik değerlendirmeleri yapılmış; bu yaklaşımların uygun maliyetli bakım ve operasyonel planlamalar sağladığı gösterilmiştir. Bu tezin ikinci bölümünde, gaz fiziği ve aktif ağ elemanlarının açma/kapama kararlarının ele alındığı çokdönemli doğal gaz depolama problemine odaklanılmıştır. Kararlı hal koşulları altında, bu problem dışbükey olmayan karma tamsayılı doğrusal olmayan bir program olarak modellenmiştir. Sıkı eşiz sınırlar elde etmek amacıyla bu karmaşık problemin karışık tamsayılı doğrusal ve ikinci dereceden konik gevşetmeleri önerilmiştir. Önerilen modeller, literatürden alınan farklı problem örnekleri kullanılarak karşılaştırılmış ve değerlendirmeleri yapılmıştır. Önerilen yaklaşımların etkinliği ve (yakın) küresel çözümler elde etme başarımı, küresel bir çözücü ile karşılaştırılarak gösterilmiştir.

ACKNOWLEDGEMENTS

I would first like thank both Dr. Burak Kocuk and Dr. Beste Başçiftci for their support and patience during this inexplicable academic journey. I would also like to thank my committee members Prof. Tonguç Ünlüyurt, Dr. Esra Koca and Dr. Ayşe Selin Kocaman.

The second part of this thesis is supported by the Scientific and Technological Research Council of Turkey (TÜBİTAK) under grant #119M855. I would further like to thank to TÜBITAK for their support to my thesis.

TABLE OF CONTENTS

LIST OF TABLES

LIST OF FIGURES

1. INTRODUCTION

The world's increasing consumption has motivated the energy industry to perform better system operations. While carrying out these operations, the need for their reliability and security has introduced numerous challenges to the industry. Motivated by the problems emerged from these challenges, the academic literature has produced a great deal of research throughout the years. In this thesis, we aim to contribute to the literature by approaching two energy system problems in different aspects.

In the first part of this thesis, we focus on the short-term condition-based integrated maintenance and operations planning problem in power systems. This problem plays a key role in system operations under uncertainty as it helps system operators ensure a reliable and secure power grid. In terms of uncertainty, the unexpected failures of generators as well as transmission lines are considered in this problem. Moreover, a joint chance-constraint consisting of Poisson Binomial random variables is introduced to account for failure risks. The resulting problem is a joint chance-constrained stochastic mixed-integer program. Unfortunately, producing optimal maintenance schedules from this program is quite challenging due to the intractability of the joint chance-constraint as well as the exponentially many failures scenarios.

In the second part of this thesis, we focus on the multi-period gas storage optimization problem in natural gas networks. This problem has become more important to the industry with the recent advances in power-to-gas technologies. However, it contains highly nonlinear and nonconvex aspects of the underlying gas physics and gas losses as well as the switching status of active network elements. In view of these aspects, it belongs to the class of nonconvex mixed-integer nonlinear programs. Therefore, obtaining globally optimal solutions is not an easy task. In the recent years, certain convex relaxations of various optimization problems in gas networks have drawn attention by the academic literature to obtain tight dual bounds, and further (near) globally optimally solutions based on the solutions produced by these relaxations.

The remainder of this thesis is organized as follows: In Chapter 2, we focus on the short-term condition-based integrated maintenance and operations planning problem in power systems. In Chapter 3, we consider the multi-period gas network optimization problem. In each chapter, we review the relevant literature, and present the mathematical formulations, the solution framework along with the results of the extensive computational experiments. We conclude this thesis with final remarks and future works in Chapter 4.

2. A Joint Chance-Constrained Stochastic Programming Approach for the Maintenance and Operations Scheduling Problem

2.1 Introduction

The competitive power industry has challenged the system operators with prohibitive penalty costs to continue their operations uninterruptedly. A natural way to avoid such interruptions with these penalties is scheduling maintenance for the system components while leveraging their condition information. Such condition-based maintenance increases the operational lifetime of the aging power grid; however, ignoring power system capabilities when performing maintenance may cause large-scale blackouts resulting in additional maintenance and operational costs (see, for example Florida blackout in 2008 FRCC (2008)). Thus, the condition-based maintenance schedules for generators as well as transmission lines must be coordinated with operational schedules in order to preserve the security of the power grid.

Maintenance schedules of generators and transmission lines have a great effect on power generation as well as power flow. Still, obtaining optimal maintenance schedules for generators has aroused considerably more interest than for transmission lines in the power system literature (Canto, 2008; Conejo, Garcia-Bertrand & Diaz-Salazar, 2005; Wu, Shahidehpour & Li, 2008). In transmission maintenance planning problem, mathematical complexity ensues from the removal of transmission lines for their unavailable periods due to maintenance, which results in a change in the network topology. Besides, such removals may cause congestion in the power system affecting the reliability and the security of the system. In this respect, the joint optimization of generator and transmission line maintenance (hereafter referred to as the *integrated maintenance*) planning problem becomes more critical in power systems to ensure reliable system operations by capturing the complex nature of the problem.

In the competitive power industry, cost-effective maintenance schedules and demand-delivery under failure uncertainty have become more and more important. Recent advances in grid modernization such as condition-monitoring are widely employed to deal with this failure uncertainty (Basciftci, Ahmed, Gebraeel & Yildirim, 2018; Yildirim, Sun & Gebraeel, 2016a). In condition-monitoring systems, sensors connected to the power grid monitor the emerging health conditions of degrading system components. These systems can be used as a basis for estimating the residual lifetime of the components by means of degradation signals obtained from real-time sensor information. When scheduling maintenance, such condition-based information on the underlying uncertainty avails system operators of correcting natural causes from degradation and increasing the overall operational lifetime of the aging power infrastructure.

Many optimization problems in power systems can be modeled as large-scale stochastic mixed-integer programs (SMIPs) as they involve various uncertainties and risks as well as a vast number of binary variables related to maintenance schedules, commitment status of generators and switching status of transmission lines. In view of handling uncertainties, building SMIP models with scenario-dependent variables and constraints is the most prevalent approach. The SMIP models, even with a limited number of scenarios, may become computationally demanding, and moreover, solutions for these SMIPs given by the state-of-the-art solvers can be suboptimal. Thus, these SMIP models necessitate developing novel decomposition-based solution algorithms to achieve tractability. To handle risks, on the other hand, the SMIP models can be built with chance-constraints. There are only a limited number of cases where a chance-constraint is computationally tractable and whenever this is not the case, it can be replaced with its safe approximation which imposes conservatism on the underlying problem. Thus, it becomes critical to provide an equivalent description of these chance-constraints whenever possible within the modeling process.

In this thesis, we study an integrated short-term condition-based maintenance scheduling problem in coordination with operations planning by taking account of unexpected failures of generators as well as transmission lines. We explicitly depict the underlying failure uncertainty as a continuous stochastic degradation process and utilize sensor-driven real-time information to estimate the remaining lifetime distribution (RLD) of system components. Furthermore, we identify those system components prone to failure within the planning horizon and construct failure scenarios based on their estimated RLDs. Additionally, we propose a joint chance-constraint for simultaneously restricting the total number of corrective maintenance occurring due to unexpected failures for generators and transmission lines within the planning horizon along with its exact and safe representation approaches. We develop a

decomposition-based cutting-plane framework to efficiently solve the resulting large-scale problem and obtain optimal condition-based daily maintenance schedules, and hourly operational decisions. We validate these maintenance schedules by evaluating them over a larger size of failure scenarios over all system components under a sample average approximation (SAA) approach.

This thesis makes the following contributions:

- We develop a stochastic optimization framework which combines the short-term condition-based generator and transmission line maintenance, and operations planning problems while explicitly considering the impacts of unexpected failures of generators as well as transmission lines on power system operations. Our framework differs from the existing studies in considering condition-based transmission line maintenance with generator maintenance. By engaging real-time degradation-based sensor information in the elaborate failure characterization under a Bayesian approach, we predict the RLDs of generators and transmission lines, and identify a specific subset of these power system components prone to failure within the planning horizon.

- To account for the failure uncertainty of both generators and transmission lines in our stochastic optimization model, we generate failure scenarios based on their estimated RLDs. We also introduce a joint chance-constraint to mitigate the unexpected failure risks for generators and transmission lines. Because of its intractability, we develop a cutting-plane method to obtain an exact reformulation of the joint chance-constraint through a separation subroutine and a set of improved cuts. Our solution framework leverages Poisson Binomial random variables in this joint chance-constraint, which can be extended to the settings under similar forms. Moreover, we derive a second-order cone programming based safe approximation of this constraint.

- We develop a decomposition-based algorithm by improving the integer L-shaped method with various algorithmic enhancements. We exploit the nice and special structure of the scenario subproblems and introduce two concepts: time-decomposability and status of system components. We benefit from these concepts to decrease the total number of scenario subproblems solved and moreover, generate various sets of stronger optimality cuts than the integer L-shaped optimality cuts. We employ parallel computing to implement our decomposition algorithm more efficiently and further present preprocessing steps for identifying redundant transmission line constraints.

- We conduct a computational study with various modified IEEE instances to

illustrate the computational efficiency of each algorithmic enhancement. We also compare the proposed decomposition algorithm with an existing state-of-the-art solver. For all instances, the underlying problem can be solved orders of magnitude faster with the proposed decomposition algorithm than this solver. Our computational study also shows that the proposed stochastic framework provides $14-31\%$ cost savings using both the exact reformulation and safe approximation of the joint chance-constraint in comparison with the deterministic model.

The remainder of our thesis is organized as follows. In Section 2.2, we review the relevant literature. In Section 2.3, we describe the integrated short-term condition-based maintenance scheduling with operations planning problem, the degradation signal modeling and decomposition structure in detail. The solution methodology with various algorithmic enhancements is presented in Section 2.4. The computational experiments and extensive numerical results follow in Section 2.5. We conclude the thesis with final remarks in Section 2.6.

2.2 Literature Review

In this section, we review the relevant power system literature on maintenance planning problem (Section 2.2.1), failure uncertainty (Section 2.2.2) and stochastic model (Section 2.2.3). We explicate the contributions of this thesis in each section.

2.2.1 Maintenance Planning in Power Systems

Maintenance planning problem in power systems has been widely studied in the literature (for a recent review, see Froger, Gendreau, Mendoza, Pinson & Rousseau (2016)). This problem concerns both generators and transmission lines, and ideally attempts to identify the unavailability of these components while ensuring a reliable power grid. However, the majority of the existing studies have focused more on obtaining optimal maintenance schedules for generators subject to various operational and network constraints (Basciftci et al., 2018; Canto, 2008; Conejo et al., 2005; Wu et al., 2008; Yildirim, Sun & Gebraeel, 2016b) than for transmission lines (Abbasi,

Fotuhi-Firuzabad & Abiri-Jahromi, 2009; Abiri-Jahromi, Fotuhi-Firuzabad & Abbasi, 2009; Lv, Wang & Sun, 2012; Marwali & Shahidehpour, 2000; Pandzic, Conejo, Kuzle & Caro, 2012). This is because of the fact that the power network topology will inherently change due to the maintenance actions for transmission lines, and this varying network topology exceedingly influences the power generation and further complicates the resulting problem.

The integrated maintenance problem can yield more cost-effective maintenance and operational schedules; however, another source of complexity arises when coordinating the maintenance schedules for both generators and transmission lines. Therefore, the integrated maintenance planning problem has attracted only very few researchers in power systems. The coordination of generator and transmission line maintenance schedules coupled with the security constrained UC is analyzed by Fu, Shahidehpour & Li (2007) and Fu, Li, Shahidehpour, Zheng & Litvinov (2009). Optimization models in these works can be utilized both in vertically integrated and restructured power systems. Geetha & Swarup (2009) coordinate integrated maintenance schedules with an acceptable level of reliability between independent actors in restructured power systems. These studies do not account for the uncertainty resulting from the unexpected failures of system components, which strongly affects the maintenance planning problem. The study by Wang, Zhong, Xia, Kirschen & Kang (2016) models the generators and transmission maintenance planning problem incorporating N-1 security criterion; however, this deterministic model may provide infeasible maintenance schedules when multiple failures of system components occur in the power system. Wu, Shahidehpour & Fu (2010) formulate an integrated maintenance problem in coordination with the security-constrained UC considering various uncertainties including forced outages of generators and transmission lines over a long-term planning horizon. They model these forced outage rates as a Markov process by using predetermined constant failure characteristics, which may not be a realistic assumption in a dynamic power network. Wang, Li, Shahidehpour, Wu, Guo & Zhu (2016) propose a similar approach to jointly optimize the underlying problem with the security-constrained UC by updating outage scenarios in an iterative manner. However, the authors neglect to consider the effects of these scenarios on operations planning and do not leverage sensor-driven condition information to identify critical system components prone to failure, which is imperative for securing overall power system operations.

2.2.2 Failure Uncertainty in Power Systems

Quantifying the failure uncertainty in power system operations has been instrumental in the maintenance planning problem. In order to achieve cost-effective maintenance schedules and to ensure the reliability and the security of the aging power infrastructure, the stochasticity arising from failures of system components must be considered in real-time operations. Power system components depict degradation symptoms over time from increasing wear and tear. This continuous degradation process may eventually lead to unexpected failures resulting in unscheduled shutdowns, congested transmission lines, voltage instability and sudden increase in power demand. To extenuate the disruptive impacts of the failures of these system components, many existing operational strategies such as N-1 contingency criterion (Stott, Alsac & Monticelli, 1987) and reserve requirements, and maintenance strategies such as periodic and manufacturer-recommended maintenance schedules (Shahidehpour, Yamin & Li, 2002) are used in power systems. These deterministic strategies remain as half measures and are not enough to improve the utilization of the power grid and therefore, many energy companies have recently started to adapt condition-monitoring techniques because of their potential benefits (for a comprehensive review, see Han & Song (2003)). In particular, these are widely employed to estimate the RLDs of system components by tracking degradation of these components using sensors in order to account for unexpected failures.

Although the failure uncertainty of system components has been considered in the literature for modeling power system operations, most studies neglect component-specific condition information and further assume that system components carry constant failure characteristics over the planning horizon (Papavasiliou & Oren, 2013; Wu et al., 2010). As this approach becomes insufficient in capturing the condition information of the components, a few studies recently consider the underlying failure uncertainty by incorporating degradation-based approaches. Wang et al. (2016) adopt a degradation-based model by extending the traditional hazard model and dynamically updating failure characteristics of system components. Furthermore, a deterministic mixed-integer optimization model integrated with condition-based sensor information is presented to obtain optimal maintenance schedules for generators (Yildirim et al., 2016a,1). Recently, Basciftci, Ahmed & Gebraeel (2020) propose a similar framework by leveraging time-varying load-dependency to obtain condition-based maintenance schedules for a fleet of generators by presenting a decision-dependent stochastic program to capture the RLDs of the components depending on the operational decisions. Nevertheless, these studies either have been conducted in a deterministic fashion and/or do not take into account scenario-dependent failure uncertainty for both generators and transmission lines at the same time. The optimization framework proposed by Basciftci et al. (2018) embodies

sensor-driven condition-based information in the long-term generator maintenance and operations planning problem considering only failure scenarios of generators; however, the authors do not consider the failure uncertainty of transmission lines and their effects on power system operations. The existing literature still lacks a unified framework for addressing the integrated condition-based maintenance planning by considering the impacts of the sensor-driven failure uncertainty of both generators and transmission lines on power system operations. As this unified framework becomes critical in ensuring cost-effective and reliable operations of the power systems, the complexities arisen from the integration of line maintenance decisions and their failure possibilities need to be addressed by developing various stochastic optimization techniques, which consists a significant part of the contributions of this study, that can also be extended to problem settings with similar structure.

2.2.3 Stochastic Programming Approaches in Power Systems

Stochastic programming arises as an important tool for modeling power system operations under uncertainty. Many existing studies in the literature describe the underlying uncertainties with a set of scenarios, i.e., a set of possible realizations of random variables (Basciftci et al., 2018; Papavasiliou & Oren, 2013; Papavasiliou, Oren & Rountree, 2015; Wu et al., 2008). Still, conventional methods may not be sufficient to solve the resulting problem in a reasonable amount of time as the scenario set can consist of an extremely large number of scenarios. As this set grows exponentially fast in the size of the network components, solving large-scale problems in power systems necessitates specialized decomposition techniques. Fortunately, the majority of such large-scale problems in power systems can be intrinsically decoupled into many smaller problems, and then recast as two-stage stochastic programs under suitable conditions. Van Slyke & Wets (1969) introduced the continuous L-shaped method as a cutting plane technique to solve the two-stage stochastic linear programs with recourse. A common criticism for this method is that the linear programming duality cannot be readily applied when integer decisions exist in the second-stage problems. In particular, SMIPs are known to have their combinatorial challenges attributed to the non-convex (even discontinuous) nature of the expected second-stage objective function. The integer L-shaped method, proposed by Laporte & Louveaux (1993), can be applied to solve the two-stage mixed-integer stochastic programs with pure binary first-stage decisions and mixed-integer second-stage decisions. As this algorithm can be extendable to our problem setting, we propose a decomposition-based algorithm in Section 2.4.1 by using the features of the integer

L-shaped method to solve the integrated short-term condition-based maintenance scheduling with operations planning problem. By exploiting the special structure of this problem, we provide algorithmic enhancements which significantly decreases the computational effort required to solve the second-stage problems, and derive stronger optimality cuts than the integer L-shaped optimality cuts, which are integrated into our solution procedure implemented in a parallel fashion in Section 2.4.3.2.

Chance constraints are widely used in modeling power systems operations as they are subject to various risks associated with many uncertainties (for a comprehensive review, see Geng & Xie (2019)). Although chance-constraints have great importance for mitigating risks in power system operations, the feasible set defined by a chance-constraint is in general nonconvex, and obtaining an exact representation of such a constraint can be difficult even under the assumption of convexity. A very well-known case in which such issues do not appear is when a random variable associated with the chance-constraint follows a Gaussian distribution and the probability level of the chance constraint is at least 0.5. In this case, the corresponding feasible set can be represented as a second-order conic set (Nemirovski, 2012). Many studies in power systems follow this Gaussian assumption and obtain such deterministic equivalents of the chance-constraints (Roald, Misra, Krause & Andersson, 2017; Wu, Shahidehpour, Li & Tian, 2014). In practice, it may happen that the probability distribution of the random variable is not Gaussian and such tractable representations may not be readily available. Whenever this is the case, safe approximations can be obtained as an alternative, though conservative, representations of the chance-constraints. Recently in maintenance planning literature, Basciftci et al. (2018) introduce a single chance-constraint consisting of the sum of independent Bernoulli random variables, i.e., a Poisson Binomial random variable. The authors ignore this useful information on the underlying distribution and propose a deterministic safe approximation of the chance-constraint by using Markov and Bernstein bounds. Joint chance-constraints are relatively more difficult to handle than a single chance-constraint. Many studies in the literature reformulate the feasible set of the joint chance-constraint by using Bonferroni-based safe approximation (Ozturk, Mazumdar & Norman, 2004; Xiong & Jirutitijaroen, 2013); however, this safe approximation is likely to be overly conservative. Thus, for the chance-constraints, there is a trade-off between searching for exact reformulations or deriving safe approximations to provide their alternative representations.

To mitigate failure risks of generators and transmission lines, we introduce a joint chance-constraint which restricts the total number of these system components under corrective maintenance, which is an undesirable and costly maintenance in case

of an unexpected failure. Our joint chance-constraint consists of Poisson Binomial random variables by leveraging the RLDs of the system components. In contrast to the recent work by Basciftci et al. (2018) with a single chance-constraint, we exploit the underlying distribution and propose an exact reformulation of the joint chance-constraint in Section 2.4.2.1. Our proposed decomposition algorithm under exact reformulation can be used for any two-stage joint chance-constrained stochastic program with pure binary first-stage decisions and independent Poisson Binomial random variables associated with this joint chance-constraint. Further, we investigate the separation problem over the joint chance-constraint and develop a separation subroutine within our decomposition algorithm. By exploiting the distributional information on the Poisson Binomial random variables, we strengthen the cutting planes which are generated within the separation subroutine. We propose an exact reformulation of the joint chance-constraint under the assumption that a probability oracle exists and computes the exact value of the probability of the non-convex joint chance-constraint by using the knowledge on the distribution of the random variables in Section 2.4.2.1. Further, we investigate the separation problem over the joint chance-constraint and use this probability oracle as a separation subroutine within our proposed decomposition algorithm to check the feasibility of a given solution and generate violated cover inequalities, if such an equality exists. This cutting-plane method guarantees an exact solution but may show slow convergence and require more computational effort as the size of the problem increases. To solve large-scale instances, we also propose a second-order cone programming based safe approximation of the joint chance-constraint in Section 2.4.2.2. Without any assumption on the underlying distribution of the independent random variables associated with the joint chance-constraint, our decomposition algorithm under safe approximation can also be extended to handle any two-stage joint chance-constrained stochastic program with pure binary first-stage decisions.

2.3 Stochastic Optimization Model

In this section, we first describe the problem setting (Section 2.3.1) and present the joint chance-constrained stochastic optimization model (Section 2.3.2). We explain how to characterize the underlying failure uncertainty by using degradation signal modeling in detail in Section 2.3.3. We provide the compact formulation and decomposition-based reformulation of our optimization model in Section 2.3.4.

2.3.1 Problem Setting

In our study, we consider a power network $\mathcal{N} = (\mathcal{B}, \mathcal{L})$, where $\mathcal{B}$ and $\mathcal{L}$ represent the sets of buses and transmission lines, respectively (see, Figure 2.1). We denote the set of generators linked to buses as $\mathcal{G} \subseteq \mathcal{B}$. In particular, $\mathcal{G}(i)$ denotes the set of generators attached to bus i. We let $\delta^+(i)$ and $\delta^-(i)$ be the sets of outgoing and incoming neighbors of bus i, respectively. We define $\mathcal{G}'$ as the set of generators which potentially need to be maintained, and $\mathcal{G}''$ as the set of generators which are not scheduled for maintenance within the planning horizon due to their low failure probabilities as detailed below. Similarly, we define the sets $\mathcal{L}'$ and $\mathcal{L}''$ for representing the transmission lines requiring and not requiring maintenance, respectively. In the remainder of this thesis, we use the term "component" to refer both generators and transmission lines and let the set of components to be $\mathcal{H} = \mathcal{H}' \cup \mathcal{H}''$, where $\mathcal{H}' = \mathcal{G}' \cup \mathcal{L}'$ and $\mathcal{H}'' = \mathcal{G}'' \cup \mathcal{L}''$. We explicitly specify the type of components with subscripts when necessary.

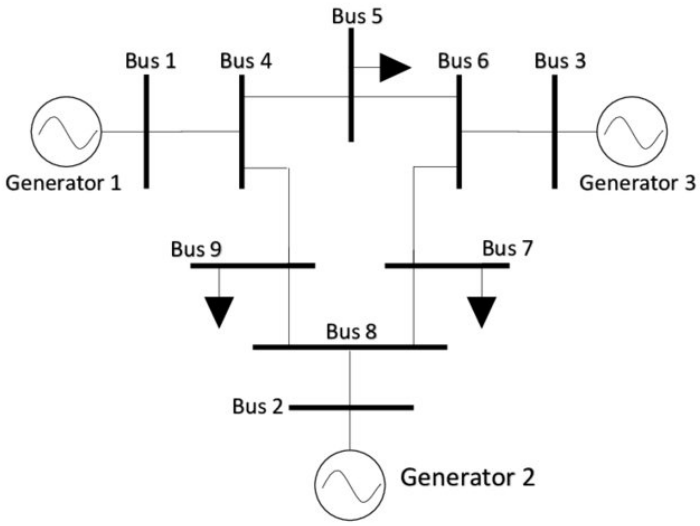

Figure 2.1 9-bus instance.

The proposed stochastic optimization model incorporates the uncertainty in failure times of system components. In addition to the introduced joint chance-constraint that ensures the reliable operations of the system based on RLDs, we represent the uncertainty in the optimization model with a finite set of scenarios, denoted by $\mathcal{K}$, where scenario k contains a possible realization of random failure time ξ_h^k of component h. We also consider a finite set of maintenance periods, denoted by $\mathcal{T}$, and a finite set of hourly subperiods in each maintenance period, denoted by $\mathcal{S}$. Additionally, we define an extended planning horizon as $\bar{\mathcal{T}} = \mathcal{T} \cup \{|\mathcal{T}| + 1\}$ for cases in which components do not fail within the planning horizon. We identify subset $\mathcal{H}'$

based on the RLDs of system components. The main reason of this subset selection is that scheduling all system components for short-term maintenance is impractical and unnecessary in real-time power system operations. We explain how to obtain a characterization on the RLDs in detail in Section 2.3.3. Here, we outline the main steps for identifying subset $\mathcal{H}'$. Suppose we are given a probability threshold $\bar{p}_{fail} \in [0,1]$ (e.g., $\bar{p}_{fail} = 0.1$). For component $h \in \mathcal{H}$, we first obtain its failure probability p^h_{fail} within the planning horizon. If $p^h_{fail} \geq \bar{p}_{fail}$, we add component h to set $\mathcal{H}'$. After having identified the set $\mathcal{H}'$, we sample failure scenarios for each component $h \in \mathcal{H}'$ from its unique RLD based on the scenario generation procedure proposed by Basciftci et al. (2018). If a component h does not fail within the planning horizon under scenario k, we let $\xi^k_h = |\bar{\mathcal{T}}|$. We note that the components in $\mathcal{H}'$ are assumed to enter maintenance at most once, whereas components belonging to set $\mathcal{H}''$ are not scheduled for maintenance within the planning horizon since their failure probabilities are negligible. In our solution evaluation scheme, however, we assume that all components from set $\mathcal{H}$ may fail within the planning horizon.

2.3.2 Mathematical Model and Formulation

In this section, we first introduce the necessary notations for our optimization model. In Table 2.1, we present the notation used for the decision variables and parameters along with their definitions. The scenario-dependent decisions variables (also parameters) are associated with the superscript k.

Next, we introduce the mathematical notation used in the formulation of the joint chance-constraint. This constraint aims to restrict the number of generators and lines that enter corrective maintenance with high probability. To this end, we let ζ_{ht} be a Bernoulli random variable which takes the value 1 if $t \geq \xi_h$, and 0 otherwise, where ξ_h represents the failure time of component h. Let us first define the following quantities $R_i(w) = \sum_{t \in \bar{\mathcal{T}}} \zeta_{it} w_{it}$ for every $i \in \mathcal{G}$ and $R_{ij}(z) = \sum_{t \in \bar{\mathcal{T}}} \zeta_{ijt} z_{ijt}$ for every $(i,j) \in \mathcal{L}$. Here, $R_i(w)$ ($R_{ij}(z)$) takes the value 1 if generator $i \in \mathcal{G}$ (transmission line $(i,j) \in \mathcal{L}$) enters the corrective maintenance within the planning horizon, and 0 otherwise. Further, we let $E_{\mathcal{G}}(w)$ be the event that the total number of generators under corrective maintenance is less than a predetermined threshold $\rho_{\mathcal{G}}$ as:

$$E_{\mathcal{G}}(w) = \Big\{ \sum_{i \in \mathcal{G}} R_i(w) \leq \rho_{\mathcal{G}} \Big\}.$$

Here, a component is considered to enter corrective maintenance if its scheduled

Parameters	
π^k	Probability of scenario k.
ξ_i^k	Failure time of generator i in scenario k.
ξ_{ij}^k	Failure time of transmission line (i,j) in scenario k.
$\tau_{\mathcal{G}}^p(\tau_{\mathcal{G}}^c)$	Predictive (corrective) maintenance duration of generators.
$\tau_{\mathcal{L}}^p(\tau_{\mathcal{L}}^c)$	Predictive (corrective) maintenance duration of transmission lines.
$C_i^p(C_i^c)$	Predictive (corrective) maintenance cost of generator i in period t.
$C_{ij}^p(C_{ij}^c)$	Predictive (corrective) maintenance cost of transmission line (i,j) in period t.
C_i^g	Generation cost of generator i.
C_i^n	No-load cost of generator i.
C_i^s	Start-up cost of generator i.
C_i^d	Demand curtailment cost of generator i.
$\delta_i^{\max}(\delta_i^{\min})$	Maximum (minimum) voltage angle at bus i.
$p_i^{\max}(p_i^{\min})$	Maximum (minimum) power generation of generator i.
$MU_i(MD_i)$	Minimum up (down) time of generator i.
$RU_i(RD_i)$	Ramp up (down) rate of generator i.
$\bar{f}_{ij}$	Maximum power flow along transmission line (i,j).
B_{ij}	Susceptance of transmission line (i,j).
d_{its}	Power demand of bus i in operational subperiod s of period t.
M_{ij}	Sufficiently large number for a flow constraint of transmission line (i,j).
Decision Variables	
w_{it}	1 if generator i enters maintenance in period t, and 0 otherwise.
z_{ijt}	1 if transmission line (i,j) enters maintenance in period t, and 0 otherwise.
δ_{its}^k	Voltage angle at bus i in subperiod s of period t in scenario k.
q_{its}^k	Demand curtailed at bus i in subperiod s of period t in scenario k.
x_{its}^k	Commitment status of generator i in subperiod s of period t in scenario k.
p_{its}^k	Power generation of generator i in subperiod s of period t in scenario k.
u_{its}^k	1 if generator i starts up in subperiod s of period t in scenario k, and 0 otherwise.
ν_{its}^k	1 if generator i shuts down in subperiod s of period t in scenario k, and 0 otherwise.
y_{ijts}^k	Switch status of transmission line (i,j) in subperiod s of period t in scenario k.
f_{ijts}^k	Power flow along transmission line (i,j) in subperiod s of period t in scenario k.

Table 2.1 Problem parameters and decision variables.

maintenance time is later than its time of failure. If the scheduled maintenance time is before the time of failure, then the maintenance is considered as predictive and prevents this undesirable failure event. We note that $R_i(w)$ can take at most the value 1, since the components can enter maintenance at most once within the planning horizon. Furthermore, this event is defined over the set $\mathcal{G}$ to capture the failure possibilities over all generators.

Similarly, we let $E_{\mathcal{L}}(z)$ be the event that the total number of transmission lines under corrective maintenance is less than a predetermined threshold $\rho_{\mathcal{L}}$ as:

$$E_{\mathcal{L}}(z) = \Big\{ \sum_{(i,j)\in\mathcal{L}} R_{ij}(z) \leq \rho_{\mathcal{L}} \Big\}.$$

We define event $E_{\mathcal{H}}(v)$ as the intersection of events $E_{\mathcal{G}}(w)$ and $E_{\mathcal{L}}(z)$. Also, we let $R_i(w) = \zeta_{i|\bar{\mathcal{T}}|}$ for $i \in \mathcal{G}''$ and $R_{ij}(z) = \zeta_{ij|\bar{\mathcal{T}}|}$ for $(i,j) \in \mathcal{L}''$. Note that this is equivalent to the assumption that component $h \in \mathcal{H}''$ is not scheduled for maintenance within the planning horizon.

Now, we are ready to present the mathematical formulation of the joint chance-constrained stochastic optimization problem:

$$\begin{aligned}
\min\ & \sum_{k\in\mathcal{K}} \pi^k \Big(\sum_{i\in\mathcal{G}'} \sum_{t=1}^{\xi_i^k-1} C_i^p w_{it} + \sum_{i\in\mathcal{G}'} \sum_{t=\xi_i^k:\xi_i^k\neq|\bar{\mathcal{T}}|}^{|\bar{\mathcal{T}}|} C_i^c w_{it} \Big) \\
& + \sum_{k\in\mathcal{K}} \pi^k \Big(\sum_{(i,j)\in\mathcal{L}'} \sum_{t=1}^{\xi_{ij}^k-1} C_{ij}^p z_{ijt} + \sum_{(i,j)\in\mathcal{L}'} \sum_{t=\xi_{ij}^k:\xi_{ij}^k\neq|\bar{\mathcal{T}}|}^{|\bar{\mathcal{T}}|} C_{ij}^c z_{ijt} \Big) \\
& + \sum_{k\in\mathcal{K}} \sum_{i\in\mathcal{G}} \sum_{t\in\mathcal{T}} \sum_{s\in\mathcal{S}} \pi^k (C_i^g p_{its}^k + C_i^n x_{its}^k + C_i^s u_{its}^k) \\
& + \sum_{k\in\mathcal{K}} \sum_{i\in\mathcal{B}} \sum_{t\in\mathcal{T}} \sum_{s\in\mathcal{S}} \pi^k C_i^d q_{its}^k && \text{(2.1a)} \\
\text{s.t. } & \mathbb{P}(E_{\mathcal{G}}(w) \cap E_{\mathcal{L}}(z)) \geq 1-\alpha && \text{(2.1b)} \\
& \sum_{t\in\bar{\mathcal{T}}} w_{it} = 1 \quad i\in\mathcal{G}' && \text{(2.1c)} \\
& \sum_{t\in\bar{\mathcal{T}}} z_{ijt} = 1 \quad (i,j)\in\mathcal{L}' && \text{(2.1d)}
\end{aligned}$$

For each scenario $k \in \mathcal{K}$:

$$\begin{aligned}
& x_{its}^k \leq 1 - \sum_{e=0}^{\tau_{\mathcal{G}}^p-1} w_{i(t-e)} \quad i\in\mathcal{G}', s\in\mathcal{S}, t\in\{1,\ldots,\xi_i^k+\tau_{\mathcal{G}}^p-1\}, && \text{(2.1e)} \\
& x_{its}^k \leq \sum_{t'=1}^{\xi_i^k-1} w_{it'} \quad i\in\mathcal{G}', s\in\mathcal{S}, t\in\{\xi_i^k,\ldots,\xi_i^k+\tau_{\mathcal{G}}^c-1\} && \text{(2.1f)} \\
& y_{ijts}^k \leq 1 - \sum_{e=0}^{\tau_{\mathcal{L}}^p-1} z_{ij(t-e)} \quad (i,j)\in\mathcal{L}', s\in\mathcal{S}, t\in\{1,\ldots,\xi_{ij}^k+\tau_{\mathcal{L}}^p-1\} && \text{(2.1g)} \\
& y_{ijts}^k \leq \sum_{t'=1}^{\xi_{ij}^k-1} z_{ijt'} \quad (i,j)\in\mathcal{L}', s\in\mathcal{S}, t\in\{\xi_{ij}^k,\ldots,\xi_{ij}^k+\tau_{\mathcal{L}}^c-1\} && \text{(2.1h)} \\
& z_{ijt} + y_{ijts}^k = 1 \quad (i,j)\in\mathcal{L}', t\in\mathcal{T}, s\in\mathcal{S} && \text{(2.1i)} \\
& \sum_{i'\in\mathcal{G}(i)} p_{i'ts}^k + q_{its}^k - d_{its} = \sum_{j\in\delta^+(i)} f_{ijts}^k - \sum_{j\in\delta^-(i)} f_{jits}^k \quad i\in\mathcal{B}, t\in\mathcal{T}, s\in\mathcal{S} && \text{(2.1j)} \\
& B_{ij}(\delta_{its}^k - \delta_{jts}^k) = f_{ijts}^k \quad (i,j)\in\mathcal{L}'', t\in\mathcal{T}, s\in\mathcal{S} && \text{(2.1k)} \\
& B_{ij}(\delta_{its}^k - \delta_{jts}^k) - M_{ij}(1-y_{ijts}^k) \leq f_{ijts}^k \\
& \quad \leq B_{ij}(\delta_{its}^k - \delta_{jts}^k) + M_{ij}(1-y_{ijts}^k) \quad (i,j)\in\mathcal{L}', t\in\mathcal{T}, s\in\mathcal{S} && \text{(2.1l)} \\
& -\bar{f}_{ij} \leq f_{ijts}^k \leq \bar{f}_{ij} \quad (i,j)\in\mathcal{L}'', t\in\mathcal{T}, s\in\mathcal{S} && \text{(2.1m)} \\
& -\bar{f}_{ij} y_{ijts}^k \leq f_{ijts}^k \leq \bar{f}_{ij} y_{ijts}^k \quad (i,j)\in\mathcal{L}', t\in\mathcal{T}, s\in\mathcal{S} && \text{(2.1n)} \\
& p_i^{\min} x_{its}^k \leq p_{its}^k \leq p_i^{\max} x_{its}^k \quad i\in\mathcal{G}, t\in\mathcal{T}, s\in\mathcal{S} && \text{(2.1o)} \\
& x_{it(s-1)}^k - x_{its}^k + u_{its}^k \geq 0 \quad i\in\mathcal{G}, t\in\mathcal{T}, s\in\mathcal{S} && \text{(2.1p)} \\
& x_{its}^k - x_{it(s-1)}^k + \nu_{its}^k \geq 0 \quad i\in\mathcal{G}, t\in\mathcal{T}, s\in\mathcal{S} && \text{(2.1q)}
\end{aligned}$$

$$-RD_i \leq p^k_{its} - p^k_{it(s-1)} \leq RU_i \quad i \in \mathcal{G}, t \in \mathcal{T}, s \in \mathcal{S} \tag{2.1r}$$

$$x^k_{its} - x^k_{it(s-1)} \leq x^k_{its'} \quad i \in \mathcal{G}, t \in \mathcal{T}, s \in \mathcal{S}, s' \in \{s+1, s+MU_i-1\} \tag{2.1s}$$

$$x^k_{it(s-1)} - x^k_{its} \leq 1 - x^k_{its'} \quad i \in \mathcal{G}, t \in \mathcal{T}, s \in \mathcal{S}, s' \in \{s+1, s+MD_i-1\} \tag{2.1t}$$

$$w \in \{0,1\}^{|\mathcal{G}'|\times|\bar{\mathcal{T}}|},\ z \in \{0,1\}^{|\mathcal{L}'|\times|\bar{\mathcal{T}}|} \tag{2.1u}$$

$$x^k, v^k \in \{0,1\}^{|\mathcal{G}|\times|\mathcal{T}|\times|\mathcal{S}|}, y^k \in \{0,1\}^{|\mathcal{L}'|\times|\mathcal{T}|\times|\mathcal{S}|} \tag{2.1v}$$

$$u^k_{its} \in [0,1] \quad i \in \mathcal{G}, t \in \mathcal{T}, s \in \mathcal{S} \tag{2.1w}$$

$$\delta^k_{its} \in [\delta_i^{\min}, \delta_i^{\max}], q^k_{its} \geq 0 \quad i \in \mathcal{B}, t \in \mathcal{T}, s \in \mathcal{S}. \tag{2.1x}$$

The objective function (2.1a) aims to minimize the expected total cost, which consists of the expected maintenance costs of components and expected operational costs. For each component $h \in \mathcal{H}'$ under each scenario $k \in \mathcal{K}$, we incur its predictive maintenance cost if this component fails in that scenario, i.e., $\xi^k_h < |\bar{\mathcal{T}}|$, and a maintenance is scheduled before its failure time; or this component does not fail, i.e., $\xi^k_h = |\bar{\mathcal{T}}|$, and a maintenance is scheduled within the planning horizon. Otherwise, its corrective maintenance cost is incurred for the first case and no cost is incurred for the latter. The operational costs correspond to power generation, commitment, start-up, and demand curtailment.

Constraint (2.1b) is a joint chance-constraint which holds with probability $1-\alpha$. This constraint limits the total number of generators and transmission lines going under corrective maintenance by predetermined thresholds $\rho_{\mathcal{G}}$ and $\rho_{\mathcal{L}}$, respectively. Constraints (2.1c) and (2.1d) imply that exactly one maintenance must be scheduled within the extended planning horizon for every component. Constraints (2.1e) and (2.1g) ensure that if a component undergoes a predictive maintenance, it becomes unavailable until this predictive maintenance is completed whereas constraints (2.1f) and (2.1h) ensure the unavailability of a component from its failure time until a corrective maintenance is completed. On the other hand, constraint (2.1i) guarantees that a transmission line is available unless it is under maintenance. Equation (2.1j) represents the linearized power flow equations (Kirchhoff's Current Law) for each bus. Notice that heavily penalized power curtailment (q_{its}) is further added to (2.1j). This guarantees that we always obtain a feasible solution when the network fails to provide sufficient power supply to meet total power demand, which is a common practice in power systems. Equation (2.1k) is the power flow definition derived from Ohm's Law. When a transmission line is switched on ($y^k_{ijts} = 1$), constraint (2.1l) ensures that power flow is defined according to Ohm's Law, otherwise both upper bounds and lower bounds become redundant. Constraints (2.1m) and (2.1n) limit the power flow for each transmission line whereas constraint (2.1o) limits the power generation for each generator. Constraints (2.1p) and (2.1q) couple commitment

status with start-up and shut-down variables, respectively. Constraint (2.1r) is the ramping constraint which guarantees that the power generation difference between consecutive hours does not exceed ramp-up and ramp-down limits. Constraints (2.1s) and (2.1t) are the minimum up and down times restrictions for each generator. Constraints (2.1u), (2.1v), (2.1w) and (2.1x) are for binary and nonnegativity restrictions. Note that binary start-up variables are relaxed to continuous variables since they are associated with positive cost coefficients in (2.1a). Although this relaxation will expand the feasible region, it does not change the optimal value of our stochastic optimization problem (see, O'Neill, Hedman, Krall, Papavasiliou & Oren (2010)).

2.3.3 Degradation Signal Modeling

In this section, we explain our modeling framework for the RLDs of system components under a Bayesian setting. A degradation signal progress has two main levels: Phase I and Phase II (Gebraeel, 2006). Phase I is referred to as the "non-defective" stage when a component does not show any sign of failure whereas Phase II is known as the "defective" stage in which degradation signal of system components aggressively deteriorates and results in failure when degradation signal reaches some predetermined threshold Λ. When modeling failure uncertainty of system components, we focus on the defective stage of their degradation signals.

In this thesis, we assume that we can identify degradation signal of each component using real-time sensor information. Then, we model each degradation signal as a stochastic continuous process and denote this process as $\mathcal{D} = \{D_h(t) : t \geq 0\}$ with $D_h : \mathbb{R} \to \mathbb{R}$ given by

$$D_h(t) = \upsilon_h + \beta_h t + \sigma_h W(t), \tag{2.2}$$

where υ_h is the initial signal amplitude and β_h is the linear drift parameter for each $h \in \mathcal{H}$. The independent stochastic parameters υ_h and β_h of the degradation signal model are presumed to follow some prior distributions which are assumed to be the same across every population (i.e., generators and transmission lines). The stochastic process $\mathcal{W} = \{W(t) : t \geq 0\}$ is the standard Brownian motion with $W(0) = 0$. We also assume that the standard deviation σ_h of degradation signal of component h is known and constant over the planning horizon. Furthermore, the standard deviation has the same value across every population. When the

degradation signal level of a component exceeds the predefined threshold Λ, we assume that it fails. In particular, we define the failure time of component h as the first passage time, i.e., $\xi_h = \min\{t \geq 0 : D_h(t) \geq \Lambda\}$.

Next, we estimate the RLDs by using Bayesian inference combining both degradation signal model parameters and real-time condition-based sensor information. For every $h \in \mathcal{H}$, we assume that the prior distribution of the initial signal amplitude is $\upsilon_h \sim \mathcal{N}(\mu_0, \kappa_0^2)$ and the prior distribution of the linear drift is $\beta_h \sim \mathcal{N}(\mu_1, \kappa_1^2)$. We let $D_h(t_h^i)$ be the degradation signal level of component h at time t_h^i. We define D_h^i as the increment between times t_h^i and t_h^{i-1}, given by $D_h^i = D_h(t_h^i) - D_h(t_h^{i-1})$ for $i = 2, \ldots, t_h^k$ with $D_h^1 = D_h(t_h^1)$ where t_h^k, $k \in \mathbb{Z}_+$ is the random observation time of the degradation signal of component h. Given the observed degradation signal data, we can mathematically derive the posterior distribution of the initial amplitude υ_h and the linear drift β_h for every $h \in \mathcal{H}$ with a closed form expression (Proposition 2 by Gebraeel, Lawley, Li & Ryan (2005)). By using the posterior distribution of the drift parameter β_h, we estimate the RLD of component h as in Proposition 2.1.

Proposition 2.1 *Given the observed signal increments D_h^i at time $i = t_h^1, \ldots, t_h^k$ with prior parameters (υ_h, β_h), and the predefined failure threshold Λ, the posterior mean of the drift parameter of component h is given by:*

$$\mu_h' = \frac{(\kappa_1^2 \sum_{i=1}^{t_h^k} D_h^i + \mu_1 \sigma_h^2)(\kappa_0^2 + \sigma_h^2 t_h^1) - \kappa_1^2 (D_h^1 \kappa_0^2 + \mu_0 \sigma_h^2 t_h^1)}{(\kappa_0^2 + \sigma_h^2 t_h^1)(\kappa_1^2 t_h^k + \sigma_h^2) - \kappa_0^2 \kappa_1^2 t_h^1}. \tag{2.3}$$

Then, the remaining lifetime of component h at time t_h^k follows the inverse Gaussian distribution $\mathcal{IG}(t + t_h^k | \mu, \lambda)$ with shape parameter $\mu = \frac{\Lambda - \sum_{i=1}^{t_h^k} D_h^i}{\mu_h'}$ and scale parameter $\lambda = \frac{(\Lambda - \sum_{i=1}^{t_h^k} D_h^i)^2}{\sigma_h^2}$.

2.3.4 Decomposition of the Stochastic Optimization Model

In this section, we present a compact formulation of the joint chance-constrained stochastic optimization model (2.1). For ease of notation, we let v be the decision vector containing the elements v_{ht} corresponding to the maintenance decision of component $h \in \mathcal{H}'$ in maintenance period $t \in \bar{\mathcal{T}}$. Additionally, we define the binary vector η^k consisting of commitment status, switch status and shut-down decisions under scenario k, and the continuous vector ϕ^k denoting the demand curtailment, voltage angle, power flow, power generation and start-up decisions under scenario

k. We also let $E_{\mathcal{H}}(v)$ be the intersection of $E_{\mathcal{G}}(w)$ and $E_{\mathcal{L}}(z)$ (introduced in Section 2.3.3). The compact formulation now can be stated as follows:

$$\min \sum_{k\in\mathcal{K}} \pi^k \Big(a^\top \eta^k + b^\top \phi^k + c_k^\top v) \tag{2.4a}$$

$$\text{s.t. } \mathbb{P}(E_{\mathcal{H}}(v)) \geq 1-\alpha \tag{2.4b}$$

$$Av = l \tag{2.4c}$$

$$B^k v + D\eta^k \leq n \qquad k\in\mathcal{K} \tag{2.4d}$$

$$F\eta^k + G\phi^k \leq r \qquad k\in\mathcal{K} \tag{2.4e}$$

$$v \in \{0,1\}^{|\mathcal{H}'|\times|\bar{\mathcal{T}}|} \tag{2.4f}$$

$$\eta^k \in \{0,1\}^{(2|\mathcal{G}|+|\mathcal{L}'|)\times|\mathcal{T}|\times|\mathcal{S}|} \qquad k\in\mathcal{K}. \tag{2.4g}$$

Next, we explain the correspondence between constraints in (2.4) and constraints in (2.1). Constraint (2.4b) corresponds to the joint chance-constraint (2.1b) for which we propose two different representation in Section 2.4.2. Constraint (2.4c) refers to the maintenance constraints (2.1c) and (2.1d) restricting the total number of maintenance schedules for each component within the planning horizon. Constraint (2.4d) corresponds to the coupling constraints (2.1e) - (2.1i) between maintenance and operational decisions. Constraint (2.4e) represents the operational constraints (2.1j) - (2.1t) and domain restrictions (2.1w) and (2.1x). Constraints (2.4f) and (2.4g) correspond to the binary restrictions (2.1u) and (2.1v) for maintenance decision v and operational decision η, respectively. We introduce the set of feasible maintenance decisions as $\hat{\mathcal{V}} = \{v \in \{0,1\}^{|\mathcal{H}'|\times|\bar{\mathcal{T}}|} : (2.4b), (2.4c)\}$. We can then reformulate (2.4) as a two-stage stochastic program given by:

$$\min_v \ \Big\{ \sum_{k\in\mathcal{K}} \pi^k \Big(c_k^\top v + \mathcal{Q}(v,\xi_k)\Big) : v\in\hat{\mathcal{V}}\Big\}, \tag{2.5}$$

where $\mathcal{Q}(v,\xi_k)$ is the recourse function under scenario k defined as follows:

$$\begin{aligned}\mathcal{Q}(v,\xi_k) = \min_{\eta^k,\phi^k} \Big\{ a^\top\eta^k + b^\top\phi^k : \ & D\eta^k \leq n - Bv, \\ & F\eta^k + G\phi^k \leq r, \\ & \eta^k \in \{0,1\}^{(2|\mathcal{G}|+|\mathcal{L}'|)\times|\mathcal{T}|\times|\mathcal{S}|}\Big\}.\end{aligned} \tag{2.6}$$

The first-stage decisions correspond to the maintenance decisions and the second-stage decisions correspond to the operational decisions. Note that the first-stage decisions are restricted to be binary and the second-stage decisions are restricted to be mixed-integer. We also denote the expected recourse function as $\mathcal{Q}(v,\xi)$ given by $\sum_{k\in\mathcal{K}} \pi^k \mathcal{Q}(v,\xi_k)$.

Even with a small number of failure scenarios, the presented two-stage stochastic program (2.5) can still be challenging to solve. Given a first-stage maintenance decision v and a realization of random failure times ξ_k, we observe that maintenance periods under scenario k become independent from each other. Fortunately, this allows us to further decompose each scenario subproblem into smaller and independent subproblems. We refer to this property as *time-decomposability* of scenario subproblems. We can formulate each smaller scenario subproblem under scenario k by replacing (2.6) with $\sum_{t\in\mathcal{T}} \mathcal{Q}_t(v,\xi_k)$ where $\mathcal{Q}_t(v,\xi_k)$ is defined as follows:

$$\mathcal{Q}_t(v,\xi_k) = \min_{\eta_t^k,\phi_t^k} \Big\{ a_t^\top \eta_t^k + b_t^\top \phi_t^k : \; D_t\eta_t^k \le n_t - B_t v, \; F_t\eta_t^k + G_t\phi_t^k \le r_t, \; \eta^k \in \{0,1\}^{(2|\mathcal{G}|+|\mathcal{L}'|)\times|\mathcal{S}|} \Big\}. \tag{2.7}$$

Before moving to the next section, let us first obtain an equivalent MIP formulation for (2.5) by introducing an auxiliary variable θ^k for the recourse function $\mathcal{Q}(v,\xi_k)$ for $k \in \mathcal{K}$. Consider the following mixed-integer master problem:

$$\min_{v,\theta} \; \sum_{k\in\mathcal{K}} \pi^k (c_k^\top v + \theta^k) \tag{2.8a}$$

$$\text{s.t.} \; v \in \hat{\mathcal{V}} \tag{2.8b}$$

$$\theta \ge L \tag{2.8c}$$

$$(v,\theta) \in \Theta \tag{2.8d}$$

Constraints (2.8c) are used to impose a lower bound on the recourse function. A trivial lower bound on the recourse function $\mathcal{Q}(v,\xi_k)$ is zero since all cost coefficients and their corresponding variables are nonnegative under scenario subproblem k. However, one can obtain a valid (and possibly better) lower bound L^k on $\mathcal{Q}(v,\xi_k)$ by solving the following linear program:

$$L^k = \min_{\eta^k,\phi^k,v} \{ a^\top \eta^k + b^\top \phi^k : \; D\eta^k + Bv \le n, \; F\eta^k + G\phi^k \le r, (2.4c), v \in [0,1]^{|\mathcal{H}'|\times|\bar{\mathcal{T}}|} \}, \tag{2.9}$$

under scenario subproblem $k \in \mathcal{K}$. We refer to set Θ in constraint (2.8d) as the set of optimality cuts added to the relaxed master problem until some iteration. In particular, set Θ is called valid if for every $v \in \hat{\mathcal{V}}, (v,\theta) \in \Theta$ implies that $\theta^k \ge \mathcal{Q}(v,\xi_k)$ for $k \in \mathcal{K}$. Note that since (2.5) has relatively complete recourse, we are not particularly interested in generating feasibility cuts which enforce the feasibility of each scenario subproblem. Suppose that a valid and finite set of optimality cuts Θ indeed exists for the joint chance-constrained stochastic program (2.5), (2.8) is

then equivalent to (2.5). We can also obtain a different equivalent MIP formulation for (2.5) by utilizing the time-decomposability of scenario subproblems. For this purpose, we replace θ^k in (2.8a) with $\sum_{t\in\mathcal{T}}\theta_t^k$. Similarly, one can obtain a valid lower bound L_t^k on $\mathcal{Q}_t(v,\xi_k)$ by utilizing time-decomposability and solving (2.9) under scenario k in maintenance period t.

We observe that set Θ may contain exponentially many constraints. Instead of adding all of these cuts to the problem, it might be more practical to consider a so-called relaxed master problem containing a small subset of Θ (possibly an empty set). In the next section, we propose an iterative algorithm with various algorithmic enhancements where the relaxed master problem is solved until we obtain the optimal solution to the two-stage joint chance-constrained stochastic program (2.5).

2.4 Solution Methodology

In this section, we first explain our decomposition algorithm to solve (2.5) and explain various algorithmic enhancements in detail (Section 2.4.1). Two different representations of the joint chance-constraint are explained in Section 2.4.2. The set of optimality cuts used in our proposed algorithm are presented in Section 2.4.3. We further present a prepossessing step to address the potential redundancy in transmission flow limits in Section 2.4.4. Finally, we use a SAA approach within the proposed decomposition algorithm to obtain statistical bounds on the true optimality gap in Section 2.4.5.

2.4.1 Decomposition Algorithm

We benefit from the features of the integer L-shaped method to develop a decomposition-based algorithm (Algorithm 1) to solve our two-stage joint chance-constrained stochastic program (2.5). Given a first-stage decision, solving many similar mixed-integer scenario subproblems can be computationally expensive. We propose an algorithmic enhancement to avoid this situation by exploiting the time decomposability of scenario subproblems and identifying the "status" of system components.

Let us first devise a concept of status of system components, which is utilized in our decomposition algorithm. This concept is used to characterize the availability of system components. Given a feasible maintenance decision $v \in \hat{\mathcal{V}}$, the status of component $h \in \mathcal{H}'$, denoted by $u^k_{ht}(v)$, takes a value of 1 if the corresponding component is available in maintenance period $t \in \mathcal{T}$ under scenario $k \in \mathcal{K}$, and 0 otherwise. We corroborate this concept with a simplified instructive example. Consider our stochastic optimization problem (2.1) under a single scenario with $|\mathcal{G}'| = |\mathcal{L}'| = 1$, $|\mathcal{T}| = 4$ and $(\tau^p_{\mathcal{G}}, \tau^c_{\mathcal{G}}, \tau^p_{\mathcal{L}}, \tau^c_{\mathcal{L}}, \xi^1_1, \xi^1_2) = (1, 2, 1, 2, 1, 4)$. Suppose we are given a feasible maintenance decision $v = [0, 1, 0, 0, 0; 0, 1, 0, 0, 0]$, which corresponds to the case where the components enter maintenance in the second period and let these components correspond to the generator and the transmission line, respectively. The status vector of component 1 is $[0, 0, 1, 1]$ as the scheduled predictive maintenance at period 2 is at a later period than its failure time at period 1. Thus, it is under corrective maintenance and is unavailable for two consecutive maintenance periods. On the other hand, the status vector of component 2 is $[1, 0, 1, 1]$ since the scheduled predictive maintenance at period 2 prevents the failure at period 4, and this component is only unavailable for one maintenance period. By combining these status vectors of components, we obtain $u^1(v) = [0, 0, 1, 1; 1, 0, 1, 1]$ where column t consists of the status of components in maintenance period t for every $t \in \mathcal{T}$. Now, suppose we are given another feasible maintenance decision under the same single scenario problem as $\tilde{v} = [0, 0, 1, 0, 0; 0, 0, 0, 1, 0]$. Similarly, we obtain $u^1(\tilde{v}) = [0, 0, 1, 1; 1, 1, 0, 1]$. In the remainder of this thesis, we let $u^k_t(v)$ denote the column t of $u^k(v)$ given maintenance decision v for every $k \in \mathcal{K}$ and $t \in \mathcal{T}$. Observe that $u^1_1(v)$ and $u^1_4(v)$ are the same with $u^1_1(\tilde{v})$ and $u^1_4(\tilde{v})$, respectively. This implies that the components have the same status for the first and fourth periods under this scenario for the solutions v and $\tilde{v}$. To generalize, decomposing a scenario subproblem into maintenance periods given different feasible maintenance decisions may yield to some identical scenario subproblems depending on the availability of the components. Eventually, we exploit this observation and adapt the concept of status in our decomposition algorithm. This allows us to uniquely determine the nature of each scenario subproblem given different feasible maintenance (first-stage) decisions.

Next, we explain our proposed decomposition-based algorithm to solve (2.5), which is summarized in Algorithm 1. For representing the joint chance-constraint (2.4b), this algorithm considers both an exact reformulation and a deterministic safe approximation, which are further explained in Section 2.4.2 in detail. When the exact reformulation is used, Algorithm 1 employs a cutting-plane method over the joint chance-constraint (2.4b) as follows: At the beginning of each iteration, we obtain a maintenance decision v by solving the relaxed master problem (2.14). We call

the separation subroutine `RepresentChance`(v) with input v to check whether this maintenance decision is feasible with respect to (2.4b). When the infeasibility of v is detected, a cutting plane is generated and added to set $\mathcal{C}$. This separation subroutine and violated cover inequalities are further explained in Section 2.4.2.1. When the deterministic safe approximation is used, we always obtain a feasible maintenance decision $v \in \hat{\mathcal{V}}$ since this approximation provides a conservative representation of the joint chance-constraint. After obtaining a feasible maintenance decision $v \in \hat{\mathcal{V}}$ and failure uncertainty is revealed for every scenario, Algorithm 1 proceeds to the second-stage. For storing the status vectors in period t, we define set Υ_t which corresponds to the set of unique status vectors identified at that iteration. Also, we define set Ψ_t to represent the set of all unique status vectors until termination within Algorithm 1. After identifying the unique status vectors (Step 12) for every maintenance period $t \in \mathcal{T}$, Algorithm 1 continues to solve only the subproblems with these newly identified status vectors (Step 20). By restricting ourselves to set Ψ_t, it suffices to solve $\sum_{t\in\mathcal{T}} |\Psi_t|$ many scenario subproblems until termination, which could be significantly less than the total number of scenario subproblems to be solved throughout the algorithm. Finally, Algorithm 1 initializes `OptimalityCut`(v, ξ, L) with input v, ξ and L to generate and add optimality cuts to set Θ in Step 27. Algorithm 1 continues to iterate until a relative optimality gap within a tolerance ϵ is achieved. The implementation of our decomposition-based algorithm is in parallel in order to achieve computational efficiency. At the initialization of Algorithm 1 (Step 2), linear relaxations of the subproblems are solved to obtain lower bounds on the objectives of these problems. Due to the independence of scenario subproblems and time-decomposability, these subproblems are solved within a distributed environment. Similarly, scenario subproblems corresponding to the unique status vectors (Step 20) are solved to optimality with parallelization.

2.4.2 Reformulations of the Joint Chance-Constraint

In this section, we specify two different approximations of the joint chance-constraint (2.4b). First recall the set of feasible maintenance decisions defined as $\hat{\mathcal{V}} = \{v \in \{0,1\}^{|\mathcal{H}'|\times|\bar{\mathcal{T}}|} : (2.4b), (2.4c)\}$. We first obtain an approximation of $\hat{\mathcal{V}}$ by using a probability oracle which provides the exact value of the left-hand side of the joint chance-constraint (2.4b) and further, prove that this approximation is in fact exact. However, this exact representation requires an exponential reformulation of $\hat{\mathcal{V}}$. Thus, we employ a cutting-plane method using the separation subroutine `RepresentChance(`v`)` within Algorithm 1 to efficiently solve our two-stage joint

Algorithm 1 Decomposition

Input: $A, B, D, F, G, a, b, c, l, n, r, \epsilon, \mathcal{Q} : (v, \xi) \to \mathbb{R}$.
Output: ϵ-optimal solution v^* and ϵ-optimal objective value c^*.

Set $UB = \infty, LB = -\infty, \Theta = \mathcal{C} = \emptyset, \Psi_t = \emptyset$ for all $t \in \mathcal{T}$.
Compute the lower bound L of $\mathcal{Q}(v, \xi)$ *(in parallel).*
while $LB/UB < 1 - \epsilon$ **do**
  if the joint chance-constraint representation is exact **then**
    Solve a relaxed master problem (2.14) to obtain a solution (v, θ).
    $flagFeasible \leftarrow$ `RepresentChance(`v`)`.
  else
    Solve a relaxed master problem (2.8) to obtain a feasible solution (v, θ).
    $flagFeasible \leftarrow$ **true**.
  if $flagFeasible$ is **true then**
    $LB \leftarrow max(\sum_{k \in \mathcal{K}} \pi^k (c_k^\top v + \sum_{t \in \mathcal{T}} \theta_t^k),\ LB)$.
    Identify the status vector $u_t^k(v) \in \{0,1\}^{|\mathcal{H}'|}$ for $(k, t) \in \mathcal{K} \times \mathcal{T}$.
    Set $\Upsilon_t = \Gamma_t = \emptyset$ for all $t \in \mathcal{T}$.
    for all $(k, t) \in \mathcal{K} \times \mathcal{T}$ **do**
      if $u_t^k(v) \in \Psi_t$ **then**
        Find an index $\hat{k}$ such that $u_t^k(v) = u_t^{\hat{k}}(v) \in \Psi_t$, and $\Gamma_t \leftarrow \Gamma_t \bigcup \{(\hat{k}, k)\}$.
      else
        $\Upsilon_t \leftarrow \Upsilon_t \bigcup \{u_t^k(v)\}$.
    $\hat{\Upsilon} \leftarrow \bigcup_{t \in \mathcal{T}} \Upsilon_t$, and $\Psi_t \leftarrow \Psi_t \bigcup \Upsilon_t$ for all $t \in \mathcal{T}$.
    for all $u_t^k(v) \in \hat{\Upsilon}$ *(in parallel)* **do**
      Solve scenario subproblem (2.7) associated with $u_t^k(v)$ and obtain $\mathcal{Q}_t(v, \xi_k)$.
    for all $t \in \mathcal{T}$ **do**
      $\mathcal{Q}_t(v, \xi_{\hat{k}}) \leftarrow \mathcal{Q}_t(v, \xi_k)$ for all $(\hat{k}, k) \in \Gamma_t$.
    $c^* \leftarrow \sum_{k \in \mathcal{K}} \pi^k (c_k^\top v + \sum_{t \in \mathcal{T}} \mathcal{Q}_t(v, \xi_k))$.
    if $UB > c^*$ **then**
      $(UB, v^*) \leftarrow (c^*, v)$.
    Initialize `OptimalityCut(`v, ξ, L`)` and add the optimality cut to set Θ.
  else
    continue
return Optimal solution v^* and optimal value c^*.

chance-constrained stochastic program (2.5). Still, this cutting-plane method may not be efficient as the number of components increases. To address this issue, we also develop a second-order cone programming (SOCP) based deterministic safe approximation of (2.4b).

2.4.2.1 Exact Reformulation

Suppose we are given a feasible maintenance decision $v = (w, z) \in \hat{\mathcal{V}}$. Let us first consider the quantity $R_i(w) = \sum_{t \in \bar{\mathcal{T}}} \zeta_{it} w_{it}$ for every $i \in \mathcal{G}$ as defined in Section 2.3.2. Here, we calculate the failure probability for generators $i \in \mathcal{G}$ within the planning horizon. Recall constraint (2.1c) in the joint chance-constrained stochastic optimization model (2.1), that is, $\sum_{t \in \bar{\mathcal{T}}} w_{it} = 1$ for $i \in \mathcal{G}'$. This implies that the quantity $R_i(w)$ is a Bernoulli random variable with the success probability $\mathbb{P}(\xi_i \leq m_i(w))$ where $m_i(w)$ is the maintenance period in which a maintenance is scheduled for generator $i \in \mathcal{G}'$, and if no maintenance is scheduled, we let $m_i(w)$ be $|\mathcal{T}|$ for generator $i \in \mathcal{G}'$. Recall also the following assumption that there is no maintenance scheduled for generators $i \in \mathcal{G}''$, thus, we also let $m_i(w)$ be $|\mathcal{T}|$ for $i \in \mathcal{G}''$. Then, the quantity $R_i(w)$ is also a Bernoulli random variable with the success probability $\mathbb{P}(\xi_i \leq |\mathcal{T}|)$ for $i \in \mathcal{G}''$.

Let us now consider the quantity $R_{ij}(z) = \sum_{t \in \bar{\mathcal{T}}} \zeta_{ijt} z_{ijt}$ for every $(i, j) \in \mathcal{L}$ as defined in Section 2.3.2. The similar results also hold for the transmission lines with constraint (2.1d) in the stochastic optimization model. Therefore, the quantity $R_{ij}(z)$ is a Bernoulli random variable with the success probability $\mathbb{P}(\xi_{ij} \leq m_{ij}(z))$ for $(i, j) \in \mathcal{L}'$. Similarly, the quantity $R_{ij}(z)$ is also a Bernoulli random variable with the success probability $\mathbb{P}(\xi_{ij} \leq |\mathcal{T}|)$ for $(i, j) \in \mathcal{L}''$.

Next, we define the following random variables $\hat{\zeta}_{\mathcal{G}}(w) = \sum_{i \in \mathcal{G}} R_i(w)$ and $\hat{\zeta}_{\mathcal{L}}(z) = \sum_{(i,j) \in \mathcal{L}} R_{ij}(z)$ as the sum of independent Bernoulli random variables.

Remark 2.1 *The random variables $\hat{\zeta}_{\mathcal{G}}(w)$ and $\hat{\zeta}_{\mathcal{L}}(z)$ follow Poisson Binomial distributions with success probabilities $\{\mathbb{P}(\xi_i \leq m_i(w));\ i \in \mathcal{G}\}$ and $\{\mathbb{P}(\xi_{ij} \leq m_{ij}(z));\ (i, j) \in \mathcal{L}\}$, respectively.*

By Remark 2.1, we observe that the left hand-side expression of the joint chance-constraint (2.4b) is equivalent to the following joint cumulative distribution function of two Poisson Binomial random variables, i.e., $\mathbb{P}(\hat{\zeta}_{\mathcal{G}}(w) \leq \rho_{\mathcal{G}}, \hat{\zeta}_{\mathcal{L}}(z) \leq \rho_{\mathcal{L}})$. By using the independence of these two random variables, joint chance-constraint (2.4b) can

be rewritten as:

$$\mathbb{P}(\hat{\zeta}_{\mathcal{G}}(w) \leq \rho_{\mathcal{G}})\mathbb{P}(\hat{\zeta}_{\mathcal{L}}(z) \leq \rho_{\mathcal{L}}) \geq 1-\alpha. \tag{2.10}$$

Finally, we can recast $\hat{\mathcal{V}}$ as follows:

$$\hat{\mathcal{V}} = \{(w,z) \in \{0,1\}^{|\mathcal{G}'|\times|\mathcal{L}'|} : (2.10), (2.4c)\}. \tag{2.11}$$

Next, we derive the exact representation of our joint chance-constraint (2.10). For any maintenance decision $v = (w,z)$, we first suppose that there exists a probability oracle $\mathcal{P}(v)$ which recognizes v and provides the exact value of the left hand-side of relation (2.10). We then introduce the index set $N = \{(h,t) : h \in \mathcal{H}', t \in \bar{\mathcal{T}}\}$. We call a set $C \subseteq N$ a *scheduling set* if it satisfies the following property:

$$\text{there exists a unique } t(h) \in \bar{\mathcal{T}} : (h,t(h)) \in C, \text{ for every } h \in \mathcal{H}'.$$

In other words, this set includes a unique maintenance period for every component from set $\mathcal{H}'$. Let us consider the maintenance decision $v(C)$ depending on a given a scheduling set $C \subseteq N$. Further, we call this set C a *cover* for $\hat{\mathcal{V}}$ if $\mathcal{P}(v(C)) < 1-\alpha$, that is, $v(C) \notin \hat{\mathcal{V}}$.

Proposition 2.2 *Given a cover $C \subseteq N$, the following set of cover inequalities is valid for $\hat{\mathcal{V}}$:*

$$\sum_{(h,t)\in C} v_{ht} \leq |\mathcal{H}'| - 1. \tag{2.12}$$

Proof 2.2 *Let $\hat{v} \in \hat{\mathcal{V}}$. Assume for the sake of contradiction that $\sum_{(h,t)\in C} \hat{v}_{ht} \geq |\mathcal{H}'|$. Since $\sum_{t\in\bar{\mathcal{T}}} \hat{v}_{ht} = 1$ for every $h \in \mathcal{H}'$, it must be that $\hat{v}_{ht} = 1$ for every $(h,t) \in C$. Then contradiction follows immediately since $\mathcal{P}(\hat{v}) < 1-\alpha$ implies that $\hat{v} \notin \hat{\mathcal{V}}$.*

We can ensure that at least one of the elements of the maintenance schedule defined by the set C need to be rescheduled by simply using a cover inequality in (2.12). In particular, if we find every valid cover inequality defined in (2.12) for every cover which is a subset of N, we can obtain an equivalent formulation of $\hat{\mathcal{V}}$. We show this result in Proposition 2.3.

Proposition 2.3 *Consider the following set:*

$$\hat{\mathcal{V}}_1 = \{(w,z) \in \{0,1\}^{|\mathcal{G}'|\times|\mathcal{L}'|} : \sum_{(h,t)\in C} v_{ht} \leq |\mathcal{H}'| - 1, (2.4c), \quad \forall C \subseteq N \text{ s.t. } C \text{ is a cover}\}. \tag{2.13}$$

Sets defined in (2.13) *and* (2.11) *are equivalent.*

Proof 2.3 *We only prove that* $\hat{\mathcal{V}}_1 \subseteq \hat{\mathcal{V}}$ *by contraposition since the converse is proven in Proposition 2.2. Let* $\tilde{v} = (\tilde{w}, \tilde{z}) \notin \hat{\mathcal{V}}$ *such that constraints* (2.4c),(2.4f) *hold for* $\tilde{v}$ *but* $\mathbb{P}(\hat{\zeta}_{\mathcal{G}}(\tilde{w}) \leq \rho_{\mathcal{G}},\ \hat{\zeta}_{\mathcal{L}}(\tilde{z}) \leq \rho_{\mathcal{L}}) < 1-\alpha$. *Then, there must exist at least one subset* $\tilde{C} \subseteq N$ *such that* $\tilde{C}$ *is a cover, which directly implies by definition that* $\tilde{v} \notin \hat{\mathcal{V}}_1$.

Unfortunately, set (2.13) requires finding an exponential number of valid inequalities to obtain the feasible space for $\hat{\mathcal{V}}$. In the remainder of this section, we address a separation subroutine using the probability oracle $\mathcal{P}$ to check the feasibility status of the current maintenance solution and further find valid cover inequalities, if such equalities exist (see, for instance, Wu & Küçükyavuz (2019)). We first consider the relaxed master problem of (2.8):

$$\min\{\sum_{k\in\mathcal{K}} \pi^k(c_k^\top v + \theta^k) :\ \theta \geq L,\ (v,\theta) \in \Theta,\ v \in \hat{\mathcal{V}} \cap \mathcal{C}\}, \tag{2.14}$$

where $\mathcal{C}$ is the set of cover inequalities generated and added to the relaxed master problem until some iteration. Algorithm 1 starts with a possibly empty subset of $\mathcal{C}$. After obtaining a maintenance decision $\hat{v} = (\hat{w}, \hat{z})$ at the end of step 5, we initialize the separation subroutine (Algorithm 2) which employs the probability oracle $\mathcal{P}(\hat{v})$ to compute the exact value of the left hand-side of (2.4b) when $\hat{v}$ is a feasible maintenance decision. Algorithm 1 leaves the separation subroutine without generating a valid inequality if the current solution is feasible. Otherwise, we define a cover as $C = \bigcup_{h\in\mathcal{H}'}\{(h,t) \in N : \hat{v}_{ht} = 1,\ t \in \bar{\mathcal{T}}\}$ and generate a cover inequality as in (2.12) to separate the current solution from the set of maintenance decisions and add the corresponding inequality to set $\mathcal{C}$.

Next, we explain the monotonicity property of the probability oracle in the thesis. Given any maintenance decision v, let us define the index set of components and maintenance periods as follows:

$$\mathcal{I}(v) = \bigcup_{h\in\mathcal{H}'} \{(h,t) : v_{ht} = 1,\ t \in \bar{\mathcal{T}}\}.$$

We say that $\mathcal{P}$ is monotonically non-increasing if any v', v'' pair has the following property:

$$(h,t') \leq (h,t'') \text{ for } (h,t') \in \mathcal{I}(v'),\ (h,t'') \in \mathcal{I}(v'') \text{ and } h \in \mathcal{H}'.$$

This implies that $\mathcal{P}(v') \geq \mathcal{P}(v'')$, i.e., $\mathbb{P}(\hat{\zeta}_{\mathcal{G}}(w') \leq \rho_{\mathcal{G}})\mathbb{P}(\hat{\zeta}_{\mathcal{L}}(z') \leq \rho_{\mathcal{L}}) \geq \mathbb{P}(\hat{\zeta}_{\mathcal{G}}(w'') \leq \rho_{\mathcal{G}})\mathbb{P}(\hat{\zeta}_{\mathcal{L}}(z'') \leq \rho_{\mathcal{L}})$. We state this property in Proposition 2.4.

Proposition 2.4 *Probability oracle $\mathcal{P}(v)$ is a monotonically non-increasing function in v.*

The proof of Proposition 2.4 is given in Appendix A which leverages the fact that the random variables have Poisson Binomial distribution as discussed in Remark 2.1. We use Proposition 2.4 to strengthen the formulation in (2.12). Without loss of generality, we assume a pair of maintenance decisions $v' \neq v''$ with the following property:

$$\begin{aligned}\text{there exists a unique } h_* \text{ and } t'_* < t''_* : (h_*, t'_*) \in \mathcal{I}(v'),\ (h_*, t''_*) \in \mathcal{I}(v''),\\ (h', t') = (h'', t'')\\ \text{for } (h', t') \in \mathcal{I}(v') \setminus \{(h_*, t'_*)\},\\ (h'', t'') \in \mathcal{I}(v'') \setminus \{(h_*, t''_*)\}.\end{aligned}$$

In other words, component h_* is scheduled for maintenance in period t'_* under decision v', and it is scheduled for maintenance in a later period t''_* than t'_* under decision v''. For each component $h \in \mathcal{H}' \setminus \{h_*\}$, maintenance schedules are the same under both decisions. By Proposition 2.4, we have $\mathcal{P}(v') > \mathcal{P}(v'')$. We observe that if v' is infeasible w.r.t. constraint (2.4b), i.e., $\mathcal{P}(v') < 1 - \alpha$, then clearly v'' is also infeasible w.r.t. constraint (2.4b). In particular, we observe that any other maintenance plan for component h_* in a later period than t'_* will lead to infeasibility. We can extend this observation when multiple components have different maintenance schedules under decisions v' and v''. Then, we can strengthen (2.12) as follows: when an infeasible maintenance decision v is obtained within Algorithm 1 at some iteration, we can generate a cover C as explained previously. Bearing in mind our observation, we define a set $E(C)$ depending on C as follows:

$$E(C) = \bigcup_{h \in \mathcal{H}'} \{(h,t) : t = t(h), t(h)+1, \ldots, |\bar{\mathcal{T}}| \text{ where } (h, t(h)) \in C\}. \tag{2.15}$$

We call a set $E(C)$ defined as in (2.15) an *extended cover* for $\hat{\mathcal{V}}$ if C is a cover. By using this set, we can obtain stronger cover inequalities than (2.12). We state our claim in Proposition 2.5.

Proposition 2.5 *Given a cover $C \subseteq N$, the following set of extended cover inequalities is valid and stronger than the set of cover inequalities given by* (2.12) *whenever $E(C) \setminus C \neq \emptyset$:*

$$\sum_{(h,t) \in E(C)} v_{ht} \leq |\mathcal{H}'| - 1. \tag{2.16}$$

Proof 2.5 *By using Proposition 2.2 and Proposition 2.4, we have the proof of validity. To prove the strength of* (2.16)*, suppose* $E(C) \setminus C \neq \emptyset$ *holds, then we have* $\sum_{(h,t)\in E(C)} v_{ht} \geq \sum_{(h,t)\in C} v_{ht}$ *since* $C \subsetneq E(C)$*. This completes the proof.*

Finally, we present our separation subroutine (Algorithm 2) within Algorithm 1.

Algorithm 2 `RepresentChance`

Input: $v, \mathcal{P} : v \to \mathbb{R}$.
Output: **true** if v is feasible w.r.t. (2.4b), **false** otherwise.
1: Compute $\mathcal{P}(v)$.
2: **if** $\mathcal{P}(v) \geq 1-\alpha$ **then**
3: **return true**
4: **else**
5: Generate and add the cover inequality of form (2.16) to set $\mathcal{C}$.
6: **return false**

2.4.2.2 Deterministic Safe Approximation

As an alternative representation of the joint chance-constraint (2.4b), we propose an SOCP-based safe approximation. The proposed safe approximation is an extension of the deterministic safe approximation of a single chance-constraint by Basciftci et al. (2018) by introducing two additional continuous variables and reformulating $\hat{\mathcal{V}}$ as a second-order conic set by lifting it to a higher-dimensional space.

Proposition 2.6 *The following system of equations provides a safe approximation of the joint chance-constrained set* $\hat{\mathcal{V}}$*, i.e., any maintenance decision* v *satisfying* (2.17) *and* (2.4c) *belongs to set* $\hat{\mathcal{V}}$*:*

$$\sum_{i\in\mathcal{G}} \sum_{t\in\bar{\mathcal{T}}} \mathbb{E}[\zeta_{it}] w_{it} \leq \rho_{\mathcal{G}}(1-\bar{\alpha}_{\mathcal{G}}) \tag{2.17a}$$

$$\sum_{(i,j)\in\mathcal{L}} \sum_{t\in\bar{\mathcal{T}}} \mathbb{E}[\zeta_{ijt}] z_{ijt} \leq \rho_{\mathcal{L}}(1-\bar{\alpha}_{\mathcal{L}}) \tag{2.17b}$$

$$\bar{\alpha}_{\mathcal{G}}\bar{\alpha}_{\mathcal{L}} \geq 1-\alpha \tag{2.17c}$$

$$\bar{\alpha}_{\mathcal{G}}, \bar{\alpha}_{\mathcal{L}} \in [0,1] \tag{2.17d}$$

Proof 2.6 *Consider* $\hat{\mathcal{V}}_S = \{(w,z) \in \mathcal{G}' \times \mathcal{L}' : (2.17), (2.4c)\}$*. Note that by the independence assumption, set* $\hat{\mathcal{V}}$ *is equivalent to:*

$$\hat{\mathcal{V}} = \{(w,z) \in \{0,1\}^{|\mathcal{G}'|\times|\mathcal{L}'|} :$$

$$\mathbb{P}(\sum_{i\in\mathcal{G}}\sum_{t\in\bar{\mathcal{T}}}\zeta_{it}w_{it}\leq\rho_{\mathcal{G}})\mathbb{P}(\sum_{i\in\mathcal{L}}\sum_{t\in\bar{\mathcal{T}}}\zeta_{ijt}z_{ijt}\leq\rho_{\mathcal{L}})\geq 1-\alpha,\ (2.4c)\}$$

To show that $\hat{\mathcal{V}}_S\subseteq\hat{\mathcal{V}}$*, we let* $(\tilde{w},\tilde{z})\in\hat{\mathcal{V}}_S$*. As proven in Basciftci et al. (2018), we have* $\mathbb{P}(\sum_{i\in\mathcal{G}}\sum_{t\in\bar{\mathcal{T}}}\zeta_{it}\tilde{w}_{it}\geq\rho_{\mathcal{G}})\leq\frac{\sum_{i\in\mathcal{G}}\sum_{t\in\bar{\mathcal{T}}}\mathbb{E}[\zeta_{it}]\tilde{w}_{it}}{\rho_{\mathcal{G}}}$*. By using* (2.17a)*, we obtain* $\mathbb{P}(\sum_{i\in\mathcal{G}}\sum_{t\in\bar{\mathcal{T}}}\zeta_{it}\tilde{w}_{it}\leq\rho_{\mathcal{G}})\geq\bar{\alpha}_{\mathcal{G}}$*. Similarly, we also have* $\mathbb{P}(\sum_{i\in\mathcal{L}}\sum_{t\in\bar{\mathcal{T}}}\zeta_{ijt}\tilde{z}_{ijt}\leq\rho_{\mathcal{L}})\geq\bar{\alpha}_{\mathcal{L}}$*. By combining these results with relations* (2.17c) *and* (2.17d)*, we have* $\mathbb{P}(\sum_{i\in\mathcal{G}}\sum_{t\in\bar{\mathcal{T}}}\zeta_{it}\tilde{w}_{it}\leq\rho_{\mathcal{G}})\mathbb{P}(\sum_{i\in\mathcal{L}}\sum_{t\in\bar{\mathcal{T}}}\zeta_{ijt}\tilde{z}_{ijt}\leq\rho_{\mathcal{L}})\geq 1-\alpha$ *proving that* $(\tilde{w},\tilde{z})\in\hat{\mathcal{V}}$*.*

In this formulation, the variables $\bar{\alpha}_{\mathcal{G}}$ and $\bar{\alpha}_{\mathcal{L}}$ are used to represent the probabilities in the joint chance-constraint (2.10). Inequalities (2.17a) and (2.17b) are affine and expectations are efficiently computable (since the random vector ζ consists of Bernoulli random variables), also (2.17c) is an SOCP constraint so that the proposed deterministic safe approximation of (2.1b) is convex and tractable. Note that this approximation may be too conservative in some cases entailing an early maintenance planning when α gets smaller.

2.4.3 Optimality Cut Families

In this section, we introduce various sets of optimality cuts which are generated by `OptimalityCut`(v,ξ,L) in Algorithm 1. In Section 2.4.3.1, we specify the well-known classical integer L-shaped optimality cuts introduced by Laporte & Louveaux (1993). We introduce new optimality cuts by strengthening the classical integer L-shaped optimality cuts in Section 2.4.3.2. We explain the rationale behind these optimality cuts in detail and provide the proofs of their validity and strength.

2.4.3.1 Integer L-Shaped Optimality Cuts

The idea of the integer L-shaped method is to approximate the expected recourse function by adding optimality cuts as the supporting hyperplanes of $\mathcal{Q}(v,\xi)$. These cuts depend on a given maintenance decision $v^{(r)}\in\hat{\mathcal{V}}$ at some iteration r and a realization of the random vector ξ, and gradually reduce the feasible region defined in the (v,θ)-space. We first introduce the index set at iteration r as $V_h(v^{(r)}):=\{t\in\bar{\mathcal{T}}:v_{ht}^{(r)}=1\}$ for every $h\in\mathcal{H}'$ and define $\mathcal{Q}(v^{(r)},\xi)$ as the expected second-stage value. Note that the set $V_h(v^{(r)})$ is a singleton by constraints (2.1c) and (2.1d). The

structure of the stochastic program with independent scenarios allows us to define multi-cuts. Given a feasible maintenance decision $v^{(r)} \in \hat{\mathcal{V}}$, the classical integer L-shaped optimality cut for subproblem k added to the master problem at the iteration r is defined as:

$$\theta^k \geq (\mathcal{Q}(v^{(r)},\xi_k) - L^k) \sum_{h\in\mathcal{H}'} \Big(\sum_{t\in V_h(v^{(r)})} (v_{ht}-1) - \sum_{t\notin V_h(v^{(r)})} v_{ht} \Big) + \mathcal{Q}(v^{(r)},\xi_k), \tag{2.18}$$

where L^k is a valid lower bound on the expected second-stage value of subproblem k. We can also obtain the single-cut version of the optimality cut by summing over all scenarios on both sides of the relation (2.18):

$$\sum_{k\in\mathcal{K}} \theta^k \geq \sum_{k\in\mathcal{K}} (\mathcal{Q}(v^{(r)},\xi_k) - L^k) \sum_{h\in\mathcal{H}'} \Big(\sum_{t\in V_h(v^{(r)})} (v_{ht}-1) - \sum_{t\notin V_h(v^{(r)})} v_{ht} \Big) + \sum_{k\in\mathcal{K}} \mathcal{Q}(v^{(r)},\xi_k). \tag{2.19}$$

For ease of notation, we will not carry the superscript (r) in the remainder of this section.

2.4.3.2 New Optimality Cuts

Next, we introduce a new set of optimality cuts by adapting the multi-cut version of the integer L-shaped optimality cut (2.18) to better approximate the expected recourse function $\mathcal{Q}$.

Proposition 2.7 *Given a feasible maintenance decision $v^* \in \hat{\mathcal{V}}$, the following set of optimality cuts is valid and stronger than the classical L-shaped optimality cut (2.18):*

$$\theta^k \geq (\mathcal{Q}(v^*,\xi_k) - L^k) \sum_{h\in\mathcal{H}'} \Big(\sum_{t\in V_h(v^*)} v_{ht} - 1 \Big) + \mathcal{Q}(v^*,\xi_k). \tag{2.20}$$

Proof 2.7 *Suppose we are given a maintenance decision $v^* \in \hat{\mathcal{V}}$. We consider the following quantity $Q_h := \sum_{t\in V_h(v^*)} v_{ht}$. If $Q_h = 1$ for every $h \in \mathcal{H}'$, then the cut in (2.20) becomes $\theta^k \geq \mathcal{Q}(v^*,\xi_k)$. If $Q_h = 0$ for some $h \in \mathcal{H}'$, then we have $\sum_{h\in\mathcal{H}'} Q_h - |\mathcal{H}'| \leq -1$. In this case, the optimality cut (2.20) becomes redundant since $\theta^k \geq L^k + A$ where $A \leq 0$. To prove the strength of the cut, we also consider the following quantity $\bar{Q}_h := \sum_{t\notin V_h(v^*)} v_{ht}$ such that $\bar{Q}_h \in \{0,1\}$ for every $h \in \mathcal{H}'$. Then, clearly we have $Q_h - \bar{Q}_h - |V_h(v^*)| \leq Q_h - |V_h(v^*)|$ for every $h \in \mathcal{H}'$. This implies that (2.20) is stronger than (2.18).*

We obtain the single-cut version of (2.20) by summing over all scenarios on both sides:

$$\sum_{k\in\mathcal{K}}\theta^k \geq \sum_{k\in\mathcal{K}}(\mathcal{Q}(v^*,\xi_k)-L^k)\sum_{h\in\mathcal{H}'}\Big(\sum_{t\in V_h(v^*)}v_{ht}-1\Big)+\sum_{k\in\mathcal{K}}\mathcal{Q}(v^*,\xi_k). \tag{2.21}$$

Next, we explain how to derive even stronger optimality cuts than (2.20). The key idea of deriving such optimality cuts is to identify a set of maintenance decisions which will yield the same operational cost. Given a maintenance decision $v^* \in \hat{\mathcal{V}}$, we introduce the set $R^k(v^*)$ as the set of all feasible maintenance decisions which will have the same second-stage value under scenario k:

$$R^k(v^*) = \{v \in \hat{\mathcal{V}} :\ \mathcal{Q}(v,\xi_k) = \mathcal{Q}(v^*,\xi_k)\}.$$

Further, we can define $\hat{\mathcal{T}}_h^k(v^*)$ as the set of maintenance period indices of each component h under scenario k such that maintaining component h in period t will yield to the same operational cost for every $t \in \hat{\mathcal{T}}_h^k(v^*)$:

$$\hat{\mathcal{T}}_h^k(v^*) = \{t \in \bar{\mathcal{T}} :\ \exists v \in R^k(v^*) \text{ such that } v_{ht} = 1\}.$$

Proposition 2.8 *Given a feasible maintenance decision $v^* \in \hat{\mathcal{V}}$, the following set of optimality cuts is valid and stronger than the set of optimality cuts given by* (2.20)*:*

$$\theta^k \geq (\mathcal{Q}(v^*,\xi_k)-L^k)\sum_{h\in\mathcal{H}'}\Big(\sum_{t\in\hat{\mathcal{T}}_h^k(v^*)}v_{ht}-1\Big)+\mathcal{Q}(v^*,\xi_k). \tag{2.22}$$

Proof 2.8 *Given a maintenance decision $v^* \in \hat{\mathcal{V}}$, consider the following quantity $Q_h := \sum_{t\in\hat{\mathcal{T}}_h^k(v^*)} v_{ht}$. By constraint* (2.4c)*, we know that $Q_h \in \{0,1\}$ for every $h \in \mathcal{H}'$, then the proof of validity follows as in Proposition 2.7. To prove the strength of the cut, let the maintenance decision of component h under v^* be in maintenance period t', which clearly implies that $t' \in \hat{\mathcal{T}}_h^k(v^*)$ for every $k \in \mathcal{K}$ and $V_h(v^*) = \{t'\}$. Then, we have the following relation $\sum_{t\in\hat{\mathcal{T}}_h^k(v^*)} v_{ht} \geq \sum_{t\in V_h(v^*)} v_{ht}$ since $V_h(v^*) \subseteq \hat{\mathcal{T}}_h^k(v^*)$ holds for every $k \in \mathcal{K}$. This implies that* (2.22) *is stronger than* (2.20)*.*

Given a maintenance decision $v^* \in \hat{\mathcal{V}}$, obtaining set $R^k(v^*)$ for every $k \in \mathcal{K}$ might be computationally expensive; however, in our setting, we can obtain a subset of $\hat{\mathcal{T}}_h^k(v^*)$ by identifying whether each component $h \in \mathcal{H}'$ enters predictive or corrective maintenance depending on decision v^* and the failure times under scenario k. In particular, if component h is scheduled for predictive maintenance under scenario k, we define this subset as the period that this component is scheduled for maintenance.

On the other hand, if component h enters corrective maintenance under scenario k, this subset consists of all maintenance periods from the failure time of component h to the end of the planning horizon.

Corollary 2.1 *Given $v^* \in \hat{\mathcal{V}}$ and a subset $\hat{\mathcal{T}}'(v^*) \subseteq \hat{\mathcal{T}}_h^k(v^*)$, the following set of optimality cuts is valid and stronger than the set of optimality cuts given by* (2.20)*:*

$$\theta^k \geq (\mathcal{Q}(v^*,\xi_k) - L^k) \sum_{h\in\mathcal{H}'} \Big(\sum_{t\in\hat{\mathcal{T}}'(v^*)} v_{ht} - 1 \Big) + \mathcal{Q}(v^*,\xi_k). \tag{2.23}$$

As before, we can obtain the single-cut version of (2.22) by summing over all scenarios on both sides:

$$\sum_{k\in\mathcal{K}} \theta^k \geq \sum_{k\in\mathcal{K}} (\mathcal{Q}(v^*,\xi_k) - L^k) \sum_{h\in\mathcal{H}'} \Big(\sum_{t\in\hat{\mathcal{T}}_h^k(v^*)} v_{ht} - 1 \Big) + \sum_{k\in\mathcal{K}} \mathcal{Q}(v^*,\xi_k). \tag{2.24}$$

Next, we explain how to derive a different set of optimality cuts by exploiting the status idea (explained in Section 2.4.1). We first provide an overview of the idea on how to derive these alternative optimality cuts. After obtaining a maintenance decision by solving (2.8), we observe that there is no coupling constraint between maintenance periods in scenario subproblems. This allows us to obtain even smaller subproblems by decomposing with respect to independent maintenance periods. We refer to this property as time-decomposability of scenario subproblems before and the formulation of these subproblems are introduced in (2.7). By using this property, we can rewrite (2.20) in the following form:

$$\theta_t^k \geq (\mathcal{Q}_t(v^*,\xi_k) - L_t^k) \sum_{h\in\mathcal{H}'} \Big(\sum_{t\in V_h(v^*)} v_{ht} - 1 \Big) + \mathcal{Q}_t(v^*,\xi_k). \tag{2.25}$$

Recall that given a maintenance decision v^*, we define the status vector for maintenance period t, denoted by $u_t^k(v^*)$, representing the availability of all components under scenario k. This property allows us to represent each scenario subproblem with respect to their status vectors and as a consequence, we restrict ourselves to the scenario subproblems such that corresponding status vectors are all unique. Given a maintenance decision v^*, we first define $\tilde{\mathcal{T}}_{ht}^k(v^*)$ as the set of periods such that maintaining a component h in period t will yield the same status $u_{ht}^k(v^*)$ under scenario k:

$$\tilde{\mathcal{T}}_{ht}^k(v^*) := \Big\{ t' \in \bar{\mathcal{T}} : \exists v \in \hat{\mathcal{V}} \text{ such that } v_{ht'} = 1,\ u_{ht}^k(v^*) = u_{ht}^k(v) \Big\}.$$

After identifying the status for component $h \in \mathcal{H}'$ in maintenance period $t \in \bar{\mathcal{T}}$ (explained in Section 2.4.1), we can easily obtain a subset of $\tilde{\mathcal{T}}^k_{ht}(v^*)$ under each scenario $k \in \mathcal{K}$.

Proposition 2.9 *Given a feasible maintenance decision $v^* \in \hat{\mathcal{V}}$, the following set of optimality cuts is valid:*

$$\theta^k_t \geq (\mathcal{Q}_t(v^*, \xi_k) - L^k_t) \sum_{h \in \mathcal{H}'} \Big(\sum_{t' \in \tilde{\mathcal{T}}^k_{ht}(v^*)} v_{ht'} - 1 \Big) + \mathcal{Q}_t(v^*, \xi_k). \tag{2.26}$$

Proof 2.9 *The proof of validity is similar as in Proposition 2.8.*

Corollary 2.2 *Given $v^* \in \hat{\mathcal{V}}$ and a subset $\tilde{\mathcal{T}}'(v^*) \subseteq \tilde{\mathcal{T}}^k_{ht}(v^*)$, the following set of optimality cuts is valid:*

$$\theta^k_t \geq (\mathcal{Q}_t(v^*, \xi_k) - L^k_t) \sum_{h \in \mathcal{H}'} \Big(\sum_{t' \in \tilde{\mathcal{T}}'(v^*)} v_{ht'} - 1 \Big) + \mathcal{Q}_t(v^*, \xi_k). \tag{2.27}$$

Remark 2.2 *The set of optimality cuts in 2.26 neither dominates nor is dominated by the set of optimality cuts in 2.22. Nevertheless, 2.26 is at least as strong as 2.22 if $\sum_{t \in \mathcal{T}} L^k_t = L^k$ for every $k \in \mathcal{K}$. We compare the computational times obtained by these optimality cuts over an illustrative small instance. Our results indicate that 2.26 is empirically better than 2.22, which is evident from Table 2.3.*

We conclude this section by proving the property of finite convergence of our decomposition algorithm (Algorithm 1).

Proposition 2.10 *Algorithm 1 converges in finitely many iterations.*

Proof 2.10 *We observe that there are only finitely many feasible first-stage decisions since each maintenance decision is pure binary. In view of this observation and the integer L-shaped algorithm, when the safe approximation of the joint chance-constraint is used, we can add finitely many optimality cuts that lead to the convergence of Algorithm 1 in finitely many iterations. When the exact representation of the joint chance-constraint is used, we can add a finite number of violated cover inequalities that can be identified through Algorithm 2 since this constraint includes only the first-stage decisions.*

2.4.4 Flow Limit Analysis

Optimization problems in power systems may involve redundant transmission flow limits. When this redundancy is identified and handled efficiently, computational requirements for solving the optimization problem may potentially decrease. Given a power demand vector $\bar{d}$, the following relaxation of the operational subproblem can be used to identify such redundancy:

$$\max_{f,y,x,\delta,p,q,d} \; f^*_{i',j'}(\bar{d}) \tag{2.28a}$$

$$\text{s.t. } q_i \le d_i \le \bar{d}_i \qquad i \in \mathcal{B} \tag{2.28b}$$

$$\sum_{i' \in \mathcal{G}(i)} p_{i'} + q_i - d_i = \sum_{j \in \delta^+(i)} f_{ij} - \sum_{j \in \delta^-(i)} f_{ji} \qquad i \in \mathcal{B} \tag{2.28c}$$

$$B_{ij}(\delta_i - \delta_j) = f_{ij} \qquad (i,j) \in \mathcal{L}'' \tag{2.28d}$$

$$\begin{aligned} B_{ij}(\delta_i - \delta_j) - M_{ij}(1 - y_{ij}) &\le f_{ij} \\ \le B_{ij}(\delta_i - \delta_j) + M_{ij}(1 - y_{ij}) & \qquad (i,j) \in \mathcal{L}' \end{aligned} \tag{2.28e}$$

$$-\bar{f}_{ij} y_{ij} \le f_{ij} \le \bar{f}_{ij} y_{ij} \qquad (i,j) \in \mathcal{L}' \tag{2.28f}$$

$$p_i^{min} x_i \le p_i \le p_i^{max} x_i \qquad i \in \mathcal{G} \tag{2.28g}$$

$$y \in [0,1]^{|\mathcal{L}'|},\; x \in [0,1]^{|\mathcal{G}|}, \delta \in [\delta^{\min}, \delta^{\max}], q \ge 0. \tag{2.28h}$$

In this formulation, the decision variables f, y, x, p, δ, q represent power flow, switching status of transmission lines, commitment status and power generation of generators, voltage angle and demand curtailment of buses, respectively. We also define another continuous decision variable d_i which represents power demand for $i \in \mathcal{B}$. Constraint (2.28b) ensures that d_i remains feasible for the operational subproblems. The remaining constraints are operational constraints implied by the power network. We note that (2.28) is a relaxation of the original operational problem, since switching variables are considered as continuous and start-up, shut-down restrictions are omitted by focusing the analysis on a single period.

Recently, Basciftci et al. (2018) solve a relaxation of the operational subproblem to identify redundant flow limits by considering the peak demand of each bus within the planning horizon. Their model (referred to as *FlowModel-I* in this thesis) is similar to (2.28) when $\bar{d} = [\max_{t \in \mathcal{T}, s \in \mathcal{S}} \{d_{its}\}; i \in \mathcal{B}]$. By utilizing the time-decomposability of operational subproblems, we improve their model (referred to as *FlowModel-II*) by replacing $\bar{d}$ with $\bar{d}_t = [\max_{s \in \mathcal{S}} \{d_{its}\}; i \in \mathcal{B}]$ and solve (2.28) for every $t \in \mathcal{T}$. Similarly, we can easily improve this model (referred to as *FlowModel-III*) by replacing $\bar{d}$ with the actual power demand in hourly subperiod s of maintenance period t, that is, $\bar{d}_{ts} = [d_{its}; i \in \mathcal{B}]$ and solve (2.28) for every $t \in \mathcal{T}$ and $s \in \mathcal{S}$. Given a transmission line (i', j') and power demand $\bar{d}$, suppose we solve the linear program (2.28) and obtain an optimal solution $f^*_{i'j'}(\bar{d})$. If $f^*_{i'j'}(\bar{d})$ is strictly less than $\bar{f}_{i'j'}$, we ensure

that flow upper limit corresponding for transmission line (i', j') will not be violated which allows us to eliminate the corresponding constraint from the optimization model (2.1). Otherwise, we impose this constraint for transmission line (i', j'). Similarly, we can also identify redundant lower flow limits by changing the objective function of (2.28) with $-f_{i'j'}(\bar{d})$. To this end, the number of constraints that can be eliminated depending on the choice of the demand parameter, and how many times the corresponding model is solved.

2.4.5 Sample Average Approximation

Since the number of scenarios of our stochastic program grows exponentially fast in the number of system components considered for maintenance, i.e., $|\bar{\mathcal{T}}|^{|\mathcal{H}'|}$, solving this program becomes computationally more demanding as the instance size increases. Thus, we solve this problem using the SAA algorithm (Algorithm 3). In our setting, the set of training scenarios are generated over the components $\mathcal{H}'$, whereas the set of test scenarios are generated over the all set of components $\mathcal{H}$ to evaluate the true performance of the proposed approach. We first generate SAA replications of size M, each consisting of independent and identically distributed (i.i.d.) failure scenarios of size N. We solve the corresponding SAA problem for each replicate and obtain their optimal values and ϵ-optimal solutions. By averaging these optimal values, we obtain the mean estimate for the true lower bound. We later evaluate each ϵ-optimal solution over a sample size of N' with $N' \gg N$ and choose the best candidate solution among all ϵ-optimal solutions by setting the corresponding objective value as the best upper bound estimate. In Step 8 and Step 10 of Algorithm 3, we construct the upper and lower statistical bounds, developed by Mak, Morton & Wood (1999), to assess the quality of the optimal solution produced by the SAA algorithm, respectively. These statistical bounds are used to construct confidence intervals (CIs) for estimating the optimality gap between the optimal value produced by Algorithm 3 and the optimal value of the true problem.

2.5 Computational Experiments

Algorithm 3 SAA

1: Generate an i.i.d. failure scenario sample of size N' considering all system components $\mathcal{H}$.
2: **for all** $i = 1, \ldots, M$ **do**
3: Generate an i.i.d. failure scenario sample of size N considering all system components $\mathcal{H}'$.
4: Solve $\hat{z}_N^i = \min\left\{\frac{1}{N}\sum_{k\in\mathcal{K}}\pi^k\left(c_k^\top v + \sum_{t\in\mathcal{T}}\mathcal{Q}_t(v,\xi_k)\right) : v \in \hat{\mathcal{V}}\right\}$ using Algorithm 1 and obtain ϵ-optimal solution $\hat{v}_N^i$.
5: Evaluate $\hat{v}_N^i$ over N' scenarios: $\hat{z}_{N'}^i(\hat{v}_N^i) = \frac{1}{N'}\sum_{k=1}^{N'}\pi^k(c_k^\top\hat{v}_N^i + \sum_{t\in\mathcal{T}}\mathcal{Q}_t(\hat{v}_N^i,\xi_k))$.
6: Select the best candidate solution $\hat{v}^* \in \arg\min\{\hat{z}_{N'}^1(\hat{v}_N^1), \ldots, \hat{z}_{N'}^M(\hat{v}_N^M)\}$ and the best upper bound estimate $\hat{\mu}_U = \hat{z}_{N'}(\hat{v}^*)$.
7: Calculate the variance estimate of the true upper bound estimate:

$$\hat{\sigma}_U^2 = \frac{1}{N'(N'-1)}\sum_{k=1}^{N'}\left(\left(c_k^\top\hat{v}^* + \sum_{t\in\mathcal{T}}\mathcal{Q}_t(\hat{v}^*,\xi_k)\right) - \hat{\mu}_U\right)^2.$$

8: Construct the approximate $(1-\alpha)$ level CI for the upper bound estimate as $\hat{\mu}_U \pm z_{\alpha/2}\hat{\sigma}_U$.
9: Calculate the mean and variance estimates of the true lower bound estimate as $\hat{\mu}_L$ and $\hat{\sigma}_L^2$ as:

$$\hat{\mu}_L = \frac{1}{M}\sum_{i=1}^{M}\hat{z}_N^i \quad \text{and} \quad \hat{\sigma}_L^2 = \frac{1}{M(M-1)}\sum_{i=1}^{M}\left(\hat{z}_N^i - \hat{\mu}_L\right)^2.$$

10: Construct the approximate $(1-\alpha)$ level CI for the lower bound estimate as $\hat{\mu}_L \pm t_{\alpha/2,M-1}\hat{\sigma}_L$.
11: Construct the approximate $(1-\alpha)$ level CI for the true objective value as $(\hat{\mu}_L - t_{\alpha/2,M-1}\hat{\sigma}_L,\ \hat{\mu}_U + z_{\alpha/2}\hat{\sigma}_U)$.

To demonstrate the computational performance and efficiency of the proposed algorithm, we conduct an extensive computational study on various modified IEEE instances from MATPOWER (Zimmerman, Murillo-Sánchez & Thomas, 2011). In Section 2.5.1, we explain the experimental setup in detail. In Section 2.5.2, we show the computational efficiency of our algorithmic enhancements and sets of optimality cuts with parallelization in comparison with the state-of-the-art solver `GUROBI`. We provide the statistical results on the true optimal value produced by the SAA algorithm with different sizes of failure scenarios in Section 2.5.3. We evaluate the quality of the maintenance schedules obtained by the proposed stochastic models in Section 2.5.4. Lastly, we investigate the effects of the cardinality of the sets $\mathcal{G}'$ and $\mathcal{L}'$ in Section 2.5.5.

2.5.1 Experimental Setup

2.5.1.1 Instance Creation

For our joint chance-constrained stochastic program model, we consider a one-week planning period with daily maintenance decisions and hourly operational decisions. The planning horizon starts on a Monday at $00:00$. We obtain the weekly electricity consumption data available from the U.S. Energy Information Administration (EIA, 2020) since actual power demand parameters in standard IEEE instances are given for an hourly period for each bus. We later use this data to generate a new power demand dataset through normalization such that $\{d_{its}; t \in \mathcal{T}, s \in \mathcal{S}\}$ follows a similar trend for every $i \in \mathcal{B}$. Since corrective maintenance is undesirable and unexpected, it is more expensive and takes longer amount of time compared to predictive maintenance. Specifically, we assume that the maintenance durations are $\tau^p_{\mathcal{G}} = \tau^p_{\mathcal{L}} = 1$ and $\tau^c_{\mathcal{G}} = \tau^c_{\mathcal{L}} = 2$ days. We also assume that maintenance cost for generators is a function of generation cost and generation capacity. In particular, we let $C^p_i = \bar{p}_i c_i |\mathcal{S}|$ for $i \in \mathcal{G}$. Additionally, we let $C^c_i = 3C^p_i$ for $i \in \mathcal{G}$, $C^p_{ij} = 0.1 \sum_{i \in G} C^p_i / |\mathcal{G}|$ and $C^c_{ij} = 3C^p_{ij}$ for $(i,j) \in \mathcal{L}$. We have chosen the constant M_{ij} sufficiently large for $(i,j) \in \mathcal{L}'$ such that constraint (2.1l) becomes redundant when $y^k_{ijts} = 1$. In particular, we let $M_{ij} = B_{ij}(\delta^{\max}_i - \delta^{\min}_j)$ for $(i,j) \in \mathcal{L}'$ (e.g., see Fisher, O'Neill & Ferris (2008)). We choose the probability thresholds $p^{\mathcal{G}}_{fail} = 0.1$ and $p^{\mathcal{L}}_{fail} = 0.2$ for generators and transmission lines, respectively. We then identify those system components prone to failure within the planning horizon as explained in Section 2.3.1. For the computational experiments subject to the joint chance-constraint (2.4b), the thresholds $\rho_{\mathcal{G}}$ and $\rho_{\mathcal{L}}$ are set to 1 and $\max\{1, \lfloor |\mathcal{L}|/20 \rfloor\}$, respectively. These experiments are conducted with a probability level $\alpha = 0.1$ of the joint chance-constraint. We report the cardinality of the subsets of $\mathcal{G}$ and $\mathcal{L}$, and the threshold parameters of the joint chance-constraint for each instance in Table 2.2.

	$\lvert\mathcal{G}'\rvert$	$\lvert\mathcal{G}''\rvert$	$\lvert\mathcal{L}'\rvert$	$\lvert\mathcal{L}''\rvert$	$\rho_{\mathcal{G}}$	$\rho_{\mathcal{L}}$
9-bus	1	2	3	6	1	1
39-bus	4	6	4	42	1	2
57-bus	2	5	7	73	1	4
118-bus	4	15	9	177	1	9

Table 2.2 Cardinality of Sets and Threshold Parameters.

We generate a dataset consisting of unique degradation signals due to the lack of publicly available data to estimate the parameters of the prior distributions of υ_h and β_h for $h \in \mathcal{H}$. In power systems, it is realistic to assume that generators are more likely to fail than transmission lines (see, for example, Papavasiliou et al. (2015)). Thus, we follow this assumption with our dataset. For simplicity, we assume that the variance of υ_h and β_h are indeed known and held constant over the planning horizon for $h \in \mathcal{H}$. Therefore, we are only interested in estimating the prior mean of υ_h and β_h, denoted by μ_0 and μ_1, respectively. First, we focus on estimating μ_0 and μ_1 among the set of generators. For that purpose, we generate 100 unique degradation signals. Let us label these degradation signals with an index j where $j = 1, \ldots, 100$. We assume that degradation signal j has the functional form (2.2) with $\upsilon_j \sim \mathcal{N}(20, 10^2)$ and $\beta_j \sim \mathcal{N}(5, 0.3^2)$ and $\sigma_j = 3$ for $j = 1, \ldots, 100$. The degradation signal threshold Λ is set to 100. We observe degradation signal j at discrete time points until a failure time $\xi_j = \{t : D_j(t) \geq 100,\ t \geq 0\}$ for $j = 1, \ldots, 100$. We remind the reader that D_j^i is defined as the increment of degradation signals between times t_j^i and t_j^{i-1} for $i = 2, \ldots, \xi_j$ where $D_j^1 = D_j(1)$, for $j = 1, \ldots, 100$. We find the point estimate of μ_0 with $\sum_{j=1}^{100} D_j^1/100$. To obtain the point estimate of μ_1, we first compute the prior mean estimate of β_j as $\hat{\mu}_j = (\sum_{i=1}^{\xi_j} D_j^i - D_j^1)/\xi_j$ for $j = 1, \ldots, 100$. Then, we find the point estimate of μ_1 with $\sum_{j=1}^{100} \hat{\mu}_j/100$. Eventually, we obtain the prior mean estimate among the set of generators. Secondly, to estimate μ_0 and μ_1 among the set of transmission lines, we follow a similar procedure after generating 100 unique degradation signals with $\upsilon_j \sim \mathcal{N}(15, 5^2)$ and $\beta_j \sim \mathcal{N}(3, 0.3^2)$ and $\sigma_j = 1$ for $j = 1, \ldots, 100$. Finally, we obtain the prior mean estimates of the stochastic parameters υ_h and β_h of the degradation signal model for every $h \in \mathcal{H}$.

Next, we obtain the posterior distribution of the unknown parameters of υ_h and β_h for $h \in \mathcal{H}$ with a Bayesian approach given the recently observed real-time condition-based information. For that purpose, we generate 100 unique degradation signals with a random initial signal amplitude. For the sake of easier modeling, we assume that these degradation signals were observed at some random discrete times. We further assume that random observation time t_h^k for component h follows a uniform distribution on $[1, (\Lambda - \mu_0)/(\mu_1 + 3\kappa_1)]$. This assumption implies that degradation signal for component $h \in \mathcal{H}$ was observed when it had been drastically degrading with a gradual linear drift. Under these assumptions, we obtain the posterior mean of the drift parameter β_h of form (2.3), which easily yields us to identify the RLD of each component $h \in \mathcal{H}$ (Proposition 2.1). Consequently, we select set $\mathcal{H}'$ by means of RLDs as discussed in Section 2.3.1.

2.5.1.2 Computational Setup

The code for each algorithm is written in Python using Spyder IDE. We use a 64-bit computer with Intel Xeon W-2255 CPU with a 2.20 GHz processor and 32 GB of memory space, running on the Windows operating system. The Gurobi Optimizer (`GUROBI`) is used to solve the pure binary integer first-stage problem (2.5) and the mixed-integer operational subproblems (2.6). To benefit from the decomposition of the operational subproblems throughout the implementation, we employ Joblib library for parallel computing. We use PoissonBinomial library (PyPI, 2020) as our probability oracle. We allow `GUROBI` to use 20 threads for solving (2.5), however, we set the number of parallel threads parameter `Threads` to 1 for solving (2.6) when using parallelization. We use the relative optimality gap, $\%(UB - LB)/UB$, as a stopping criteria within Algorithm 1. For each computational experiment, the relative optimality gap tolerance `MIPGap` is chosen as the same as the tolerance parameter ϵ of Algorithm 1. Time limit for all experiments is set to 6 hours. The wall-clock time for computational experiments is measured in seconds. Note that each operational subproblem is solved to optimality within the tolerance ϵ.

2.5.2 Performance of the Proposed Algorithm

In this section, we illustrate the computational efficiency of the proposed algorithm from three aspects. We first benchmark the performance of the proposed optimality cuts and algorithmic enhancements against the standard integer L-shaped optimality cut and the state-of-the-art solver `GUROBI` for different sizes of failure scenarios under exact and approximate representations of the joint chance-constraint. Secondly, we present the speedup of the proposed algorithm gained from parallel computing. We conclude this section by comparing the performance of each $FlowModel$ used for transmission line flow analysis over different instances.

2.5.2.1 Benchmark of the Proposed Algorithm

We derive different sets of optimality cuts based on the integer L-shaped optimality cuts (Section 2.4.3) and introduce various algorithmic enhancements such as time-decomposability of scenario subproblems and status of system components (Section

	$\|\mathcal{K}\|$	intLS	optCut	optCut$_+$	intLS*	optCut*	optCut$^*_{++}$	GUROBI	Speedup
	50	2222.29	2139.21	871.66	232.13	123.04	11.29	2576.07	×228.27
SP_{exact}	100	4184.08	4025.15	1884.74	400.89	256.71	18.00	5311.97	×295.04
	200	8165.64	7971.17	4235.76	772.62	604.62	29.30	16488.76	×562.73
	50	334.07	334.70	350.69	11.85	12.36	9.30	576.33	×61.99
SP_{safe}	100	639.34	637.40	766.17	18.63	17.83	12.36	2007.75	×162.45
	200	1268.76	1270.58	1879.29	28.23	29.63	19.02	6155.00	×323.65

Table 2.3 Computational Times for the 9-bus Instance.

2.4.1). By using both the exact representation (referred to as SP_{exact}) and the SOCP-based safe approximation (referred to as SP_{safe}) of the joint chance-constraint, we compare them against each other over the illustrative 9-bus instance under failure scenarios of size $50, 100$ and 200. When using GUROBI for SP_{exact}, we first relax our optimization model by removing the joint chance-constraint and obtain a solution within the time limit. Then, we check the feasibility status of this solution with respect to the joint chance-constraint with Algorithm 2. When this solution is feasible, we conclude that it is indeed optimal. Otherwise, we discard this solution from the set of feasible solutions by adding (2.16) to our optimization model and resolve it by GUROBI. We investigate the differences between these optimality cuts and algorithmic enhancements by setting the tolerance parameter ϵ to 10^{-2}. Our computational results are shown in Table 2.3 for the following cases of Algorithm 1:

- intLS: The set of classical integer L-shaped optimality cuts in (2.19).
- optCut: The set of improved optimality cuts in (2.21).
- optCut$_+$: The set of improved optimality cuts in (2.24).
- intLS*: The set of classical integer L-shaped optimality cuts in (2.19) with time-decomposability of scenario subproblems and status of system components.
- optCut*: The set of improved optimality cuts in (2.21) with time-decomposability of scenario subproblems and status of system components.
- optCut$^*_{++}$: The set of improved optimality cuts in (2.26) with time-decomposability of scenario subproblems and status of system components.
- GUROBI: The state-of-the-art solver GUROBI.

The "Speedup" column represents the speedup of $\texttt{optCut}^*_{++}$ against GUROBI. For each scenario size, GUROBI is able to provide a feasible solution within the time limit; however, its computational time is even larger than intLS. For SP_{exact}, the computational times under intLS and optCut increase linearly with the size of scenarios whereas $\texttt{optCut}_+$ reduces these computational times almost by half. Surprisingly for SP_{safe}, intLS and optCut outperform $\texttt{optCut}_+$ under different sets of scenarios. The time-decomposability of scenario subproblems and status of system components provide the most computational gain in both SP_{exact} and SP_{safe} as these algorithmic enhancements prevent many unnecessary resolves of scenario subproblems within Algorithm 1. Under these enhancements, $\texttt{optCut}^*_{++}$ outperforms $\texttt{intLS}^*$ and $\texttt{optCut}^*$ for both exact and safe approaches. We observe that speedup gains for SP_{exact} are more than for SP_{safe} as the feasible region induced by the joint chance-constraint is smaller in the latter, which reduces the effects of the optimality cuts. Still, $\texttt{optCut}^*_{++}$ provides a substantial speedup compared to GUROBI for both SP_{exact} and SP_{safe}.

Based on our preliminary computations of the SAA method, we observe that we can obtain maintenance and operational schedules within 2% optimality under failure scenarios of size 50 and 100 (see Section 2.5.3). We extend our computational study for all IEEE instances by setting the tolerance parameter ϵ to 10^{-4}. In Table 2.4, we investigate the computational efficiency of $\texttt{optCut}^*_{++}$ against GUROBI by reporting the following metrics:

- # Iter: The number of iterations within Algorithm 1.
- Time: The time for solving the joint chance-constrained stochastic program in seconds.
- Gap: The percentage relative optimality gap obtained within the 6-hour time limit.

		SP_{exact}					SP_{safe}				
		$\texttt{optCut}^*_{++}$			GUROBI		$\texttt{optCut}^*_{++}$			GUROBI	
	$\lvert\mathcal{K}\rvert$	# Iter	Time	Gap	Time	Gap	# Iter	Time	Gap	Time	Gap
9-bus	50	30	11.29	0.00	TL	0.08	21	10.02	0.00	736.25	0.00
	100	31	18.00	0.00	TL	0.12	21	13.30	0.00	2931.43	0.01
39-bus	50	311	3610.20	0.00	TL	6.44	75	506.32	0.00	TL	0.72
	100	348	7334.40	0.00	TL	30.63	73	598.75	0.00	TL	7.59
57-bus	50	329	2509.55	0.00	TL	0.24	393	2110.02	0.00	TL	0.07
	100	364	7708.44	0.01	TL	0.29	386	3889.33	0.01	TL	0.16
118-bus	50	90	TL	3.80	TL	69.88	699	TL	0.79	TL	5.33
	100	78	TL	4.35	TL	NA	580	TL	1.55	TL	NA

Table 2.4 Comparison of $\texttt{optCut}^*_{++}$ with GUROBI for Different Instances.

The "TL" (under column "Time") is used whenever the 6-hour time limit is reached. The "NA" (under column "Gap") is used if no feasible solution is found within the time limit. According to Table 2.4, $\texttt{optCut}^*_{++}$ and GUROBI produce an optimal solution within the time limit for the 9-bus instance under SP_{safe}; however, $\texttt{optCut}^*_{++}$ attains these solutions in less than 20 seconds whereas the computational time of GUROBI rapidly increases when 100 failure scenarios are used. For all instances, $\texttt{optCut}^*_{++}$ outperforms GUROBI in terms of the percentage relative optimality gap. For the 118-bus instance, GUROBI fails to produce a feasible solution within the time limit under scenario size of 100 whereas $\texttt{optCut}^*_{++}$ produces a feasible solution for both SP_{exact} and SP_{safe}. Our computational study shows that $\texttt{optCut}^*_{++}$ has significant computational gains compared to GUROBI under both SP_{exact} and SP_{safe}, and can be used to produce high-quality feasible solutions for large-scale instances.

2.5.2.2 Parallel Computing

A significant property of Algorithm 1 is that the linear relaxations (Step 2) and the second-stage problems (Step 20) can be solved in parallel. In order to demonstrate the effect of parallelism within Algorithm 1, we solve the 9-bus instance with a scenario size of 1000 by using the exact reformulation of the joint chance-constraint. The results of our computational experiment are presented in Figure 2.2 with respect to different number of threads.

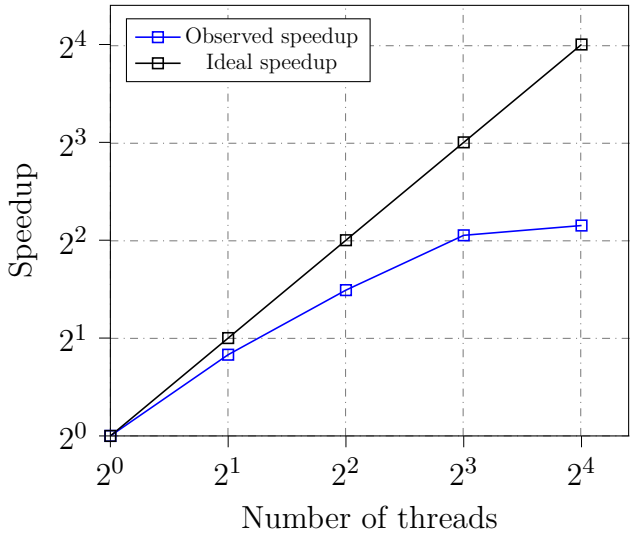

Figure 2.2 Speedup ratios with parallel computing.

Our empirical study indicates a sublinear growth in the parallel speedup ratios. We

note that the data size of 9-bus instance is relatively small and the results are only representative, nevertheless, the utilization of the parallel computing becomes more apparent as the size of the problem increases.

2.5.2.3 Flow Limit Analysis

As a preprocessing step for Algorithm 1, we identify the redundancy in constraints (2.1m) as explained in Section 2.4.4. We summarize the computational results in Table 2.5 by reporting the following metrics:

- Time: The preprocessing time in seconds.
- UB: The redundancy ratio in the upper bound flow constraints.
- LB: The redundancy ratio in the lower bound flow constraints.

We note that we do not report 57-bus instance in Table 2.5 since all upper and lower flow limits are redundant. The redundancy ratios under UB and LB columns are given as follows:

- The redundancy ratio over $|\mathcal{L}''|$ in *FlowModel-I*.
- The redundancy ratio over $|\mathcal{L}''| \times |\mathcal{T}|$ in *FlowModel-II*.
- The redundancy ratio over $|\mathcal{L}''| \times |\mathcal{T}| \times |\mathcal{S}|$ in *FlowModel-III*.

	9-bus			39-bus			118-bus		
	UB	LB	Time	UB	LB	Time	UB	LB	Time
FlowModel-I	0.500	0.333	0.011	0.476	0.548	0.114	0.819	0.819	3.541
FlowModel-II	0.500	0.476	0.035	0.514	0.548	0.740	0.819	0.822	24.432
FlowModel-III	0.602	0.640	0.593	0.560	0.548	17.650	0.831	0.832	574.311

Table 2.5 Flow Limit Analysis.

Each *FlowModel* identifies redundacy less than a second for the 9-bus instance whereas the differences between the preprocessing times become more evident as the instance size increases. For 39-bus and 118-bus instances, the differences between the redundancy ratios given by *FlowModel-I* and *FlowModel-II* remain almost identical. Thus, one can potentially consider the trade-off between the computational effort and redundancy in the choice of *FlowModel*. As instance size increases, the

difference between the redundancy ratios tends to decrease. Still, our computational results show that *FlowModel-III* provides the best ratio within a reasonable time limit for all instances. Therefore, we use *FlowModel-III* to identify such redundant flow limits in the remainder of our computational experiments.

2.5.3 Sample Average Approximation Results

In this section, we present our computational results by solving the SAA problems of the joint chance-constrained stochastic program by evaluating the obtained solutions through Algorithm 3. For that purpose, we let $M = 5$, $N' = 1000$, $N = 50$ and $N = 100$ with significance level of 0.05 of the SAA algorithm. We generate i.i.d. samples for each replicate and solve them with Algorithm 1 for various IEEE test instances. We remind the readers that the training scenarios are generated over the set of components $\mathcal{H}'$ whereas solutions are evaluated over the failure possibilities of all components $\mathcal{H}$. The resulting 95% CIs for the lower and upper bound estimates (in 100.000$) are presented in Table 2.6. We also report the estimated optimality gaps between the optimal value associated with the candidate optimal solutions produced by the SAA method and the true optimal value in Table 2.6.

		SP_{exact}			SP_{safe}		
	$\|\mathcal{K}\|$	CI of LB	CI of UB	Gap (%)	CI of LB	CI of UB	Gap (%)
9-bus	50	(1.61, 1.64)	(1.63, 1.64)	2.30	(1.64, 1.67)	(1.66, 1.67)	2.03
	100	(1.63, 1.64)	(1.63, 1.64)	1.17	(1.64, 1.66)	(1.66, 1.67)	1.65
39-bus	50	(31.50, 31.80)	(31.69, 31.88)	1.21	(36.29, 36.41)	(36.39, 36.47)	0.48
	100	(31.65, 31.88)	(31.69, 31.89)	0.72	(36.32, 36.38)	(36.39, 36.47)	0.41
57-bus	50	(36.63, 36.79)	(36.91, 37.02)	1.07	(36.72, 36.83)	(36.97, 37.08)	0.98
	100	(36.67, 36.78)	(36.90, 37.02)	0.95	(36.74, 36.85)	(36.97, 37.08)	0.93
118-bus	50	(5.48, 5.52)	(5.53, 5.55)	1.22	(5.49, 5.52)	(5.53, 5.55)	1.12
	100	(5.50, 5.52)	(5.53, 5.55)	0.86	(5.49, 5.51)	(5.53, 5.55)	1.10

Table 2.6 SAA Results.

According to Table 2.6, the estimated gap decreases as the size of scenarios increases for all instances, as expected. For the 9-bus instance, the scenario size of 100 reduces the estimated gap significantly compared to the scenario size of 50 whereas this reduction is less significant in other instances. Additionally, the estimated confidence intervals are almost identical for the 118-bus instance for both SP_{exact} and SP_{safe}. The results of our computational study indicate that these sample sizes along with the choice of the system components considered for maintenance are indeed large

enough to obtain the corresponding tight bounds on the true optimal value of our optimization model.

2.5.4 Model Comparison

In this section, we evaluate the quality of the maintenance schedules obtained from the proposed stochastic models, SP_{exact} and SP_{safe}, in terms of the average failures of system components, maintenance and operational costs under 50 failure scenarios. In order to quantify the effects of these schedules when the unexpected failures are not considered, we compare the maintenance schedules of SP_{exact} and SP_{safe} with those of a deterministic model (DM), which assumes that none of the system components will fail within the planning horizon. We evaluate each maintenance schedule over failure scenarios of size 1000 and report the average failures in Table 2.7.

		$\mathcal{G}'$			$\mathcal{L}'$			$\mathcal{G}'' \cup \mathcal{L}''$			JCC-Violation		
	$(\lvert\mathcal{G}'\rvert, \lvert\mathcal{L}'\rvert)$	SP_{exact}	SP_{safe}	DM	SP_{exact}	SP_{safe}	DM	SP_{exact}	SP_{safe}	DM	SP_{exact}	SP_{safe}	DM
9-bus	$(1,3)$	0.014	0.014	1.000	0.254	0.000	1.390	0.043			0.000	0.000	0.417
39-bus	$(4,4)$	0.559	0.022	3.075	0.335	0.000	3.950	0.095			0.097	0.003	1.000
57-bus	$(2,7)$	0.010	0.010	1.894	0.190	0.000	6.067	0.259			0.000	0.000	0.999
118-bus	$(4,9)$	0.064	0.062	3.798	0.340	0.091	6.776	0.124			0.006	0.006	1.000

Table 2.7 Average Failures under Stochastic and Deterministic Models.

The "JCC-Violation" column represents the total number of joint chance-constraint violations under different maintenance plans by evaluating the number of components entering corrective maintenance under each scenario against the desired thresholds. For all instances, these violations are less than the probability level of the joint chance-constraint for both SP_{exact} and SP_{safe}; however, these are adversely higher under DM as it does not consider the risks associated with the unexpected failures. Furthermore, SP_{safe} provides a more conservative approach with less number of failures and lower violation of the joint-chance constraint, compared to the SP_{exact} approach. In Table 2.8, we also report the maintenance and operational costs incurred under these different maintenance schedules.

		GM			TLM			Operations			Cost Improv. (%)	
	$(\lvert\mathcal{G}'\rvert, \lvert\mathcal{L}'\rvert)$	SP_{exact}	SP_{safe}	DM	SP_{exact}	SP_{safe}	DM	SP_{exact}	SP_{safe}	DM	SP_{exact}	SP_{safe}
9-bus	(1,3)	0.32	0.32	0.91	0.04	0.05	0.06	1.28	1.30	1.39	30.67	29.52
39-bus	(4,4)	2.73	2.42	5.88	0.26	0.22	0.64	28.80	33.79	35.91	25.08	14.14
57-bus	(2,7)	3.78	3.78	10.09	1.13	1.20	2.95	32.05	32.05	31.98	17.89	17.74
118-bus	(4,9)	1.13	1.12	3.07	0.22	0.22	0.49	4.20	4.19	4.26	29.07	29.05

Table 2.8 Cost Comparison of Stochastic and Deterministic Models.

The "GM" and "TLM" columns provide the generator and transmission line maintenance costs, respectively. The "Operations" column gives the operational costs. All costs are reported in 100.000$. The "Cost Improv. (%)" represents the total cost improvements in percentages achieved by stochastic models compared to the deterministic model.

Table 2.7 shows that the average failures for $\mathcal{G}'$ and $\mathcal{L}'$ significantly decrease under both SP_{exact} and SP_{safe} as DM ignores the power system capabilities. Accordingly, generator and transmission line maintenance costs obtained under these stochastic methods are less than under those of DM for all instances. We also observe a slight increase in the operational costs in the DM approach, except the 57-bus instance; however, DM still incurs a higher total cost than SP_{exact} and SP_{safe}. This is due to the fact that the effects of the unexpected failures of system components on power system operations are ignored in DM. Our computational study shows that $14-31\%$ cost savings can be obtained under stochastic models in comparison with DM. As a result, the coordination between maintenance and operational schedules when considering the unexpected failures of system components yields significant cost savings as well as less interruptions due to these failures.

2.5.5 Sensitivity Analysis

In this section, we examine the effects of different choices of sets $\mathcal{G}'$ and $\mathcal{L}'$ on average failures, maintenance and operational costs under 50 failure scenarios. For that purpose, we first select $(p^{\mathcal{G}}_{fail}, p^{\mathcal{L}}_{fail}) = (0.2, 0.4)$ which decreases the cardinality of these sets compared to the baseline setting; however, this selection of subsets results in infeasibilities. This is because of the fact that components in $\mathcal{H}''$ are not scheduled for maintenance within the planning horizon, which causes the violation of the joint chance-constraint. Then, we analyze the effects of the size of sets $\mathcal{G}'$ and $\mathcal{L}'$ when $(p^{\mathcal{G}}_{fail}, p^{\mathcal{L}}_{fail}) = (0.01, 0.02)$ that considers more components for maintenance. We evaluate the maintenance schedules obtained by stochastic and deterministic

models over 1000 failure scenarios, which are the same in Section 2.5.4. We report the average failures and joint chance-constraint violations in Table 2.9.

		$\mathcal{G}'$			$\mathcal{L}'$			$\mathcal{G}'' \cup \mathcal{L}''$			JCC-Violation		
	$(\lvert\mathcal{G}'\rvert, \lvert\mathcal{L}'\rvert)$	SP_{exact}	SP_{safe}	DM	SP_{exact}	SP_{safe}	DM	SP_{exact}	SP_{safe}	DM	SP_{exact}	SP_{safe}	DM
9-bus	(2,3)	0.057	0.065	1.043	0.254	0.000	1.390	0.000			0.000	0.000	0.417
39-bus	(5,5)	0.452	0.065	3.118	0.046	0.046	3.996	0.006			0.062	0.003	1.000
57-bus	(3,10)	0.041	0.041	1.925	0.381	0.192	6.259	0.036			0.000	0.000	0.999
118-bus	(5,10)	0.108	0.089	3.825	0.407	0.144	6.829	0.044			0.008	0.006	1.000

Table 2.9 Average Failures under Stochastic and Deterministic Models with Larger $\mathcal{H}'$.

We observe that the average failures of set $\mathcal{G}'$ and $\mathcal{L}'$ increase; however, this is an expected result since more system components are under study for maintenance. Table 2.10 demonstrates the maintenance and operational costs incurred when the failure probability thresholds are decreased.

		GM			TLM			Operations			Cost Improv. (%)	
	$(\lvert\mathcal{G}'\rvert, \lvert\mathcal{L}'\rvert)$	SP_{exact}	SP_{safe}	DM	SP_{exact}	SP_{safe}	DM	SP_{exact}	SP_{safe}	DM	SP_{exact}	SP_{safe}
9-bus	(2,3)	0.32	0.32	0.91	0.04	0.05	0.06	1.28	1.30	1.39	30.67	29.52
39-bus	(5,5)	2.52	2.42	5.88	0.22	0.22	0.64	29.73	33.79	35.91	23.47	14.14
57-bus	(3,10)	3.78	3.78	10.09	1.13	1.20	2.95	32.05	32.05	31.98	17.89	17.74
118-bus	(5,10)	1.13	1.12	3.07	0.22	0.22	0.49	4.20	4.19	4.26	28.98	29.05

Table 2.10 Cost Comparison of Stochastic and Deterministic Models with Larger $\mathcal{H}'$.

For 9-bus and 57-bus instances, increasing the sizes of sets $\mathcal{G}'$ and $\mathcal{L}'$ does not affect the quality of the maintenance schedules for both SP_{exact} and SP_{safe} as compared to the results in Section 2.5.4. For the 39-bus instance under SP_{exact}, we observe a slight decrease in both generator and transmission line maintenance costs whereas operational cost increases. On the other hand, there is a relatively small increase in maintenance and operational costs for the 118-bus instance under SP_{exact}. This is because of the fact that large-scale instances cannot be solved to optimality within tolerance as increasing the size of $\mathcal{H}'$ increases the computational time required for convergence of the solution algorithm as well. Nevertheless in all cases, there are still significant cost savings compared to DM. We observe that although we take less failure risks by decreasing probability thresholds, we might be overly cautious which can result in higher operational costs.

2.6 Conclusions

In this thesis, we study a short-term condition-based integrated maintenance planning problem in coordination with the power system operations by considering the unexpected failures of generators as well as transmission lines. We formulate this problem as a two-stage joint chance-constrained stochastic program. Under a Bayesian setting, we obtain the RLDs of generators and transmission lines by using their degradation-based sensor information. We consider a specific subset of these components which are more prone to failure for scheduling maintenance and take the effects of their unexpected failures into account based on their estimated RLDs. We introduce a joint chance-constraint to mitigate the failure risk in the power network by restricting the number of system components under corrective maintenance. We develop a decomposition algorithm by improving the integer L-shaped method with various algorithmic enhancements including derivation of stronger optimality cuts by exploiting the underlying problem structure. This algorithm also includes a separation subroutine to provide an exact representation of the joint chance-constraint by leveraging the Poisson Binomial random variables in this constraint. As an alternative approach, we also provide an SOCP-based safe approximation to represent the joint chance-constraint which provides computational advantages for larger scale instances, despite of its conservatism. Our computational experiments demonstrate the efficiency of the proposed decomposition algorithm along with the improved cut generation procedures and preprocessing steps which consistently outperforms the state-of-the-art solver for all test instances. Finally, we highlight that our proposed stochastic models can obtain $14-31\%$ cost savings against a deterministic model since maintenance and operational schedules are coordinated in these models while explicitly considering the effects of failure uncertainty on power system operations.

3. Convex Relaxations for the Multi-period Natural Gas Storage Optimization Problem

3.1 Introduction

Gas network optimization problems have been a great interest to the natural gas industry due to their potential economic benefits (Wong & Larson, 1968). The main aim of these problems is to determine the optimal nodal pressures and gas flows through pipelines as well as to balance gas supply and demand with minimum operational costs. In this respect, integrating gas storages into these problems has become highly relevant and more important to the natural gas industry since the recent advances in power-to-gas technologies allow for storing and transporting surplus electrical power in gaseous form. While this form along with the contracted gas supplies can be used to deal with supply and demand fluctuations, there remain certain mathematical and computational challenges in the gas storage optimization problem: (i) due to their physical properties, some passive and active network elements impose challenging constraints on the optimization model, such as the well-known nonconvex pressure loss equations ("Weymouth" equations) governing the gas transportation in pipes and resistors, and the nonconvex fuel consumption of compressors, (ii) disjunctive formulations are needed for representing the direction of gas flow as well as the switching decisions for active elements such as compressors and (control) valves and, (iii) the injection and withdrawal rates of gas storages and the coupling conditions of active elements necessitate the multi-period modeling of this problem. Due to its many inherent nonconvex and nonlinear features, the multi-period gas storage optimization problem belongs to the class of nonconvex mixed-integer nonlinear programming (MINLP) problems whose continuous relaxations are quite challenging to solve to optimality.

There has been a wide literature devoted to the optimization problems in gas net-

works (for an recent review, see Ríos-Mercado & Borraz-Sánchez (2015) and references therein). These problems are typically modeled as nonconvex MINLPs whose simple cases are known be computationally and practically intractable within the scope of current state-of-the-art global optimization solvers (Burer & Letchford, 2012). In the context of gas network optimization, Labbé, Plein, Schmidt & Thürauf (2021) show that the feasibility problem of booking contracts in passive networks can be solved in polynomial time; however, the existence of active network elements such as compressors and (control) valves further complicate the problem. In particular, Humpola (2014) proves the NP-hardness of the gas network optimization problem with active elements and switching decisions. In the literature, there are more results on the hardness of different types of optimization problems in gas networks, see, e.g., Gross, Pfetsch, Schewe, Schmidt & Skutella (2019) and Schewe, Schmidt & Thürauf (2020).

In order to solve these hard problems in gas networks, several studies have used nonlinear optimization methods, such as sequential linear and quadratic programming (de Wolf & Smeers, 2000; Ehrhardt & Steinbach, 2005), interior point methods (Steinbach, 2007) and primal-relaxed dual decomposition methods (Wu, Lai & Liu, 2007). As these methods require a fixed network topology, the flexibility in changing the switching status of active elements is completely ignored. Some researchers attempt to incorporate these switching decisions into nonlinear models by using complementary constraints (Pfetsch, Fügenschuh, Geißler, Geißler, Gollmer, Hiller, Humpola, Koch, Lehmann, Martin, Morsi, Rövekamp, Schewe, Schmidt, Schultz, Schwarz, Schweiger, Stangl, Steinbach, Vigerske & Willert, 2015; Schmidt, 2015). While being able to find locally optimal (feasible) solutions in reasonably short time, these local methods provide only an upper bound on the objective value without any quality guarantees of these local solutions.

The literature has also focused on various relaxations and approximations in order to deal with the nonlinear and nonconvex aspects of gas physics, see, e.g., piecewise convex relaxations (Wu, Nagarajan, Zlotnik, Sioshansi & Rudkevich, 2017) and Taylor approximation (Ordoudis, Pinson & Morales, 2019) of nonconvex constraints, convex approximations of cost functions (Babonneau, Nesterov & Vial, 2012; Wu, Ríos-Mercado, Boyd & Scott, 2000), or continuous relaxations of integrality (Andre, Bonnans & Cornibert, 2009; Zhang & Zhu, 1996) and domain restrictions (Fügenschuh & Humpola, 2013; Wu et al., 2000). Many studies use the McCormick envelopes for relaxing the bilinear terms in the nonconvex constraints, see, e.g., Borraz-Sánchez, Bent, Backhaus, Hijazi & Hentenryck (2016), Wu et al. (2017). Although this relaxation technique is quite standard in the literature, it might lead to weak formulations when the variables have large bounds, which is in-

deed the case for nodal pressure and gas flow in gas network optimization problems. Piecewise linear approximations are also widely used in the literature to handle the inherent nonlinearities by introducing binary variables (Martin, Möller & Moritz, 2006; Pfetsch et al., 2015; Wang, Yuan, Zhang, Zhao & Liang, 2018; Wu et al., 2017; Zheng, Rebennack, Iliadis & Pardalos, 2010). The main advantage of these piecewise linearizations is that the resulting mixed-integer linear programming (MILP) model can be readily given to the current state-of-the-art mixed-integer programming solvers. Still, the high-resolution solutions produced by these approximations require introducing "many" binary variables. In the existence of these variables along with the switching decisions of active elements, these MILP formulations might be prohibitively expensive within these solvers.

Recently, certain convex relaxations have attracted attention in the literature. In particular, the mixed-integer second-order cone programming (MISOCP) and the semidefinite programming (SDP) relaxations are used to obtain tight dual bounds. In Borraz-Sánchez et al. (2016), an MISOCP relaxation model is constructed for solving the gas expansion planning problem, which involves the switching status for active network elements and simplified bidirectional compressor stations. He, Shahidehpour, Li, Guo & Zhu (2018) formulate a two-stage robust model for the operational problem in the integrated energy systems. They ignore active gas network elements, and assume a radial gas network, which allows them to remove the absolute value from the Weymouth equations. Under this unrealistic assumption, they relax these equations into second-order cone constraints. More recently, Schwele, Ordoudis, Kazempour & Pinson (2019) propose a similar MISOCP-based outer-approximation of the region defined by the nonconvex Weymouth equation including the bidirectional gas flow. Ojha, Kekatos & Baldick (2017) formulate an SDP relaxation for the gas network operations problem, in which they exploit the chordal extension of the sparse natural gas network. They tighten this convex relaxation by solving moment-based relaxation problems and applying the rank reduction of the moment matrix via valid inequalities.

The optimization problems in gas networks include highly detailed nonlinear, nonconvex and discrete aspects as mentioned above. For this reason, several studies in the literature make some simplifications or completely ignore some of these aspects. For example, some studies on the gas storage optimization problems over a multi-period planning horizon do not consider the switching status of the active network elements (Correa-Posada & Sánchez-Martín, 2015; Schwele et al., 2019), or assume that there are no such elements in the gas network (He et al., 2018). While these active elements along with their switching status are modeled in some of the previous works, they assume that compressors do not incur losses in the network

(Borraz-Sánchez et al., 2016; Burlacu, Egger, Groß, Martin, Pfetsch, Schewe, Sirvent & Skutella, 2019; Schewe et al., 2020). Among the MISOCP relaxation approaches, the strong formulations are neglected. For example, the convexification approach by Schwele et al. (2019) uses weak relaxations for feasible region defined by the Weymouth equations.

In this thesis, we focus on the multi-period gas storage optimization problem by considering these aforementioned highly nonlinear and nonconvex aspects of the gas physics and gas losses as well as the switching status of active network elements such as compressors and (control) valves. We formulate this problem as a nonconvex MINLP, which has two types of nonconvexity: i) the Weymouth equations for pipes and resistors, and ii) fuel consumption equations for compressors. Since this class of optimization problems are hard to solve in general, we present different mixed-integer convex relaxations based on the outer-approximations of the feasible regions defined by (i) and (ii). Our convexification approaches use the polyhedral and second-order cone representable (SOCr) outer-approximations of the nonconvex constraints. Moreover, we present a two-step solution framework based on these mixed-integer convex relaxations, which derive (near) globally optimal solutions and high-quality (locally) feasible solutions for congested gas networks. We demonstrate the effectiveness of our framework on different GasLib instances from the literature.

The remainder of this chapter is organized as follows: Section 3.2 introduces the physical and operational constraints in the multi-period gas storage optimization problem along with its mathematical formulations. Section 3.3 and Section 3.4 present our proposed outer-approximations of the feasible regions defined by the nonconvex constraints for compressors and passive elements, respectively. The two-step solution framework is explained in Section 3.5. The results of our computational study are presented in Section 3.6. Section 3.7 concludes this chapter with final remarks.

3.2 Problem Formulation

In this section, we first describe the problem setting (Section 3.2.1), and explain the constraints used in the gas network modeling along with the decision variables and problem parameters (Section 3.2.2). Then, we present the mathematical formulation (Section 3.2.3) and the MINLP formulation (Section 3.2.4) for the multi-period gas

storage optimization problem.

3.2.1 Problem Setting

In our work, we consider an isothermal and stationary natural gas network $\mathcal{G} = (\mathcal{N}, \mathcal{E})$, where $\mathcal{N}$ denotes the set of nodes, and $\mathcal{E}$ denotes the set of arcs. Figure 3.1 shows an example of a small-scale gas network (taken from Burlacu et al. (2019)). The set $\mathcal{N}$ consists of the set $\mathcal{N}_{source}$ of source nodes, the set $\mathcal{N}_{inner}$ of inner nodes and the set $\mathcal{N}_{sink}$ of sink nodes. We let $\mathcal{E} = \mathcal{P} \cup \mathcal{A}$ where $\mathcal{P}$ and $\mathcal{A}$ denote the set of passive and active elements, respectively. In our notation, we also let $\mathcal{P} = \mathcal{P}' \cup \mathcal{P}'' \cup \mathcal{P}'''$, where these subsets denote the set of pipes, resistors and connections (i.e., short pipes), respectively. Also, we split $\mathcal{A}$ into the set $\mathcal{C}$ of compressors, the set $\mathcal{V}$ of control valves, and the set $\mathcal{R}$ of regular valves. For each arc (i, j), we say that the direction of gas flow is positive if it goes from node i to node j, and negative otherwise. We restrict ourselves to an idealized compressor station which consists of a bidirectional single compressor unit (i.e., compressor). We assume that all nodes are located horizontally (i.e., arcs are at the same height), and all arcs are cylindrical. For each node $i \in \mathcal{N}$, we define $\Delta^+(i) := \{j \in \mathcal{N} : (i, j) \in \mathcal{A}\}$ as the set of outgoing neighbors and $\Delta^-(i) := \{j \in \mathcal{N} : (j, i) \in \mathcal{A}\}$ as the incoming neighbors of node i. Also, we let $\Delta^+_{\mathcal{C}}(i) = \{j \in \mathcal{N}, (i, j) \in \mathcal{C}\}$ and $\Delta^-_{\mathcal{C}}(i) = \{j \in \mathcal{N}, (j, i) \in \mathcal{C}\}$ as the sets of outgoing and incoming neighbors of node i, which are connected to this node via a compressor. We assume that natural gas storage units (i.e., stores) are installed at some nodes $i \in \mathcal{N}$. We denote the set of natural gas stores linked to node i as $\mathcal{S}(i) \subseteq \mathcal{N}$. Finally, $\mathcal{T}$ represents the set of periods within the planning horizon.

3.2.2 Gas Network Modeling

In this section, we explain the operational and physical constraints of passive and active elements. For more detailed explanations on these physical quantities and gas network modeling, we refer the reader to the book by Koch, Pfetsch & Schewe (2015). Each node $i \in \mathcal{N}$ is associated with a pressure variable p_{it} for $t \in \mathcal{T}$ that takes values from the interval $[\underline{p}_i, \bar{p}_i]$. The gas load at node $i \in \mathcal{N}$ in period $t \in \mathcal{T}$ is denoted by q_{it}. For each period $t \in \mathcal{T}$, the variable $s_{jt} \in [\underline{s}_j, \bar{s}_j]$ represents the amount

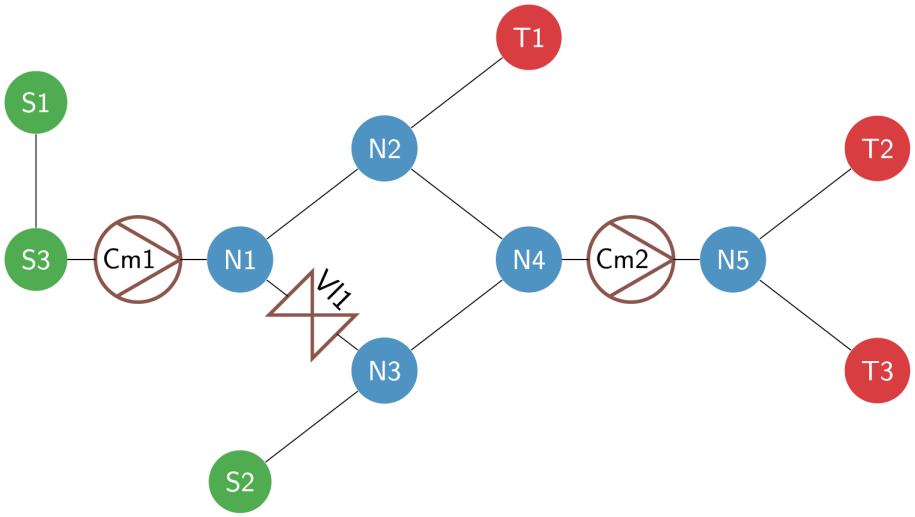

Figure 3.1 The GasLib-11 instance. $\mathcal{N}_{source} = \{\text{S1, S2, S3}\}$, $\mathcal{N}_{sink} = \{\text{T1, T2, T3}\}$, $\mathcal{N}_{inner} = \{\text{N1, N2, N3, N4, N5}\}$, $\mathcal{C} = \{\text{Cm1, Cm2}\}$, $\mathcal{R} = \{\text{Vl1}\}$, $\mathcal{P}$ is the set of unlabeled arcs.

of natural gas (the store level) at store $j \in \mathcal{S}(i)$ linked to node $i \in \mathcal{N}$, whereas the gas injected and withdrawn from node i with rates η'_j and η''_j are denoted by s'_{jt} and s''_{jt}, respectively. The gas withdrawals from store j are associated with supply costs $C^-_j > 0$. The variable f_{ijt} represents the gas flow through arc $(i,j) \in \mathcal{E}$ in period $t \in \mathcal{T}$. The gas flow through arc $(i,j) \in \mathcal{E}$ is between allowable lower and upper flow limits denoted as $\underline{f}_{ij}$ and $\bar{f}_{ij}$, respectively. For each active element $(i,j) \in \mathcal{A}$, we consider its active and closed states. We model the switching status of these network elements by using a binary variable x_{ijt}, which takes the value one if the active element (i,j) is open in period t, and zero otherwise. Moreover, each compressor $(i,j) \in \mathcal{C}$ is associated with binary start-up and shut-down variables u_{ijt} and v_{ijt}, respectively. Whenever compressor (i,j) is turned on from off state, the positive start-up cost C^{up}_{ij} is incurred.

Gas transportation in pipes is governed by the Euler equations, which are a system of hyperbolic partial differential equations (e.g., see Osiadacz (1987)). Finding a solution to this complex system is very hard. Thus, we simplify this system under isothermal and stationary assumptions, which is a common practice in the gas network literature. For each period $t \in \mathcal{T}$, we are then able to model the pressure losses due to the internal friction during gas transportation through each pipe $(i,j) \in \mathcal{P}'$ with the very well-known nonlinear and nonconvex Weymouth equation:

$$p^2_{it} - p^2_{jt} = w_{ij}|f_{ijt}|f_{ijt} \qquad (i,j) \in \mathcal{P}', t \in \mathcal{T}. \tag{3.1}$$

Here, the resistance coefficient w_{ij} is often called as the Weymouth coefficient. We

note that short pipes are artificial network elements which do not induce pressure losses, i.e., $w_{ij} = 0$ for each $(i,j) \in \mathcal{P}'''$.

Aside from the pipes, there are also different sources such as filter systems and pressure regulators, which cause pressure losses in the gas network (Koch et al., 2015). A resistor $(i,j) \in \mathcal{P}''$ is used to represent such losses. Similar to pipes, the Darcy–Weisbach equation (Finnemore & Franzini, 2002) is used to model these with a small resistance coefficient w_{ij} for each $t \in \mathcal{T}$ in each resistor $(i,j) \in \mathcal{P}''$:

$$\begin{aligned} f_{ijt} \geq 0 &\implies 2p_{it}(p_{it} - p_{jt}) = w_{ij}|f_{ijt}|f_{ijt} \\ f_{ijt} < 0 &\implies 2p_{jt}(p_{it} - p_{jt}) = w_{ij}|f_{ijt}|f_{ijt}. \end{aligned}$$

We note that the Darcy-Weisbach equation is also nonlinear and nonconvex. This equation can be replaced with the Weymouth equation (see, e.g., Schmidt (2013)) by approximating the terms $2p_{it}$ and $2p_{jt}$ by $p_{it} + p_{jt}$:

$$p_{it}^2 - p_{jt}^2 = w_{ij}|f_{ijt}|f_{ijt} \qquad (i,j) \in \mathcal{P}'', t \in \mathcal{T}. \tag{3.2}$$

In the gas network, active elements are used to control the gas flow and the pressures of their adjacent nodes. For example, compressors are used to increase the pressure of the incoming natural gas and transport it over long distances whereas control valves are used to reduce this pressure between its adjacent nodes. For an open active element, the compression ratio p_{jt}/p_{it} must lie between $[\underline{r}_{ij}, \bar{r}_{ij}]$ if the gas flow is in the positive direction. Otherwise, the ratio p_{it}/p_{jt} belongs to the same interval. Whenever the active element is closed, the gas flow between node i and node j is blocked and their nodal pressures are decoupled. These operational conditions are summarized as follows:

$$x_{ijt} = 0 \implies f_{ijt} = 0 \qquad (i,j) \in \mathcal{A}, t \in \mathcal{T} \tag{3.3a}$$

$$f_{ijt} \geq 0, x_{ijt} = 1 \implies \frac{p_{jt}}{p_{it}} \in [\underline{r}_{ij}, \bar{r}_{ij}] \qquad (i,j) \in \mathcal{A}, t \in \mathcal{T} \tag{3.3b}$$

$$f_{ijt} < 0, x_{ijt} = 1 \implies \frac{p_{it}}{p_{jt}} \in [\underline{r}_{ij}, \bar{r}_{ij}] \qquad (i,j) \in \mathcal{A}, t \in \mathcal{T}. \tag{3.3c}$$

We assume that each active element $(i,j) \in \mathcal{A}$ is bidirectional (i.e., $\underline{f}_{ij} \leq 0 \leq \bar{f}_{ij}$). Also, $1 < \underline{r}_{ij} < \bar{r}_{ij}$ for each compressor $(i,j) \in \mathcal{C}$, which results in a pressure increase at node i (node j) in case of a positive (negative) gas flow. Similar to compressors, we have $0 \leq \underline{r}_{ij} < \bar{r}_{ij} < 1$ for each control valve $(i,j) \in \mathcal{V}$. On the other hand, we assume that there is no pressure loss in valves (i.e., $w_{ij} = 0$), and thus, we have $\underline{r}_{ij} = \bar{r}_{ij} = 1$ for each, $(i,j) \in \mathcal{R}$.

We assume that each compressor $(i,j) \in \mathcal{C}$ is a so-called turbo compressor. This

type of compressors is associated with a special type of compressor drive (i.e., gas turbines) which provides the necessary power to compress the gas. Whenever a compressor (i,j) is active, its drive consumes the fuel gas directly taken from the network with cost C_{ij}^{fc}. We denote the fuel gas consumption (i.e., gas loss) incurred by each compressor (i,j) with the variable l_{ijt} for each period $t \in \mathcal{T}$. These loss variables depend on the direction of the gas flow, and some physical constants κ'_{ij} and κ. Note that κ'_{ij} is a component-specific constant. For example, the loss of compressor (i,j) depends on the compression ratio p_{jt}/p_{it} if the gas flow through compressor (i,j) is positive. For each open compressor $(i,j) \in \mathcal{C}$ with positive gas flow, the absolute difference between the pressure variables of node j and node i are between its allowable lower $\underline{\delta}_{ij}$ and upper $\bar{\delta}_{ij}$ limits. We summarize these operational conditions for compressors as follows:

$$x_{ijt} = 0 \implies f_{ijt} = 0, l_{ijt} = 0 \qquad (i,j) \in \mathcal{C}, t \in \mathcal{T} \tag{3.4a}$$

$$f_{ijt} \geq 0, x_{ijt} = 1 \implies \begin{array}{l} p_{jt} - p_{it} \in [\underline{\delta}_{ij}, \bar{\delta}_{ij}] \\ l_{ijt} = \kappa'_{ij}[(\frac{p_{jt}}{p_{it}})^{\kappa} - 1] f_{ijt} \end{array} \qquad (i,j) \in \mathcal{C}, t \in \mathcal{T} \tag{3.4b}$$

$$f_{ijt} < 0, x_{ijt} = 1 \implies \begin{array}{l} p_{it} - p_{jt} \in [\underline{\delta}_{ij}, \bar{\delta}_{ij}] \\ l_{ijt} = \kappa'_{ij}((\frac{p_{it}}{p_{jt}})^{\kappa} - 1) f_{ijt} \end{array} \qquad (i,j) \in \mathcal{C}, t \in \mathcal{T}. \tag{3.4c}$$

Finally, we consider the operational restrictions for each active element $(i,j) \in \mathcal{A}$. The minimum-up time restrictions ensure that whenever active element (i,j) is turned on, it must remain open for at least MU_{ij} many periods. Similarly, the minimum-down time restrictions impose that this network element remains closed for at least MD_{ij} many periods whenever it is turned down. We also couple the start-up and shut-down decisions with switching decisions for each compressor $(i,j) \in \mathcal{C}$. These operational conditions for active elements are given as follows:

$$x_{ijt} - x_{ij(t-1)} \leq x_{ijt'} \qquad \begin{array}{l} (i,j) \in \mathcal{A}, t \in \mathcal{T} \\ t' \in \{t+1, \ldots, t+MU_{ij}-1\} \end{array} \tag{3.5a}$$

$$x_{ij(t-1)} - x_{ij} \leq 1 - x_{ijt'} \qquad \begin{array}{l} (i,j) \in \mathcal{A}, t \in \mathcal{T} \\ t' \in \{t+1, \ldots, t+MD_{ij}-1\} \end{array} \tag{3.5b}$$

$$x_{ijt} - x_{ij(t-1)} = u_{ijt} - v_{ijt} \qquad (i,j) \in \mathcal{C}, t \in \mathcal{T} \tag{3.5c}$$

$$u_{ijt} + v_{ijt} \leq 1 \qquad (i,j) \in \mathcal{C}, t \in \mathcal{T}. \tag{3.5d}$$

We note that the switching decisions for compressors are analogous to generator commitment decisions in the unit commitment problem in power systems.

3.2.3 The Mathematical Formulation

We are now ready to present the mathematical formulation of the multi-period natural gas storage optimization problem by using the physical and operational constraints introduced in the previous section:

(3.6a)
$$\min \sum_{(i,j)\in\mathcal{C}} \sum_{t\in\mathcal{T}} (C_{ij}^{fc}|l_{ijt}| + C_{ij}^{up} u_{ijt}) + \sum_{i\in\mathcal{N}} \sum_{j\in\mathcal{S}(i)} \sum_{t\in\mathcal{T}} C_j^{wd} s''_{jt}$$

(3.6b)
$$\text{s.t. } q_{it} = \sum_{j\in\mathcal{S}(i)} (s'_{jt} - s''_{jt}) + \sum_{j\in\Delta^+(i)} f_{ijt} - \sum_{j\in\Delta^-(i)} f_{jit} + \sum_{j\in\Delta_{\mathcal{C}}^-(i)} l_{ijt} - \sum_{j\in\Delta_{\mathcal{C}}^+(i)} l_{jit} \qquad i\in\mathcal{N}, t\in\mathcal{T}$$

(3.6c) $$s_{jt} = s_{j(t-1)} + \eta'_j s'_{jt} - \eta''_j s''_{jt} \qquad i\in\mathcal{N}, j\in\mathcal{S}(i), t\in\mathcal{T}$$

(3.6d) $$\underline{s}_j \le s_{jt} \le \bar{s}_j \qquad i\in\mathcal{N}, j\in\mathcal{S}(i), t\in\mathcal{T}$$

(3.6e) $$\underline{p}_i \le p_{it} \le \bar{p}_i \qquad i\in\mathcal{N}, t\in\mathcal{T}$$

(3.6f) $$\underline{f}_{ij} \le f_{ijt} \le \bar{f}_{ij} \qquad (i,j)\in\mathcal{E}, t\in\mathcal{T}$$

(3.6g) $$x_{ijt} \in \{0,1\} \qquad (i,j)\in\mathcal{A}, t\in\mathcal{T}$$

(3.6h)
$$u_{ijt}, v_{ijt} \in \{0,1\} \qquad (i,j)\in\mathcal{C}, t\in\mathcal{T}$$
$$(3.1)-(3.5).$$

In this formulation, the objective function (3.6a) minimizes the total cost gas transportation which has two main components: the operational cost for compressors, i.e., the fuel gas consumption and start-up costs, and supply cost of gas stores. Constraint (3.6b) models natural gas flow balance by the conservation of mass at each node. We note that a positive gas load (i.e., supply) is assigned for each $i\in\mathcal{N}_{source}$ and a negative gas load (i.e., demand) is assigned for each $i\in\mathcal{N}_{sink}$. We let $q_{it}=0$ for each $i\in\mathcal{N}_{inner}$. Constraint (3.6c) corresponds to the inventory balance equation for the amount of the natural gas stored at each store. Constraints (3.6d), (3.6e) and (3.6f) are the operational limit constraints for store level, pressure and flow variables, respectively. Constraints (3.6g) and (3.6h) represent the binary restrictions for switching decisions for active arcs, and start-up and shut-down variables for compressors, respectively. The additional physical constants and parameters describing the gas physics are further explained in Appendix B.

3.2.4 MINLP Formulation

In the previous section, we introduce the mathematical formulation for our problem, which cannot be directly given to an optimization solver. In this context, we provide the MINLP formulation of formulation (3.6) by defining new variables in this section. We first observe that one type of nonlinearity is in the form of $p_i^2 - p_j^2$ in equations (3.1) and (3.2). In order to capture this, we define the squared pressure variable $\pi_{it} \in [\underline{\pi}_i, \bar{\pi}_i]$ for each node $i \in \mathcal{N}$ and each period $t \in \mathcal{T}$, where $\bar{\pi}_i = (\bar{p}_i)^2$ and $\underline{\pi}_i = (\underline{p}_i)^2$. Still, pressure variables of neighbor nodes connected by compressors appear linearly in constraints (3.4b) and (3.4c). Thus, we enforce the following two coupling constraints $p_{it}^2 = \pi_{it}$ and $p_{jt}^2 = \pi_{jt}$ in our optimization model for each compressor $(i,j) \in \mathcal{C}$ and each period $t \in \mathcal{T}$. Then, we have the following system of nonlinear and nonconvex equations:

$$\pi_{it} - \pi_{jt} = w_{ij} |f_{ijt}| f_{ijt} \qquad (i,j) \in \mathcal{P}' \cup \mathcal{P}'', t \in \mathcal{T} \tag{3.7a}$$

$$\pi_{it} = p_{it}^2, \pi_{jt} = p_{jt}^2 \qquad (i,j) \in \mathcal{C}, t \in \mathcal{T}. \tag{3.7b}$$

In order to linearize system (3.3), we define two binary variables $x_{ijt}^+ \in \{0,1\}$ and $x_{ijt}^- \in \{0,1\}$ for each active element $(i,j) \in \mathcal{A}$ and each period $t \in \mathcal{T}$. To be precise, x_{ijt}^+ (x_{ijt}^-) takes the value one if the gas flow direction for an open active element (i,j) is positive (negative), and 0 otherwise. If an active element (i,j) is closed, then $x_{ijt}^+ = x_{ijt}^- = 0$ holds since the gas flow is not allowed through this network element. We also let $\underline{a}_{ij} = (\underline{r}_{ij})^2$ and $\bar{a}_{ij} = (\bar{r}_{ij})^2$. By using these variables, system (3.3) can be linearized as

$$x_{ijt} = x_{ijt}^+ + x_{ijt}^- \qquad (i,j) \in \mathcal{A}, t \in \mathcal{T} \tag{3.8a}$$

$$\pi_{jt} \geq \underline{a}_{ij} \pi_{it} + (1 - x_{ijt}^+)(\underline{\pi}_j - \underline{a}_{ij} \bar{\pi}_i) \qquad (i,j) \in \mathcal{A}, t \in \mathcal{T} \tag{3.8b}$$

$$\pi_{jt} \leq \bar{a}_{ij} \pi_{it} + (1 - x_{ijt}^+)(\bar{\pi}_j - \bar{a}_{ij} \underline{\pi}_i) \qquad (i,j) \in \mathcal{A}, t \in \mathcal{T} \tag{3.8c}$$

$$\pi_{it} \geq \underline{a}_{ji} \pi_{jt} + (1 - x_{ijt}^-)(\underline{\pi}_i - \underline{a}_{ji} \bar{\pi}_j) \qquad (i,j) \in \mathcal{A}, t \in \mathcal{T} \tag{3.8d}$$

$$\pi_{it} \leq \bar{a}_{ji} \pi_{jt} + (1 - x_{ijt}^-)(\bar{\pi}_i - \bar{a}_{ji} \underline{\pi}_j) \qquad (i,j) \in \mathcal{A}, t \in \mathcal{T} \tag{3.8e}$$

$$\underline{f}_{ij} x_{ijt}^- \leq f_{ijt} \leq \bar{f}_{ij} x_{ijt}^+ \qquad (i,j) \in \mathcal{A}, t \in \mathcal{T} \tag{3.8f}$$

$$x_{ijt} \in [0,1], x_{ijt}^+, x_{ijt}^- \in \{0,1\} \qquad (i,j) \in \mathcal{A}, t \in \mathcal{T}. \tag{3.8g}$$

Here, the continuous relaxation of the switching decisions is used since their binary nature is implied by constraint (3.8a) due to the fact that x_{ijt}^+ and x_{ijt}^- are binary.

In order to linearize system (3.4), we first define new nonnegative variables $f_{ijt}^+, f_{ijt}^-, l_{ijt}^+$ and l_{ijt}^- for each compressor $(i,j) \in \mathcal{C}$ and each period $t \in \mathcal{T}$. If $x_{ijt} = 0$,

all of these variables take the value zero. This ensures that there is no gas flow through this compressor, which implies that there is no gas loss incurred by this compressor. If $x_{ijt} = 1$, then at least one of f^+_{ijt} and f^-_{ijt} take the value zero, and the loss incurred by this compressor is given by either l^+_{ijt} or l^-_{ijt}. For example, if $f_{ijt} \geq 0$, then $f^+_{ijt}, l^+_{ijt} \geq 0$ and $f^-_{ijt} = l^-_{ijt} = 0$. The similar result also holds if $f_{ijt} < 0$. Note that the direction of the gas flow also affects the compression ratio. Thus, we also define the new variables $p^+_{it}, p^-_{it}, p^+_{jt}, p^-_{jt}, r^+_{ijt}, r^-_{ijt}$ and r'_{ijt} in order to represent this ratio depending on the direction of the gas flow. We let $x_{ijt}p_{it} = p^+_{it} + p^-_{it}$ and $x_{ijt}p_{jt} = p^+_{jt} + p^-_{jt}$ for each compressor $(i,j) \in \mathcal{C}$ and each period $t \in \mathcal{T}$. These two equations ensure that whenever a compressor is closed, both of the auxiliary pressure variables take the value zero. On the other hand, either $p^+_{it}, p^+_{jt} \geq 0$ or $p^-_{it}, p^-_{jt} \geq 0$ holds for an open compressor. In order to model the gas losses and compression conditions with these auxiliary variables, we define the following set:

$$\begin{aligned}\mathcal{L}(\underline{p}', \underline{p}'', \bar{p}', \bar{p}'', \kappa') := \Big\{(p', p'', l, f, x, r, r') : \; & l = \kappa'(r'-1)f, l \geq 0 \\ & r = p''/p' \\ & \underline{p}'x \leq p' \leq \bar{p}'x \\ & \underline{p}''x \leq p'' \leq \bar{p}''x\Big\}.\end{aligned}$$

Now, system (3.4) can be equivalently read as

$$\begin{aligned}
&\text{(3.9a)} && f_{ijt} = f^+_{ijt} - f^-_{ijt} && (i,j) \in \mathcal{C}, t \in \mathcal{T} \\
&\text{(3.9b)} && l_{ijt} = l^+_{ijt} - l^-_{ijt} && (i,j) \in \mathcal{C}, t \in \mathcal{T} \\
&\text{(3.9c)} && x_{ijt}p_{it} = p^+_{it} + p^-_{it} \;,\; x_{ijt}p_{jt} = p^+_{jt} + p^-_{jt} && (i,j) \in \mathcal{C}, t \in \mathcal{T} \\
&\text{(3.9d)} && x_{ijt}r'_{ijt} = r^{\kappa}_{ijt} && (i,j) \in \mathcal{C}, t \in \mathcal{T} \\
&\text{(3.9e)} && r_{ijt} = r^+_{ijt}x^+_{ijt} + r^-_{ijt}x^-_{ijt} && (i,j) \in \mathcal{C}, t \in \mathcal{T} \\
&\text{(3.9f)} && (p^+_{it}, p^-_{jt}, l^+_{ijt}, f^+_{ijt}, x^+_{ijt}, r^+_{ijt}, r'_{ijt}) \in \mathcal{L}(\underline{p}_i, \underline{p}_j, \bar{p}_i, \bar{p}_j, \kappa'_{ij}) && (i,j) \in \mathcal{C}, t \in \mathcal{T} \\
&\text{(3.9g)} && (p^-_{jt}, p^-_{it}, l^-_{ijt}, f^-_{ijt}, x^-_{ijt}, r^-_{ijt}, r'_{ijt}) \in \mathcal{L}(\underline{p}_j, \underline{p}_i, \bar{p}_j, \bar{p}_i, \kappa'_{ij}) && (i,j) \in \mathcal{C}, t \in \mathcal{T} \\
&\text{(3.9h)} && p_{jt} - p_{it} \leq \bar{\delta}_{ij}x^+_{ijt} - \underline{\delta}_{ji}x^-_{ijt} && \\
& && \qquad + (1 - x_{ijt})(\underline{p}_j - \bar{p}_i) && (i,j) \in \mathcal{C}, t \in \mathcal{T} \\
&\text{(3.9i)} && p_{jt} - p_{it} \geq \underline{\delta}_{ij}x^+_{ijt} - \bar{\delta}_{ji}x^-_{ijt} && \\
& && \qquad + (1 - x_{ijt})(\bar{p}_j - \underline{p}_i) && (i,j) \in \mathcal{C}, t \in \mathcal{T} \\
&\text{(3.9j)} && 0 \leq f^+_{ijt} \leq \bar{f}_{ij}x^+_{ijt} && (i,j) \in \mathcal{C}, t \in \mathcal{T} \\
&\text{(3.9k)} && 0 \leq f^-_{ijt} \leq -\underline{f}_{ij}x^-_{ijt} && (i,j) \in \mathcal{C}, t \in \mathcal{T} \\
&\text{(3.9l)} && \underline{r}_{ij} \leq r^+_{ijt}, r^-_{ijt} \leq \bar{r}_{ij} && (i,j) \in \mathcal{C}, t \in \mathcal{T}.
\end{aligned}$$

Here, constraints (3.9a) - (3.9d) are the consistency constraints which preserve the

relations between original and auxiliary variables as explained above. We note that the variable r_{ijt} can be projected out via simple substitution. Now, observe that all the nonlinearity and nonconvexity arise from constraints (3.9c) - (3.9g) in the form of quadratic terms, and also constraint (3.9d) in the form of an exponential term with a fractional exponent (i.e., $\kappa \approx 0.228$).

Now, we are in a position to present an MINLP formulation of model (3.6):

(3.10a)
$$\min \quad \sum_{(i,j)\in\mathcal{C}} \sum_{t\in\mathcal{T}} (C_{ij}^{fc}(l_{ijt}^{+} + l_{ijt}^{-}) + C_{ij}^{up} u_{ijt}) + \sum_{i\in\mathcal{N}} \sum_{j\in\mathcal{S}(i)} \sum_{t\in\mathcal{T}} C_{j}^{wd} s_{jt}''$$

(3.10b)
$$\text{s.t.} \quad \underline{\pi}_i \leq \pi_{it} \leq \bar{\pi}_i \qquad\qquad i \in \mathcal{N}, t \in \mathcal{T}$$
$$(3.6\text{b}) - (3.6\text{d}), (3.7) - (3.9).$$

Here, the absolute value $|l_{ijt}|$ in (3.6a) is replaced with the nonnegative term $l_{ijt}^{+} + l_{ijt}^{-}$ since constraints (3.9j) and (3.9k) ensure that at least one of these auxiliary loss variables take the value zero. We note that problem (3.10) is highly nonlinear and nonconvex due to constraints (3.7) and (3.9). In the next section, we present different mixed-integer convex relaxations for the MINLP formulation of the multi-period gas storage optimization problem. In particular, we derive these relaxations by focusing on the physical constraints for pipes, resistors and compressors. Throughout our convexification scheme, we utilize McCormick envelopes (see, McCormick (1976)) for linearizing the bilinear term $w = xy$, which are given by the set

$$\begin{aligned} \mathcal{M}(l_x, u_x, l_y, u_y) = \{(w,x,y) \in \mathbb{R}^3 : \; & w \geq l_y x + l_x y - l_x l_y \\ & w \leq u_y x + l_x y - l_x u_y \\ & w \leq l_y x + u_x y - u_x l_y \\ & w \geq u_y x + u_x y - u_x u_y \}. \end{aligned}$$

3.3 Convex Relaxations for Compressors

In this section, we present an outer-approximation of the feasible region defined by constraints (3.7b) and (3.9c) - (3.9g). In the remainder of this section, we drop t indices for brevity. First, we introduce the following new variables for each com-

pressor $(i,j) \in \mathcal{C}$: $R'_{ij} = x_{ij} r'_{ij}, R^+_{ij} = x^+_{ij} r^+_{ij}$ and $R^- = x^-_{ij} r^-_{ij}$. We construct the exact McCormick envelopes for these equations. We also introduce two new variables F^+_{ij} and F^-_{ij} as $F^+_{ij} = f^+_{ij} r'_{ij}$ and $F^-_{ij} = f^-_{ij} r'_{ij}$. We replace constraint (3.9d) by $R'_{ij} = r^\kappa_{ij}$ and $R'_{ij} = x_{ij} r'_{ij}$. Now, observe that equation $R'_{ij} = r^\kappa_{ij}$ defines a concave function with the endpoints $(\underline{r}_{ij}, \underline{r}^\kappa_{ij})$ and $(\bar{r}_{ij}, \bar{r}^\kappa_{ij})$ in the (R', r)-space. In order to obtain a mixed-integer convex relaxation, we replace this nonconvex equality by its linear underestimator:

$$R'_{ij} \geq m_{ij} r_{ij} - (m_{ij} \underline{r}_{ij} + \underline{r}^\kappa_{ij}) x_{ij}, \tag{3.11}$$

where $m_{ij} := (\bar{r}^\kappa_{ij} - \underline{r}^\kappa_{ij})/(\bar{r}_{ij} - \underline{r}_{ij})$. Finally, we introduce the following set which is used as an outer-approximation of $\mathcal{L}$:

$$\mathcal{L}'(l_r, u_r, l_{p'}, u_{p'}, \kappa') := \Big\{ (p', p'', l, F, f, x, r) : l = \kappa'(F - f) \\ (p'', r, p') \in \mathcal{M}(l_r, u_r, l_{p'}, u_{p'}) \Big\}.$$

Now, consider the following set of constraints:

$$\pi_i \geq p_i^2, \pi_j \geq p_j^2 \qquad (i,j) \in \mathcal{C} \tag{3.12a}$$
$$r_{ij} = R^+_{ij} + R^-_{ij} \qquad (i,j) \in \mathcal{C} \tag{3.12b}$$
$$(p^+_i, p^+_j, l^+_{ij}, F^+_{ij}, f^+_{ij}, x^+_{ij}, r^+_{ij}) \in \mathcal{L}'(0, 0, \bar{p}_i, \bar{p}_j, \kappa'_{ij}) \qquad (i,j) \in \mathcal{C} \tag{3.12c}$$
$$(p^-_j, p^-_i, l^-_{ij}, F^-_{ij}, f^-_{ij}, x^-_{ij}, r^-_{ij}) \in \mathcal{L}'(0, 0, \bar{p}_j, \bar{p}_i, \kappa'_{ij}) \qquad (i,j) \in \mathcal{C} \tag{3.12d}$$
$$(R'_{ij}, x_{ij}, r'_{ij}) \in \mathcal{M}(0, 1, \underline{r}^\kappa_{ij}, \bar{r}^\kappa_{ij}) \qquad (i,j) \in \mathcal{C} \tag{3.12e}$$
$$(p^+_i + p^-_i, x_{ij}, p_i) \in \mathcal{M}(0, 1, \underline{p}_i, \bar{p}_i) \qquad (i,j) \in \mathcal{C} \tag{3.12f}$$
$$(p^+_j + p^-_j, x_{ij}, p_j) \in \mathcal{M}(0, 1, \underline{p}_j, \bar{p}_j) \qquad (i,j) \in \mathcal{C} \tag{3.12g}$$
$$(R^+_{ij}, x^+_{ij}, r^+_{ij}) \in \mathcal{M}(0, 1, \underline{r}_{ij}, \bar{r}_{ij}) \qquad (i,j) \in \mathcal{C} \tag{3.12h}$$
$$(R^-_{ij}, x^-_{ij}, r^-_{ij}) \in \mathcal{M}(0, 1, \underline{r}_{ij}, \bar{r}_{ij}) \qquad (i,j) \in \mathcal{C} \tag{3.12i}$$
$$(F^+_{ij}, f^+_{ij}, r'_{ij}) \in \mathcal{M}(0, \bar{f}_{ij}, \underline{r}^\kappa_{ij}, \bar{r}^\kappa_{ij}) \qquad (i,j) \in \mathcal{C} \tag{3.12j}$$
$$(F^-_{ij}, f^-_{ij}, r'_{ij}) \in \mathcal{M}(0, -\underline{f}_{ij}, \underline{r}^\kappa_{ij}, \bar{r}^\kappa_{ij}) \qquad (i,j) \in \mathcal{C}. \tag{3.12k}$$

In this formulation, constraints (3.12e) - (3.12k) are the McCormick envelopes. Note that the linearization in constraints (3.12e) - (3.12i) is exact. Moreover, the feasible region defined by these constraints are polyhedral. Also, observe that constraint (3.12a) represents the epigraphs of two parabolas in the space of (π_i, p_i) and (π_j, p_j) variables, respectively. It is straightforward to see that these are SOCr. Moreover, these epigraphs are the convex hull of the set defined by constraint (3.7b). Then, the set defined by constraints (3.11) and (3.12) is mixed-integer second-order cone representable (MISOCr). Finally, we denote the projection of this set onto the

original space as

$$\mathcal{Y} := \{(\tilde{f}, \tilde{p}, \tilde{r}, \tilde{l}, \tilde{x}) : \exists (R', R^+, R^-, F^+, F^-) \in \mathbb{R}^5 : (3.11), (3.12)\}, \tag{3.13}$$

where we denote $\tilde{p}_{ij} = (\pi_i, \pi_j, p_i, p_j, p_i^+, p_j^+, p_i^-, p_j^-)$, $\tilde{r}_{ij} = (r_{ij}, r'_{ij}, r_{ij}^+, r_{ij}^-)$, $\tilde{f}_{ij} = (f_{ij}^+, f_{ij}^-)$, $\tilde{l}_{ij} = (l_{ij}^+, l_{ij}^-)$ and $\tilde{x}_{ij} = (x_{ij}, x_{ij}^+, x_{ij}^-)$ by dropping (i,j) indices.

Proposition 3.1 *The set $\mathcal{Y}$ forms an outer-approximation of the feasible region defined by constraints* (3.7b) *and* (3.9c) - (3.9g).

3.4 Convex Relaxations for Pipes and Resistors

In this section, we present different outer-approximations of the feasible region defined by the nonconvex Weymouth equation (3.7a) with respect to the flow and squared pressure bounds (3.6f) and (3.10b), respectively. We first let $\tilde{\mathcal{P}} := \mathcal{P} \setminus \mathcal{P}'''$, $f := f_{ij}$ and $\pi := \pi_i - \pi_j$. For each passive element $(i,j) \in \tilde{\mathcal{P}}$, we now define the following rectangle:

$$\mathcal{R}_{ij} := \{(f, \pi) : \underline{\alpha}_{ij} \leq f \leq \bar{\alpha}_{ij},\ \underline{\beta}_{ij} \leq \pi \leq \bar{\beta}_{ij}\},$$

where the bounds are defined as

$$\underline{\alpha}_{ij} := \max\left\{-\underline{f}_{ij}, -\sqrt{\frac{\bar{\pi}_j - \underline{\pi}_i}{w_{ij}}}\right\} \qquad \bar{\alpha}_{ij} := \min\left\{\bar{f}_{ij}, \sqrt{\frac{\bar{\pi}_i - \underline{\pi}_j}{w_{ij}}}\right\}$$
$$\underline{\beta}_{ij} := \max\left\{-w_{ij}(\underline{f}_{ij})^2, \underline{\pi}_i - \bar{\pi}_j\right\} \qquad \bar{\beta}_{ij} := \min\left\{w_{ij}(\bar{f}_{ij})^2, \bar{\pi}_i - \underline{\pi}_j\right\}.$$

For each passive element $(i,j) \in \tilde{\mathcal{P}}$, we concentrate on the following set defined by equation (3.7a) over the rectangle $\mathcal{R}_{ij}$:

$$\mathcal{X}_{ij} := \{(f, \pi) \in \mathcal{R}_{ij} : \pi = w_{ij} |f| f\}.$$

The red region in Figure 3.2 shows the rectangle $\mathcal{R}_{ij}$, whereas the blue curve shows the set of (f, π) points defined by $\mathcal{X}_{ij}$. We now define the binary variable $z_{ij} \in \{0, 1\}$ for each arc $(i,j) \in \tilde{\mathcal{P}}$, which takes the value one if the direction of the gas flow through this arc is positive, and 0 otherwise.

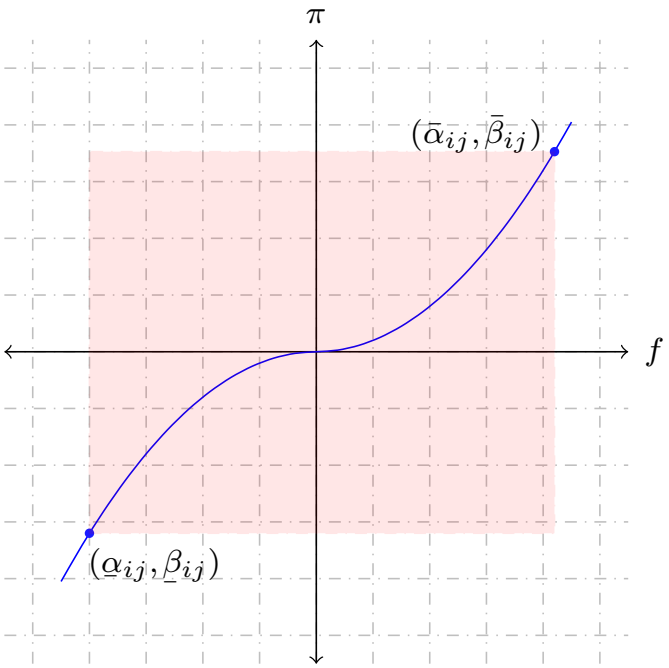

Figure 3.2 The curve in the (f, π) space.

In the remainder of this section, we construct different sets which are used as outer-approximations of $\mathcal{X}$. We present these sets by dropping (i, j) indices, and explicitly specify i or j indices whenever necessary.

Note that in some test instances, it is indeed the case that $\underline{\alpha} = \underline{\beta} = 0$. This clearly implies that the direction of the flow is known to be positive. Thus, we first present an outer-approximation of $\mathcal{X}$ for the passive elements with the bounds $\underline{\alpha} = \underline{\beta} = 0$. In such cases, the gas flows from node i to node j, and the pressure loss induced by passive arc (i, j) is given by $\pi_i - \pi_j$ for $(i, j) \in \tilde{\mathcal{P}}$. Then, equation (3.7a) reduces to the the positive half of the curve whose endpoints are $(0, 0)$ and $(\bar{\alpha}, \bar{\beta})$ in the space of (f, π). By adding the chord of this curve passing through these points, we have a linear approximation of $\mathcal{X}$ given by

$$\mathcal{K}^0_{LP} := \{(f, \pi) \in \mathbb{R}^2_+ : \pi \leq (\bar{\alpha}/\bar{\beta}) f\}.$$

Note that the formulation based on $\mathcal{K}^0_{LP}$ is very weak. By using the SOCr of the convex hull of the set defined by equation (3.7a), we also obtain a quadratic outer-approximation of $\mathcal{X}$ given by

$$\mathcal{K}^0_{SOCP} := \{(f, \pi) \in \mathbb{R}^2_+ : \pi \geq w f^2, \pi \leq (\bar{\alpha}/\bar{\beta}) f\}.$$

Note that the first constraint in $\mathcal{K}^0_{SOCP}$ is SOCr. Moreover, $\mathcal{K}^0_{SOCP}$ represents the convex hull of $\mathcal{X}$ whenever the direction of the gas flow is positive. Observe that

both $\mathcal{K}^0_{LP}$ and $\mathcal{K}^0_{SOCP}$ are defined in the original space. It is also easy to see that $\mathcal{K}^0_{SOCP} \subseteq \mathcal{K}^0_{LP}$. In the remainder of this section, we assume that $\underline{\alpha}_{ij} < 0 < \bar{\alpha}_{ij}$ and $\underline{\beta}_{ij} < 0 < \bar{\beta}_{ij}$ for each passive element $(i,j) \in \tilde{\mathcal{P}}$. Our convexification approaches use the polyhedral outer-approximation and the SOCr outer-approximations of $\mathcal{X}$, where the latter benefits from z_{ij} variables as well as auxiliary variables.

3.4.1 Polyhedrally-representable Set

In this section, we present a "cheap" approximation of $\mathcal{X}$. In particular, we use four hyperplanes to obtain an outer-approximation of this set. Our construction is geometrically summarized in Figure 3.3.

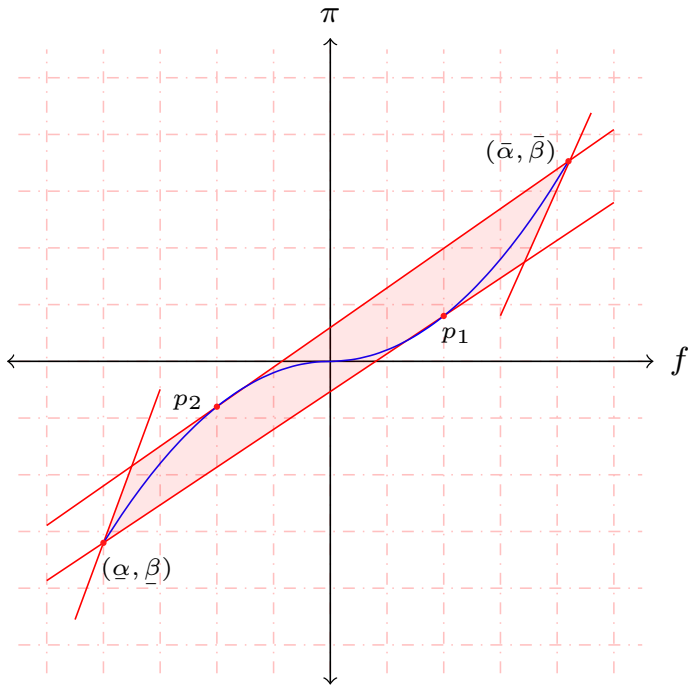

Figure 3.3 Polyhedral outer-approximation of $\mathcal{X}$.

To be precise, we first find the line passing through $(\underline{\alpha}, \underline{\beta})$ and tangent to the curve at point $p_1 = (a, wa^2)$ with $f, \pi \geq 0$. Similarly, we obtain the line passing through $(\bar{\alpha}, \bar{\beta})$ and tangent to this curve at point $p_2 = (a, -wa^2)$ with $f, \pi \leq 0$. For the remaining hyperplanes, we find two tangent lines to this curve at the points $(\underline{\alpha}, \underline{\beta})$ and $(\bar{\alpha}, \bar{\beta})$, respectively. After some simple calculations, these four hyperplanes are given by

$$\pi_i - \pi_j \geq w_{ij} a_{ij} (2 f_{ij} - a_{ij}) \qquad (i,j) \in \tilde{\mathcal{P}} \tag{3.14a}$$

$$\pi_i - \pi_j \leq w_{ij} b_{ij} (b_{ij} - 2f_{ij}) \qquad (i,j) \in \tilde{\mathcal{P}} \tag{3.14b}$$

$$\pi_i - \pi_j \geq w_{ij} \bar{\alpha}_{ij} (2f_{ij} - \bar{\alpha}_{ij}) \qquad (i,j) \in \tilde{\mathcal{P}} \tag{3.14c}$$

$$\pi_i - \pi_j \leq w_{ij} \underline{\alpha}_{ij} (\underline{\alpha}_{ij} - 2f_{ij}) \qquad (i,j) \in \tilde{\mathcal{P}}, \tag{3.14d}$$

where $a_{ij} = (1-\sqrt{2})\underline{\alpha}_{ij}$ and $b_{ij} = (1-\sqrt{2})\bar{\alpha}_{ij}$. Thus, we have a polyhedral outer-approximation of $\mathcal{X}$ given by

$$\mathcal{K}^1_{LP} := \{(f,\pi) \in \mathcal{R} : (3.14)\}.$$

Proposition 3.2 *The set $\mathcal{K}^1_{LP}$ forms an outer-approximation of $\mathcal{X}$.*

We note that $\mathcal{X}$ can be approximated better by applying piecewise linearization (see, e.g., Pfetsch et al. (2015)). However, such a formulation requires using "many" binary variables even for a single passive arc. In this case, the global solver might fail to provide even locally optimal solutions as the size of the gas network increases due to the time limit. In the next sections, we approximate $\mathcal{X}$ with MISOCr sets by using only one binary z_{ij} variable for each passive arc, which represents the direction of the gas flow through $(i,j) \in \tilde{\mathcal{P}}$.

3.4.2 MISOCr Set I

In order to remove the absolute value from the nonconvex constraint (3.7a), we define two new nonnegative variables f^+_{ij} and f^-_{ij} for each passive element $(i,j) \in \tilde{\mathcal{P}}$. If the direction of the gas flow is positive, the pressure loss $\pi_i - \pi_j = w_{ij}(f^+_{ij})^2 \geq 0$ and $f^-_{ij} = 0$. In case of a negative gas flow, the pressure loss is given by $\pi_j - \pi_i = w_{ij}(f^-_{ij})^2 \geq 0$, and $f^+_{ij} = 0$ holds. These conditions can be modeled by the following set of constraints:

$$\pi_i - \pi_j = w_{ij}((f^+_{ij})^2 - (f^-_{ij})^2) \qquad (i,j) \in \tilde{\mathcal{P}} \tag{3.15a}$$

$$f_{ij} = f^+_{ij} - f^-_{ij} \qquad (i,j) \in \tilde{\mathcal{P}} \tag{3.15b}$$

$$0 \leq f^+_{ij} \leq \bar{\alpha}_{ij} z_{ij} \qquad (i,j) \in \tilde{\mathcal{P}} \tag{3.15c}$$

$$0 \leq f^-_{ij} \leq -\underline{\alpha}_{ij}(1 - z_{ij}) \qquad (i,j) \in \tilde{\mathcal{P}} \tag{3.15d}$$

$$\underline{\beta}_{ij} \leq \pi_i - \pi_j \leq \bar{\beta}_{ij} \qquad (i,j) \in \tilde{\mathcal{P}}. \tag{3.15e}$$

Although the absolute value is removed from constraint (3.7a) by using z_{ij} variables, this formulation is still nonconvex due to equality constraint (3.15a) with quadratic terms. Now, observe that constraint (3.15a) can be equivalently rewritten as

$$\pi_i - \pi_j \geq w_{ij}((f_{ij}^+)^2 - (f_{ij}^-)^2) \qquad (i,j) \in \tilde{\mathcal{P}} \tag{3.16a}$$

$$\pi_i - \pi_j \leq w_{ij}((f_{ij}^+)^2 - (f_{ij}^-)^2) \qquad (i,j) \in \tilde{\mathcal{P}}. \tag{3.16b}$$

Also, $f_{ij}^+ \leq \bar{\alpha}_{ij}$ and $f_{ij}^- \leq -\underline{\alpha}_{ij}$ since $z_{ij} \in \{0,1\}$. By using these bounds along with constraints (3.16), we obtain the following valid constraints:

$$\pi_i - \pi_j \geq w_{ij}((f_{ij}^+)^2 + \underline{\alpha}_{ij} f_{ij}^-) \qquad (i,j) \in \tilde{\mathcal{P}} \tag{3.17a}$$

$$\pi_i - \pi_j \leq w_{ij}(\bar{\alpha}_{ij} f_{ij}^+ - (f_{ij}^-)^2) \qquad (i,j) \in \tilde{\mathcal{P}}. \tag{3.17b}$$

Observe that constraints (3.17a) and (3.17b) are SOCr. Thus, we have an outer-approximation of $\mathcal{X}$ with an MISOCr set defined as

$$\mathcal{K}^1_{SOCP} := \{(f,\pi) \in \mathbb{R}^2 : \exists (f^+, f^-, z) \in \mathbb{R}^2 \times \{0,1\} : (3.15b) - (3.15e), (3.17)\}.$$

Proposition 3.3 *The set $\mathcal{K}^1_{SOCP}$ forms an outer-approximation of $\mathcal{X}$.*

Note that a similar formulation is proposed in the work by Schwele et al. (2019) for the gas transmission problem by omitting constraint (3.16b). The big-M formulations are applied to constraint (3.16a), which results in bilinear terms with large bounds, and the McCormick envelopes are constructed for these terms.

3.4.3 MISOCr Set II

In this section, we present another exact reformulation of $\mathcal{X}$. We can easily remove the absolute value from equation (3.7a) by using z_{ij} variables. In particular, we ensure that left-hand side this constraint is $\pi_i - \pi_j$ whenever the gas flow is positive through passive arc (i,j), and $\pi_j - \pi_i$ otherwise. We model these conditions with the following set of constraints:

$$(2z_{ij} - 1)(\pi_i - \pi_j) = w_{ij} f_{ij}^2 \qquad (i,j) \in \tilde{\mathcal{P}} \tag{3.18a}$$

$$\underline{\beta}_{ij}(1 - z_{ij}) \leq \pi_i - \pi_j \leq \bar{\beta}_{ij} z_{ij} \qquad (i,j) \in \tilde{\mathcal{P}} \tag{3.18b}$$

$$\underline{\alpha}_{ij}(1 - z_{ij}) \leq f_{ij} \leq \bar{\alpha}_{ij} z_{ij} \qquad (i,j) \in \tilde{\mathcal{P}}. \tag{3.18c}$$

Observe that this formulation is nonconvex due to the bilinear terms in the equality constraint (3.18a). In order to represent the bilinear term at the left-hand side of this constraint, we introduce the variable $\bar{\pi}_{ij}$ for each passive arc $(i,j) \in \tilde{\mathcal{P}}$. After replacing $(2z_{ij}-1)(\pi_i-\pi_j)$ by $\bar{\pi}_{ij}$, constraint (3.18a) can be relaxed into a quadratic constraint. Also, the term $\bar{\pi}_{ij} = (2z_{ij}-1)(\pi_i-\pi_j)$ can be linearized with the McCormick envelopes. Finally, we obtain the following set of constraints:

$$\bar{\pi}_{ij} \geq w_{ij} f_{ij}^2 \qquad (i,j) \in \tilde{\mathcal{P}} \tag{3.19a}$$

$$(\bar{\pi}_{ij}, 2z_{ij}-1, \pi_i-\pi_j) \in \mathcal{M}(-1,1,\underline{\beta}_{ij},\bar{\beta}_{ij}) \qquad (i,j) \in \tilde{\mathcal{P}}. \tag{3.19b}$$

Here, constraint (3.19a) is SOCr whereas the set defined by constraint (3.19b) is polyhedral. In fact, constraint (3.19a) represents the epigraph of $\bar{\pi}_{ij} = w_{ij} f_{ij}^2$ in the $(f,\bar{\pi})$-space, which is also its convex hull. Note that the linearization in constraint (3.19b) is exact since z_{ij} is binary. Finally, we have an outer-approximation of $\mathcal{X}$:

$$\mathcal{K}^2_{SOCP} := \{(f,\pi) \in \mathbb{R}^2 : \exists (\bar{\pi}, z) \in \mathbb{R} \times \{0,1\} : (3.18b), (3.18c), (3.19)\}.$$

Proposition 3.4 *The set $\mathcal{K}^2_{SOCP}$ forms an outer-approximation of $\mathcal{X}$.*

Note that a similar formulation is also proposed in Borraz-Sánchez et al. (2016) without constraints (3.18b) and (3.18c) for the gas expansion planning problem.

3.4.4 MISOCr Set III

In this section, we define two new variables π'_{ij} and π''_{ji} for each $(i,j) \in \tilde{\mathcal{P}}$ in order to model the pressure loss between adjacent nodes. We enforce one of these variables to be 0 in case of the positive or negative gas flow. In the former case, $\pi'_{ij} = \pi_i - \pi_j \in [0, \bar{\beta}]$ and $\pi''_{ji} = 0$. However, if the gas flow is negative, $\pi''_{ji} = \pi_i - \pi_j \in [\underline{\beta}, 0]$ and $\pi'_{ij} = 0$. These conditions are given by the following set of constraints:

$$\pi'_{ij} - \pi''_{ji} = w_{ij} f_{ij}^2 \qquad (i,j) \in \tilde{\mathcal{P}} \tag{3.20a}$$

$$\pi_i - \pi_j \leq \pi'_{ij} \leq \pi_i - \pi_j - \underline{\beta}_{ij}(1-z_{ij}) \qquad (i,j) \in \tilde{\mathcal{P}} \tag{3.20b}$$

$$\pi_i - \pi_j - \bar{\beta}_{ij} z_{ij} \leq \pi''_{ji} \leq \pi_i - \pi_j \qquad (i,j) \in \tilde{\mathcal{P}} \tag{3.20c}$$

$$0 \leq \pi'_{ij} \leq \bar{\beta}_{ij} z_{ij} \qquad (i,j) \in \tilde{\mathcal{P}} \tag{3.20d}$$

$$\underline{\beta}_{ij}(1-z_{ij}) \leq \pi''_{ji} \leq 0 \qquad (i,j) \in \tilde{\mathcal{P}} \tag{3.20e}$$

$$\underline{\alpha}_{ij}(1-z_{ij}) \le f_{ij} \le \bar{\alpha}_{ij} z_{ij} \qquad (i,j) \in \tilde{\mathcal{P}}. \tag{3.20f}$$

Observe that this formulation is nonconvex due to constraint (3.20a), which can be relaxed into an SOCr constraint as

$$\pi'_{ij} - \pi''_{ji} \ge w_{ij} f_{ij}^2 \qquad (i,j) \in \tilde{\mathcal{P}}. \tag{3.21}$$

Note that the convex hull of the set induced by constraint (3.20a) is defined by inequality (3.21). Finally, we have an outer-approximation of $\mathcal{X}$:

$$\mathcal{K}^3_{SOCP} := \{(f,\pi) \in \mathbb{R}^2 : \exists (\pi', \pi'', z) \in \mathbb{R}^2 \times \{0,1\} : (3.20\text{b}) - (3.20\text{f}), (3.21)\}.$$

Proposition 3.5 *The set $\mathcal{K}^3_{SOCP}$ forms an outer-approximation of $\mathcal{X}$.*

3.4.5 MISOCr Set IV

For each $(i,j) \in \tilde{\mathcal{P}}$, we define new variables $f_{ij}^+, f_{ij}^-, \pi_i^+, \pi_j^+, \pi_i^-, \pi_j^-$ as $f_{ij} = f_{ij}^+ + f_{ij}^-$, $\pi_i = \pi_i^+ + \pi_i^-$ and $\pi_j = \pi_j^+ + \pi_j^-$. As before, we enforce exactly one of these new variables of each type to take the value zero depending on the direction of the gas flow. In particular, the gas flow $f_{ij}^+ \ge 0$ and the squared pressure loss is $\pi_i^+ - \pi_j^+ \ge 0$ if and only if $z = 1$. On the other hand, $z_{ij} = 0$ holds if and only if $f_{ij}^- \le 0$, and the pressure loss is $\pi_j^- - \pi_i^- \ge 0$. These conditions are modeled by the following set of constraints:

$$\pi_i^+ - \pi_j^+ = w_{ij}(f_{ij}^+)^2 \qquad (i,j) \in \tilde{\mathcal{P}} \tag{3.22a}$$
$$\pi_j^- - \pi_i^- = w_{ij}(f_{ij}^-)^2 \qquad (i,j) \in \tilde{\mathcal{P}} \tag{3.22b}$$
$$f_{ij} = f_{ij}^+ + f_{ij}^- \qquad (i,j) \in \tilde{\mathcal{P}} \tag{3.22c}$$
$$\pi_i = \pi_i^+ + \pi_i^-,\ \pi_j = \pi_j^+ + \pi_j^- \qquad (i,j) \in \tilde{\mathcal{P}} \tag{3.22d}$$
$$\underline{\pi}_i z_{ij} \le \pi_i^+ \le \bar{\pi}_i z_{ij} \qquad (i,j) \in \tilde{\mathcal{P}} \tag{3.22e}$$
$$\underline{\pi}_j z_{ij} \le \pi_j^+ \le \bar{\pi}_j z_{ij} \qquad (i,j) \in \tilde{\mathcal{P}} \tag{3.22f}$$
$$\underline{\pi}_i (1-z_{ij}) \le \pi_i^+ \le \bar{\pi}_i (1-z_{ij}) \qquad (i,j) \in \tilde{\mathcal{P}} \tag{3.22g}$$
$$\underline{\pi}_j (1-z_{ij}) \le \pi_j^+ \le \bar{\pi}_j (1-z_{ij}) \qquad (i,j) \in \tilde{\mathcal{P}} \tag{3.22h}$$
$$0 \le \pi_i^+ - \pi_j^+ \le \bar{\beta}_{ij} z_{ij} \qquad (i,j) \in \tilde{\mathcal{P}} \tag{3.22i}$$
$$\underline{\beta}_{ij} \le \pi_i^- - \pi_j^- \le 0 \qquad (i,j) \in \tilde{\mathcal{P}} \tag{3.22j}$$

$$0 \leq f_{ij}^{+} \leq \bar{\alpha}_{ij} \qquad (i,j) \in \tilde{\mathcal{P}} \tag{3.22k}$$

$$\underline{\alpha}_{ij} \leq f_{ij}^{-} \leq 0 \qquad (i,j) \in \tilde{\mathcal{P}}. \tag{3.22l}$$

Note that the set defined by system (3.22) is still nonconvex due to constraints (3.22a) and (3.22b). These constraints can be relaxed into SOCr constraints as

$$\pi_i^{+} - \pi_j^{+} \geq w_{ij}(f_{ij}^{+})^2 \qquad (i,j) \in \tilde{\mathcal{P}} \tag{3.23a}$$

$$\pi_j^{-} - \pi_i^{-} \geq w_{ij}(f_{ij}^{-})^2 \qquad (i,j) \in \tilde{\mathcal{P}}, \tag{3.23b}$$

which represent the convex hull of the sets defined by equations (3.22a) and (3.22b), respectively. Observe that all continuous variables are bounded by closed intervals in system (3.22). Thus, we tighten the formulation in system (3.23) by using the following two halfspaces:

$$\pi_i^{+} - \pi_j^{+} \leq (\bar{\beta}_{ij}/\bar{\alpha}_{ij}) f_{ij}^{+}, \quad \pi_i^{-} - \pi_j^{-} \geq (\underline{\beta}_{ij}/\underline{\alpha}_{ij}) f_{ij}^{-} \qquad (i,j) \in \tilde{\mathcal{P}}. \tag{3.24}$$

Finally, we have an outer-approximation of $\mathcal{X}$ is given by the following MISOCr set:

$$\begin{aligned} \mathcal{K}_{SOCP}^{4} := \{(f,\pi) \in \mathbb{R}^2 : \exists (\pi^{+},\pi^{-},f^{+},f^{-},z) \in \mathbb{R}^6 \times \{0,1\} \\ : (3.22c) - (3.22l), (3.23), (3.24)\}. \end{aligned}$$

Proposition 3.6 *The set $\mathcal{K}_{SOCP}^{4}$ forms an outer-approximation of $\mathcal{X}$.*

3.5 Solution Methodology

In this section, we describe our solution framework for solving the multi-period gas storage optimization problem (3.10). Our two-step procedure is summarized in Algorithm 4. The input of this algorithm is the type of the mixed-integer convex relaxation of problem (3.10). We denote the tolerance of our algorithm by ϵ. In Step 1 of Algorithm 4, a mixed-integer convex relaxation of our choice is solved to optimality. The dual bound for this relaxation provides a lower bound on the objective value of problem (3.10). In order to obtain (locally) optimal solutions, all the optimal binary values x^* produced by the relaxation are fixed, which reduces problem (3.10) to a nonlinear program (NLP). By passing the optimal continuous

values y^* produced by the relaxation as the initial point, we solve this program with a local interior point solver in Step 4. If the solver converges to a (locally) optimal solution, which is also feasible for problem (3.10), we have an upper bound on its optimal objective value. By using these lower and upper bounds, the relative optimality gap in percentages is calculated.

Algorithm 4 MINLP

Input: `convexRelaxation`.

Output: Primal and dual bounds for problem (3.10), the relative optimality gap in percentages.

1: Solve `convexRelaxation` of problem (3.10).
2: Obtain ϵ-optimal $x^* = (x, x^+, x^-, u, v)$ and $y^* = (\pi, f, s, s^+, s^-, l, l^+, l^-)$ solutions produced by `convexRelaxation`.
3: Assign the dual bound of `convexRelaxation` to LB.
4: Solve problem (3.10) by fixing x^* and passing y^* as an initial point.
5: Assign the primal bound of problem (3.10) to UB.
6: Assign the relative optimality $(1 - LB/UB)\%$ to Gap.
7: **return** LB, UB, Gap.

We conclude this section by describing the mixed-integer convex relaxations proposed for the multi-period gas storage optimization problem (3.10). These relaxations differ from each other in terms of the choice of the outer-approximation of $\mathcal{X}$ as explained in Section 3.4. Thus, we consider the following cases for `convexRelaxation` in Algorithm 4:

- `MILP`$_0$: The MILP relaxation under $\mathcal{K}^0_{LP}$.
- `MILP`$_1$: The MILP relaxation under $\mathcal{K}^1_{LP}$.
- `MISOCP`$_0$: The MISOCP relaxation under $\mathcal{K}^0_{SOCP}$.
- `MISOCP`$_1$: The MISOCP relaxation under $\mathcal{K}^1_{SOCP}$.
- `MISOCP`$_2$: The MISOCP relaxation under $\mathcal{K}^2_{SOCP}$.
- `MISOCP`$_3$: The MISOCP relaxation under $\mathcal{K}^3_{SOCP}$.
- `MISOCP`$_4$: The MISOCP relaxation under $\mathcal{K}^4_{SOCP}$.

Note that the MISOCr set $\mathcal{Y}$ as in formulation (3.13) for compressors is used in each of these relaxations.

In this section, we present the results of our computational study conducted on various GasLib test instances from the literature (Schmidt, Aßmann, Burlacu, Humpola, Joormann, Kanelakis, Koch, Oucherif, Pfetsch, Schewe, Schwarz & Sirvent, 2017). We focus on a short-term gas network operations and let $|\mathcal{T}| = 24$. Note that demand parameters in GasLib instances are given for a single-period. Thus, we generate a new demand dataset by using the 24-hour gas demand data in Schwele et al. (2019) such that the single-period demand from GasLib instances is the average gas demand within the planning horizon. Table 3.1 shows the cardinality of gas network elements for all the test instances used in our study. All computational experiments are conducted on a 64-bit workstation with two Intel(R) Xeon(R) Gold 6248R CPU (3.00GHz) processors. The workstation runs on the Windows operations system and has 256 GB 2993 Mhz RAM. All mixed-integer convex relaxations for the multi-period gas storage optimization problem are solved by using GUROBI 9.5.0 (Gurobi Optimization, 2022). After fixing the binary variables obtained from these relaxations, the resulting NLP is solved by the interior point solver IPOPT 3.11.1 (Wächter & Biegler, 2006). For these NLPs, the `the bound_relax_factor` parameter is set to 0 in IPOPT. We also compare the computational performance of our approaches by directly solving problem (3.10) over the rectangle $\mathcal{R}$ with the global solver `BARON` (Tawarmalani & Sahinidis, 2005). The wall-clock time limit for each computational experiment is set to one hour. All computational experiments are measured in seconds. In order to assess the scalability of our approaches, we also stress the gas network by scaling the gas demand from 1.25 up to 2.00 for each test instance. We present our computational results by presenting the following metrics that are obtained within Algorithm 4:

- LB: Lower bound obtained by `convexRelaxation`.
- UB: Upper bound obtained by the NLP.
- Relax. Time: CPU time in `convexRelaxation`.
- Total Time: Total CPU time.
- Gap (%): The relative optimality gap in percentages.

The abbreviation “inf” (under column “LB”) is used if the mixed-integer convex relaxation is proven to be infeasible. Under “UB” columns, we use the abbreviation “local inf” if the local solver converges to a locally infeasible solution. Under “Relax. Time” and “Total Time” columns, we use the abbreviation “TL” if the one-hour time limit has been reached.

Instance	$\lvert\mathcal{N}\rvert$	$\lvert\mathcal{N}_{source}\rvert$	$\lvert\mathcal{N}_{sink}\rvert$	$\lvert\mathcal{P}'\rvert$	$\lvert\mathcal{P}''\rvert$	$\lvert\mathcal{P}'''\rvert$	$\lvert\mathcal{R}\rvert$	$\lvert\mathcal{V}\rvert$	$\lvert\mathcal{C}\rvert$
Gaslib-11	11	3	3	8	0	0	1	0	2
Gaslib-24	24	3	5	19	1	1	0	1	3
Gaslib-40	40	3	29	39	0	0	0	0	6
Gaslib-134	134	3	45	86	0	45	0	1	1

Table 3.1 GasLib Instances.

In Table 3.2, we present our results on the GasLib-11 instance. In terms of computational times, our mixed-integer convex relaxation methods perform better than `BARON` under all demand scales. Also, all the proposed methods result in the same dual bounds. However, only $\texttt{MISOCP}_3$ is able to provide the best feasible solution among them. In fact, these solutions obtained by $\texttt{MISOCP}_3$ are optimal. Under 1.25 scale, all of these methods also solve the problem to optimality, whereas they fail to prove infeasibility under 1.75 scale. Still, we note that this small-scale instance is very easy to solve since there is no cycle consisting of passive network elements, and the directions of the gas flow through compressors are known to be positive.

We present the computational results on the GasLib-24 instance in Table 3.3. Note that all lower limits for gas flows in this instance are given as zero, which implies that the gas flow directions are all positive i.e., $\underline{\alpha} = \underline{\beta} = 0$. Hence, we use the mixed-integer convex relaxations $\texttt{MILP}_0$ and $\texttt{MISOCP}_0$. Whenever our problem is feasible, both of these methods provide the same dual bound. Also, they prove infeasibility in less than two seconds under 1.75 and 2.00 scales. Although this is a small-scale instance with unidirectional gas flows, `BARON` reaches to the one-hour time limit whenever the problem is feasible. While the optimality gaps under `BARON` are smaller than those under our methods, all of these methods result in the same feasible solution in terms of the objective value.

Scale	Method	LB	UB	Relax. Time	Total Time	Gap (%)
1.00	MILP$_1$	70463.22	70501.73	0.81	1.93	0.05
	MISOCP$_1$	70463.22	70495.16	0.91	2.21	0.05
	MISOCP$_2$	70463.22	70499.74	1.10	2.57	0.05
	MISOCP$_3$	70463.22	70474.25	0.96	2.09	0.02
	MISOCP$_4$	70463.22	70477.43	1.33	2.49	0.02
	BARON	70474.20	70474.25	-	35.25	0.00
1.25	MILP$_1$	85270.02	85272.21	0.91	3.63	0.00
	MISOCP$_1$	85270.02	85272.21	0.94	2.21	0.00
	MISOCP$_2$	85270.02	85272.21	0.95	2.10	0.00
	MISOCP$_3$	85270.02	85272.21	0.96	2.58	0.00
	MISOCP$_4$	85270.02	85272.21	1.33	2.95	0.00
	BARON	85272.13	85272.21	-	9.02	0.00
1.50	MILP$_1$	100076.83	100482.34	0.91	1.94	0.40
	MISOCP$_1$	100076.83	100447.63	0.97	2.12	0.37
	MISOCP$_2$	100076.83	100412.15	0.91	2.29	0.33
	MISOCP$_3$	100076.83	100366.10	0.96	2.29	0.29
	MISOCP$_4$	100076.83	100378.72	1.21	2.32	0.30
	BARON	100282.75	100366.10	-	TL	0.08
1.75	MILP$_1$	114883.63	local inf	0.94	2.62	NA
	MISOCP$_1$	114883.63	local inf	0.91	2.97	NA
	MISOCP$_2$	114883.63	local inf	0.94	2.78	NA
	MISOCP$_3$	114883.63	local inf	0.95	2.92	NA
	MISOCP$_4$	114883.63	local inf	1.13	3.25	NA
	BARON	inf	-	-	1.50	NA
2.00	MILP$_1$	inf	-	3.29	-	NA
	MISOCP$_1$	inf	-	4.73	-	NA
	MISOCP$_2$	inf	-	4.94	-	NA
	MISOCP$_3$	inf	-	5.03	-	NA
	MISOCP$_4$	inf	-	10.36	-	NA
	BARON	inf	-	-	1.00	NA

Table 3.2 Computational Results on GasLib-11.

Table 3.4 presents the computational results on the GasLib-40 instance. Note that this network has six fundamental cycles containing both passive and active elements. We encounter some persistent issues with BARON for this instance. Interestingly, BARON claims false infeasibility under all demand scales. We try to overcome this by solving our problem in a shorter planning horizon and decreasing the demand scales. BARON also falsely states upon termination that these cases are also infeasible. Under 1.00 scale, all of our methods are able to find the global optimal solution. Although MILP$_1$ is better than other methods in terms of computational times, the quality of the solutions obtained by this method worsens for the congested networks. MISOCP$_4$ provides better dual bounds than the other methods within one-hour time limit. Both MISOCP$_1$ and MISOCP$_4$ are able to find feasible solutions with the same

objective value except under 2.00 scale. Still, MISOCP$_4$ is faster than MISOCP$_1$ for the cases that the one-hour time limit is not reached.

Scale	Method	LB	UB	Relax. Time	Total Time	Gap (%)
1.00	MILP$_0$	134991.60	136417.26	1.22	3.65	1.05
	MISOCP$_0$	134991.60	136417.26	1.34	2.93	1.05
	BARON	135710.56	136417.26	-	TL	0.52
1.25	MILP$_0$	164525.99	165297.66	1.16	2.87	0.47
	MISOCP$_0$	164525.99	165297.66	1.34	2.90	0.47
	BARON	164776.57	165297.66	-	TL	0.32
1.50	MILP$_0$	194060.39	194268.17	1.08	3.24	0.11
	MISOCP$_0$	194060.39	194268.17	1.26	3.46	0.11
	BARON	194071.74	194268.17	-	TL	0.10
1.75	MILP$_0$	inf	-	1.51	-	NA
	MISOCP$_0$	inf	-	1.83	-	NA
	BARON	inf	-	-	1.11	NA
2.00	MILP$_0$	inf		1.57	-	NA
	MISOCP$_0$	inf	-	1.83	-	NA
	BARON	inf	-	-	1.17	NA

Table 3.3 Computational Results on GasLib-24.

In Table 3.5 presents the computational results on the Gaslib-134 instance. Note that this is a tree-structured gas network. Similar to the GasLib-40 instance, we have some interesting results for BARON. In our first experiments, BARON returns the "Problem is numerically sensitive" message and the "Best possible" objective values are inconsistent among each experiment. After multiple attempts, we present the results for BARON, which are consistent with our methods. Our methods provide the identical dual bounds for all cases. Although the difference between the upper bounds obtained by these methods is negligible under 2.00 scale, MISOCP$_2$ and MISOCP$_4$ find better feasible solutions than other methods. For most of the cases, our methods are able to find high-quality feasible solutions less than three minutes.

We summarize our observations on the computational results as follows. In our experiments, MILP$_1$ is faster than our other methods in almost all cases. However, our MISOCP-based methods are able to produce better dual bounds than those obtained by MILP$_1$. Also, MISOCP$_1$ and MISOCP$_4$ are consistently better than MISOCP$_2$ and MISOCP$_3$ in terms of the quality of the feasible solutions obtained by these methods for medium-scale instances. Still, MISOCP$_4$ is more promising in terms of (near) globally optimal solutions. Although BARON is seemingly better than our methods for the GasLib-11 instance, it is computationally very expensive compared to our methods for the GasLib-24 instance. Moreover, it produces unreliable results for medium-scale instances such as false infeasibility claims and inconsistent bounds

on the underlying problem. Our methods produce consistent results in only a few seconds, which is significantly less than the one-hour run time of BARON.

Scale	Method	LB	UB	Relax. Time	Total Time	Gap (%)
1.00	$\texttt{MILP}_1$	449864.73	449864.73	2.48	126.85	0.00
	$\texttt{MISOCP}_1$	449864.73	449864.73	3.97	57.82	0.00
	$\texttt{MISOCP}_2$	449864.73	449864.73	11.57	79.20	0.00
	$\texttt{MISOCP}_3$	449864.73	449864.73	9.29	59.86	0.00
	$\texttt{MISOCP}_4$	449864.73	449864.73	9.40	19.43	0.00
	BARON	-	-	-	334.86	NA
1.25	$\texttt{MILP}_1$	555308.41	581137.61	2.57	22.07	4.44
	$\texttt{MISOCP}_1$	576636.31	576636.31	34.36	49.91	0.00
	$\texttt{MISOCP}_2$	576636.31	588633.14	92.42	160.47	2.04
	$\texttt{MISOCP}_3$	576636.16	581908.99	428.30	513.20	0.91
	$\texttt{MISOCP}_4$	576636.31	576636.31	33.69	77.77	0.00
	BARON	-	-	-	378.10	301.39
1.50	$\texttt{MILP}_1$	688036.09	832845.33	2.59	97.55	17.39
	$\texttt{MISOCP}_1$	832839.55	832845.33	449.86	496.14	0.00
	$\texttt{MISOCP}_2$	727306.20	840945.33	TL	3696.89	13.51
	$\texttt{MISOCP}_3$	738422.20	840945.33	TL	3680.89	12.19
	$\texttt{MISOCP}_4$	832839.55	832845.33	193.24	219.18	0.00
	BARON	-	-	-	350.46	NA
1.75	$\texttt{MILP}_1$	942990.22	1325219.89	2.45	97.02	28.84
	$\texttt{MISOCP}_1$	1285470.92	1325219.89	TL	3670.79	3.00
	$\texttt{MISOCP}_2$	923227.07	1368686.13	TL	3661.49	32.55
	$\texttt{MISOCP}_3$	951265.64	1341929.24	TL	3686.94	29.11
	$\texttt{MISOCP}_4$	1297252.37	1325219.89	TL	3630.95	2.11
	BARON	-	-	-	403.74	NA
2.00	$\texttt{MILP}_1$	1460189.51	2315998.40	2.44	65.31	36.95
	$\texttt{MISOCP}_1$	2149490.27	2315980.38	TL	3643.54	7.19
	$\texttt{MISOCP}_2$	1915562.66	2307121.71	TL	3694.44	16.97
	$\texttt{MISOCP}_3$	1912566.90	2313062.68	TL	3670.58	17.31
	$\texttt{MISOCP}_4$	2158947.81	2309063.38	TL	3650.95	6.50
	BARON	-	-	-	433.66	NA

Table 3.4 Computational Results on GasLib-40.

Scale	Method	LB	UB	Relax. Time	Total Time	Gap (%)
1.00	$\texttt{MILP}_1$	76725.58	76751.89	2.38	93.99	0.03
	$\texttt{MISOCP}_1$	76725.58	76751.89	3.21	123.80	0.03
	$\texttt{MISOCP}_2$	76725.58	76751.89	3.51	118.24	0.03
	$\texttt{MISOCP}_3$	76725.58	76751.89	4.10	91.15	0.03
	$\texttt{MISOCP}_4$	76725.58	76751.89	6.28	96.03	0.03
	BARON	76751.81	76751.89	-	23.63	0.00
1.25	$\texttt{MILP}_1$	94502.47	94539.20	2.43	84.73	0.04
	$\texttt{MISOCP}_1$	94502.47	94539.20	3.25	82.78	0.04
	$\texttt{MISOCP}_2$	94502.47	94539.19	3.61	114.50	0.04
	$\texttt{MISOCP}_3$	94502.47	94539.20	3.73	129.14	0.04
	$\texttt{MISOCP}_4$	94502.47	94539.19	6.92	124.80	0.04
	BARON	94539.10	94539.19	-	31.36	0.00
1.50	$\texttt{MILP}_1$	112279.37	112329.10	2.72	102.25	0.04
	$\texttt{MISOCP}_1$	112279.37	112329.10	3.38	98.23	0.04
	$\texttt{MISOCP}_2$	112279.37	112329.10	3.61	156.15	0.04
	$\texttt{MISOCP}_3$	112279.37	112329.10	3.72	136.19	0.04
	$\texttt{MISOCP}_4$	112279.37	112329.10	6.61	98.88	0.04
	BARON	112329.04	112329.15	-	46.02	0.00
1.75	$\texttt{MILP}_1$	130056.26	130122.18	2.66	130.99	0.05
	$\texttt{MISOCP}_1$	130056.26	130122.18	3.52	93.95	0.05
	$\texttt{MISOCP}_2$	130056.26	130122.18	3.57	164.56	0.05
	$\texttt{MISOCP}_3$	130056.26	130122.18	3.75	221.40	0.05
	$\texttt{MISOCP}_4$	130056.26	130122.18	6.54	51.99	0.05
	BARON	130122.05	130122.18	-	33.47	0.00
2.00	$\texttt{MILP}_1$	147833.16	147919.02	2.60	103.00	0.06
	$\texttt{MISOCP}_1$	147833.16	147919.02	3.40	138.13	0.06
	$\texttt{MISOCP}_2$	147833.16	147919.02	3.72	195.05	0.06
	$\texttt{MISOCP}_3$	147833.16	147919.02	3.87	149.92	0.06
	$\texttt{MISOCP}_4$	147833.16	147919.02	6.99	129.03	0.06
	BARON	147919.30	147919.45	-	34.90	0.00

Table 3.5 Computational Results on GasLib-134.

3.7 Conclusion

In this work, we study a multi-period gas storage optimization problem under stationary conditions, which contains highly nonlinear, nonconvex and discrete aspects. In order to obtain (near) globally optimal solutions, we propose different mixed-integer convex relaxations for this problem. In this context, we focus on two types of nonconvexity resulting from the Weymouth and fuel gas consumption equations, and then convexify the feasible regions induced by these nonconvex equations with

different polyhedrally-representable and MISOCr sets. We conduct a computational study on small- and medium-scale test instances taken from the literature, and compare our mixed-integer convex relaxation approaches with a state-of-the-art global solver. Our mixed-integer convex relaxations offer initial points which can be used in the local solver. For medium-scale instances, they also consistently produce tight dual bounds as well as high-quality feasible solutions under congested networks. Our approaches lead to numerically more stable results in comparison with the global solver. There is still room for improvement in terms of stronger formulations for our mixed-integer convex relaxations and computational efficiency in medium-scale and congested gas networks.

4. Conclusion

Mathematical programming methods have been very useful tool to solve optimization problems in energy systems. In this thesis, we particularly focused on two of these problems, both of which have potential benefits along with certain challenging aspects. First, we studied the short-term condition-based maintenance and operations planning problem in power systems by considering the unexpected failures of both generators and transmission lines. As this problem was formulated as a two-stage joint chance-constrained stochastic program, dealing with the exponential increase in the number of failure scenarios and the nonconvex nature of the joint-chance constraint was not an easy task. Thus, we proposed a decomposition-based cutting-plane algorithm along with different algorithmic enhancements in order to solve this problem. Later, we focused on the multi-period natural gas storage optimization problem which was formulated as a nonconvex MINLP under stationary conditions. The discrete aspect of this problem was due to the switching decisions of active arcs whereas its nonlinear and nonconvex aspects emerge from the well-known Weymouth equations for pipes and resistors and loss consumption equations for compressors. In order to convexify the feasible region induced by these equations, we derived mixed-integer linear and SOCr outer-approximations. Based on these mixed-integer outer-approximations, we solved our problem with a two-step approach, and obtain (near) globally optimal and high-quality (locally) feasible solutions.

Although we consider some of the challenging aspects of the optimization problems in this thesis, there are more interesting aspects to be introduced in them. In particular, considering different sources of uncertainty such as price and demand uncertainty, and their modeling in both of these problems are recommended. While these uncertainties can be introduced by using the knowledge on the underlying distributions, which can be further exploited in the solution approaches, it may be also interesting to focus on the cases based on empirical distributions in the absence of such distributional information. The integration of gas networks into power systems is another considerable future work.

BIBLIOGRAPHY

Abbasi, E., Fotuhi-Firuzabad, M., & Abiri-Jahromi, A. (2009). Risk based maintenance optimization of overhead distribution networks utilizing priority based dynamic programming. In *2009 IEEE Power Energy Society General Meeting*, (pp. 1–11).

Abiri-Jahromi, A., Fotuhi-Firuzabad, M., & Abbasi, E. (2009). An efficient mixed-integer linear formulation for long-term overhead lines maintenance scheduling in power distribution systems. *IEEE Transactions on Power Delivery*, *24*(4), 2043–2053.

Andre, J., Bonnans, F., & Cornibert, L. (2009). Optimization of capacity expansion planning for gas transportation networks. *European Journal of Operational Research*, *197*(3), 1019–1027.

Babonneau, F., Nesterov, Y., & Vial, J.-P. (2012). Design and Operations of Gas Transmission Networks. *Operations Research*, *60*(1), 34–47.

Basciftci, B., Ahmed, S., & Gebraeel, N. Z. (2020). Data-driven maintenance and operations scheduling in power systems under decision-dependent uncertainty. *IISE Transactions*, *52*(6), 589–602.

Basciftci, B., Ahmed, S., Gebraeel, N. Z., & Yildirim, M. (2018). Stochastic optimization of maintenance and operations schedules under unexpected failures. *IEEE Transactions on Power Systems*, *33*(6), 6755–6765.

Borraz-Sánchez, C., Bent, R., Backhaus, S., Hijazi, H., & Hentenryck, P. V. (2016). Convex relaxations for gas expansion planning. *INFORMS Journal on Computing*, *28*(4), 645–656.

Burer, S. & Letchford, A. N. (2012). Non-convex mixed-integer nonlinear programming: A survey. *Surveys in Operations Research and Management Science*, *17*(2), 97–106.

Burlacu, R., Egger, H., Groß, M., Martin, A., Pfetsch, M. E., Schewe, L., Sirvent, M., & Skutella, M. (2019). Maximizing the storage capacity of gas networks: a global minlp approach. *Optimization and Engineering*, *20*(2), 543–573.

Canto, S. P. (2008). Application of benders' decomposition to power plant preventive maintenance scheduling. *European Journal of Operational Research*, *184*(2), 759–777.

Conejo, A., Garcia-Bertrand, R., & Diaz-Salazar, M. (2005). Generation maintenance scheduling in restructured power systems. *IEEE Transactions on Power Systems*, *20*(2), 984–992.

Correa-Posada, C. M. & Sánchez-Martín, P. (2015). Integrated power and natural gas model for energy adequacy in short-term operation. *IEEE Transactions on Power Systems*, *30*(6), 3347–3355.

de Wolf, D. & Smeers, Y. (2000). The gas transmission problem solved by an extension of the simplex algorithm. *Management Science*, *46*(11), 1454–1465.

Ehrhardt, K. & Steinbach, M. C. (2005). Nonlinear optimization in gas networks. In Bock, H. G., Phu, H. X., Kostina, E., & Rannacher, R. (Eds.), *Modeling, Simulation and Optimization of Complex Processes*, (pp. 139–148)., Berlin, Heidelberg. Springer Berlin Heidelberg.

EIA (2020). Weekly Electricity Consumption from the U.S. Energy Information

Administration. www.eia.gov/electricity/data/browser/.

Finnemore, E. J. & Franzini, J. B. (2002). *Fluid Mechanics with Engineering Applications*. Boston: McGraw-Hill.

Fisher, E. B., O'Neill, R. P., & Ferris, M. C. (2008). Optimal transmission switching. *IEEE Transactions on Power Systems*, *23*(3), 1346–1355.

FRCC (2008). Florida Reliability Coordinating Council Inc System Disturbance and Underfrequency Load Shedding Event Report.

Froger, A., Gendreau, M., Mendoza, J. E., Pinson, E., & Rousseau, L.-M. (2016). Maintenance scheduling in the electricity industry: A literature review. *European Journal of Operational Research*, *251*(3), 695 – 706.

Fu, Y., Li, Z., Shahidehpour, M., Zheng, T., & Litvinov, E. (2009). Coordination of midterm outage scheduling with short-term security-constrained unit commitment. *IEEE Transactions on Power Systems*, *24*(4), 1818–1830.

Fu, Y., Shahidehpour, M., & Li, Z. (2007). Security-constrained optimal coordination of generation and transmission maintenance outage scheduling. *IEEE Transactions on Power Systems*, *22*(3), 1302–1313.

Fügenschuh, A. & Humpola, J. (2013). A Unified View on Relaxations for a Nonlinear Network Flow Problem. Technical Report 13-31, ZIB, Takustr. 7, 14195 Berlin.

Gebraeel, N. (2006). Sensory-based prognostics and life prediction for components with exponential degradation. *SAE Transactions*, *115*, 867–874.

Gebraeel, N. Z., Lawley, M. A., Li, R., & Ryan, J. K. (2005). Residual-life distributions from component degradation signals: A bayesian approach. *IIE Transactions*, *37*(6), 543–557.

Geetha, T. & Swarup, K. S. (2009). Coordinated preventive maintenance scheduling of genco and transco in restructured power systems. *International Journal of Electrical Power & Energy Systems*, *31*(10), 626–638.

Geng, X. & Xie, L. (2019). Data-driven decision making in power systems with probabilistic guarantees: Theory and applications of chance-constrained optimization. *Annual Reviews in Control*, *47*, 341–363.

Gross, M., Pfetsch, M. E., Schewe, L., Schmidt, M., & Skutella, M. (2019). Algorithmic results for potential-based flows: Easy and hard cases. *Networks*, *73*(3), 306–324.

Gurobi Optimization, L. (2022). Gurobi Optimizer Reference Manual. www.gurobi.com/documentation/.

Han, Y. & Song, Y. H. (2003). Condition monitoring techniques for electrical equipment-a literature survey. *IEEE Transactions on Power Delivery*, *18*(1), 4–13.

He, Y., Shahidehpour, M., Li, Z., Guo, C., & Zhu, B. (2018). Robust constrained operation of integrated electricity-natural gas system considering distributed natural gas storage. *IEEE Transactions on Sustainable Energy*, *9*(3), 1061–1071.

Humpola, J. (2014). *Gas Network Optimization by MINLP*. PhD thesis, Technische Universität Berlin.

Koch, T., Pfetsch, M. E., & Schewe, L. (2015). *Evaluating Gas Network Capacities*. SIAM, Philadelphia: SIAM-MOS Series on Optimization.

Labbé, M., Plein, F., Schmidt, M., & Thürauf, J. (2021). Deciding feasibility of a booking in the European gas market on a cycle is in P for the case of passive

networks. *Networks*, *78*(2), 128–152.

Laporte, G. & Louveaux, F. V. (1993). The integer l-shaped method for stochastic integer programs with complete recourse. *Operations Research Letters*, *13*(3), 133–142.

Lv, C., Wang, J., & Sun, P. (2012). Short-term transmission maintenance scheduling based on the benders decomposition. In *2012 Asia-Pacific Power and Energy Engineering Conference*, (pp. 1–5).

Mak, W., Morton, D., & Wood, R. (1999). Monte carlo bounding techniques for determining solution quality in stochastic programs. *Operations Research Letters*, *24*(1–2), 47–56.

Martin, A., Möller, M., & Moritz, S. (2006). Mixed integer models for the stationary case of gas network optimization. *Mathematical Programming*, *105*(2-3), 563.

Marwali, M. & Shahidehpour, S. (2000). Short-term transmission line maintenance scheduling in a deregulated system. *IEEE Transactions on Power Systems*, *15*(3), 1117–1124.

McCormick, G. P. (1976). Computability of global solutions to factorable nonconvex programs: Part i —convex underestimating problems. *Mathematical Programming*, *10*(1), 147–175.

Nemirovski, A. (2012). On safe tractable approximations of chance constraints. *European Journal of Operational Research*, *219*(3), 707–718. Feature Clusters.

Ojha, A., Kekatos, V., & Baldick, R. (2017). Solving the natural gas flow problem using semidefinite program relaxation. In *2017 IEEE Power Energy Society General Meeting*, (pp. 1–5).

O'Neill, R. P., Hedman, K. W., Krall, E. A., Papavasiliou, A., & Oren, S. S. (2010). Economic analysis of the N-1 reliable unit commitment and transmission switching problem using duality concepts. *Energy Systems*, *1*(2), 165–195.

Ordoudis, C., Pinson, P., & Morales, J. M. (2019). An integrated market for electricity and natural gas systems with stochastic power producers. *European Journal of Operational Research*, *272*(2), 642–654.

Osiadacz, A. (1987). *Simulation and Analysis of Gas Networks*. Houston, TX: Gulf Publishing Company.

Ozturk, U., Mazumdar, M., & Norman, B. (2004). A solution to the stochastic unit commitment problem using chance constrained programming. *IEEE Transactions on Power Systems*, *19*(3), 1589–1598.

Pandzic, H., Conejo, A. J., Kuzle, I., & Caro, E. (2012). Yearly maintenance scheduling of transmission lines within a market environment. *IEEE Transactions on Power Systems*, *27*(1), 407–415.

Papavasiliou, A. & Oren, S. S. (2013). Multiarea stochastic unit commitment for high wind penetration in a transmission constrained network. *Operations Research*, *61*(3), 578–592.

Papavasiliou, A., Oren, S. S., & Rountree, B. (2015). Applying high performance computing to transmission-constrained stochastic unit commitment for renewable energy integration. *IEEE Transactions on Power Systems*, *30*(3), 1109–1120.

Pfetsch, M. E., Fügenschuh, A., Geißler, B., Geißler, N., Gollmer, R., Hiller, B., Humpola, J., Koch, T., Lehmann, T., Martin, A., Morsi, A., Rövekamp, J., Schewe, L., Schmidt, M., Schultz, R., Schwarz, R., Schweiger, J., Stangl, C., Steinbach, M. C., Vigerske, S., & Willert, B. M. (2015). Validation of

nominations in gas network optimization: models, methods, and solutions. *Optimization Methods and Software*, *30*(1), 15–53.

PyPI (2020). Poisson Binomial Package. www.pypi.org/project/poisson-binomial/.

Ríos-Mercado, R. Z. & Borraz-Sánchez, C. (2015). Optimization problems in natural gas transportation systems: A state-of-the-art review. *Applied Energy*, *147*, 536–555.

Roald, L., Misra, S., Krause, T., & Andersson, G. (2017). Corrective control to handle forecast uncertainty: A chance constrained optimal power flow. *IEEE Transactions on Power Systems*, *32*(2), 1626–1637.

Schewe, L., Schmidt, M., & Thürauf, J. (2020). Computing technical capacities in the European entry-exit gas market is NP-hard. *Annals of Operations Research*, *295*(1), 337–362.

Schmidt, M. (2013). *A Generic Interior-Point Framework for Nonsmooth and Complementarity Constrained Nonlinear Optimization*. PhD thesis, Gottfried Wilhelm Leibniz Universität Hannover.

Schmidt, M. (2015). An interior-point method for nonlinear optimization problems with locatable and separable nonsmoothness. *EURO Journal on Computational Optimization*, *3*(4), 309–348.

Schmidt, M., Aßmann, D., Burlacu, R., Humpola, J., Joormann, I., Kanelakis, N., Koch, T., Oucherif, D., Pfetsch, M., Schewe, L., Schwarz, R., & Sirvent, M. (2017). GasLib—A Library of Gas Network Instances. *Data*, *2*(4), 40.

Schwele, A., Ordoudis, C., Kazempour, J., & Pinson, P. (2019). Coordination of power and natural gas systems: Convexification approaches for linepack modeling. In *2019 IEEE Milan PowerTech*, (pp. 1–6).

Shahidehpour, M., Yamin, H., & Li, Z. (2002). *Market operations in Electric Power Systems: Forecasting, scheduling, and Risk Management*. Institute of Electrical and Electronics Engineers, Wiley-Interscience.

Steinbach, M. C. (2007). On PDE solution in transient optimization of gas networks. *Journal of Computational and Applied Mathematics*, *203*(2), 345–361. Special Issue: The first Indo-German Conference on PDE, Scientific Computing and Optimization in Applications.

Stott, B., Alsac, O., & Monticelli, A. (1987). Security analysis and optimization. *Proceedings of the IEEE*, *75*(12), 1623–1644.

Tabkhi, F., Pibouleau, L., Hernandez-Rodriguez, G., Azzaro-Pantel, C., & Domenech, S. (2010). Improving the performance of natural gas pipeline networks fuel consumption minimization problems. *AIChE Journal*, *56*(4), 946–964.

Tawarmalani, M. & Sahinidis, N. V. (2005). A polyhedral branch-and-cut approach to global optimization. *Mathematical Programming*, *103*(2), 225–249.

Van Slyke, R. M. & Wets, R. (1969). L-shaped linear programs with applications to optimal control and stochastic programming. *SIAM Journal on Applied Mathematics*, *17*(4), 638–663.

Wächter, A. & Biegler, L. T. (2006). On the implementation of an interior-point filter line-search algorithm for large-scale nonlinear programming. *Mathematical Programming*, *106*(1), 25–57.

Wang, B., Yuan, M., Zhang, H., Zhao, W., & Liang, Y. (2018). An MILP model for optimal design of multi-period natural gas transmission network. *Chemical Engineering Research and Design*, *129*, 122–131.

Wang, Y., Li, Z., Shahidehpour, M., Wu, L., Guo, C. X., & Zhu, B. (2016). Stochastic co-optimization of midterm and short-term maintenance outage scheduling considering covariates in power systems. *IEEE Transactions on Power Systems*, *31*(6), 4795–4805.

Wang, Y., Zhong, H., Xia, Q., Kirschen, D. S., & Kang, C. (2016). An Approach for Integrated Generation and Transmission Maintenance Scheduling Considering N-1 Contingencies. *IEEE Transactions on Power Systems*, *31*(3), 2225–2233.

Wong, P. & Larson, R. (1968). Optimization of natural-gas pipeline systems via dynamic programming. *IEEE Transactions on Automatic Control*, *13*(5), 475–481.

Wu, F., Nagarajan, H., Zlotnik, A., Sioshansi, R., & Rudkevich, A. M. (2017). Adaptive convex relaxations for gas pipeline network optimization. In *2017 American Control Conference (ACC)*, (pp. 4710–4716).

Wu, H., Shahidehpour, M., Li, Z., & Tian, W. (2014). Chance-constrained day-ahead scheduling in stochastic power system operation. *IEEE Transactions on Power Systems*, *29*(4), 1583–1591.

Wu, H.-H. & Küçükyavuz, S. (2019). Probabilistic partial set covering with an oracle for chance constraints. *SIAM Journal on Optimization*, *29*(1), 690–718.

Wu, L., Shahidehpour, M., & Fu, Y. (2010). Security-constrained generation and transmission outage scheduling with uncertainties. *IEEE Transactions on Power Systems*, *25*(3), 1674–1685.

Wu, L., Shahidehpour, M., & Li, T. (2008). Genco's risk-based maintenance outage scheduling. *IEEE Transactions on Power Systems*, *23*(1), 127–136.

Wu, S., Ríos-Mercado, R., Boyd, E., & Scott, L. (2000). Model relaxations for the fuel cost minimization of steady-state gas pipeline networks. *Mathematical and Computer Modelling*, *31*(2), 197–220.

Wu, Y., Lai, K. K., & Liu, Y. (2007). Deterministic global optimization approach to steady-state distribution gas pipeline networks. *Optimization and Engineering*, *8*(3), 259–275.

Xiong, P. & Jirutitijaroen, P. (2013). A stochastic optimization formulation of unit commitment with reliability constraints. *IEEE Transactions on Smart Grid*, *4*(4), 2200–2208.

Yildirim, M., Sun, X. A., & Gebraeel, N. Z. (2016a). Sensor-driven condition-based generator maintenance scheduling—part i: Maintenance problem. *IEEE Transactions on Power Systems*, *31*(6), 4253–4262.

Yildirim, M., Sun, X. A., & Gebraeel, N. Z. (2016b). Sensor-driven condition-based generator maintenance scheduling—part ii: Incorporating operations. *IEEE Transactions on Power Systems*, *31*(6), 4263–4271.

Yucekaya, A. (2013). The operational economics of compressed air energy storage systems under uncertainty. *Renewable and Sustainable Energy Reviews*, *22*, 298–305.

Zhang, J. & Zhu, D. (1996). A bilevel programming method for pipe network optimization. *SIAM Journal on Optimization*, *6*(3), 838–857.

Zheng, Q., Rebennack, S., Iliadis, N., & Pardalos, P. (2010). Optimization models in the natural gas industry. In P. Pardalos, S. Rebennack, M. Pereira, & N. Iliadis (Eds.), *Handbook of Power Systems I. Energy Systems*. Springer, Berlin, Heidelberg.

Zimmerman, R. D., Murillo-Sánchez, C. E., & Thomas, R. J. (2011). Matpower:

Steady-state operations, planning, and analysis tools for power systems research and education. *IEEE Transactions on Power Systems*, *26*(1), 12–19.

APPENDIX A

The Monotonicity of Poisson Binomial Distribution.

We state Lemma A.1 which is used in the proof of Proposition 2.4.

Lemma A.1 *The cumulative distribution function of Poisson Binomial distribution is non-increasing with respect to success probability p_i for all $i = 1, \ldots, n$.*

Proof A.1 *Let Y be a Poisson Binomial random variable with success probabilities $p_1, \ldots, p_n$. It suffices to show that the partial derivative of the cumulative distribution function of Poisson Binomial distribution with respect to p_i is nonpositive for all $i = 1, \ldots, n$. Without loss of generality, we concentrate on the nth Bernoulli random variable. The cumulative distribution function of Poisson Binomial distribution is given by:*

$$F(y, p_1, \ldots, p_n) = \mathbb{P}(Y \leq y) = \sum_{l=0}^{y} f(l, p_1, \ldots, p_n) = \sum_{l=0}^{y} \sum_{A \in \mathcal{B}_l(1,\ldots,n)} \prod_{i \in A} p_i \prod_{j \in A^c} (1 - p_j),$$

where $f(l, p_1, \ldots, p_n)$ denotes its probability mass function, i.e., the probability of l successes in n Bernoulli trials, and $\mathcal{B}_l(1, \ldots, n)$ denotes the set of all subsets of size l from $\{1, \ldots, n\}$. We can rewrite the probability mass function of Poisson Binomial distribution as follows:

$$\begin{aligned} f(y, p_1, \ldots, p_n) = & \sum_{A \in \mathcal{B}_y(1,\ldots,n): n \in A} \prod_{i \in A} p_i \prod_{j \in A^c} (1 - p_j) + \sum_{A \in \mathcal{B}_y(1,\ldots,n): n \notin A} \prod_{i \in A} p_i \prod_{j \in A^c} (1 - p_j) \\ = & \, p_n \sum_{A \in \mathcal{B}_y(1,\ldots,n): n \in A} \prod_{i \in A: i \neq n} p_i \prod_{j \in A^c} (1 - p_j) \\ & + (1 - p_n) \sum_{A \in \mathcal{B}_y(1,\ldots,n): n \notin A} \prod_{i \in A} p_i \prod_{j \in A^c: j \neq n} (1 - p_j). \end{aligned}$$

Let us now obtain the partial derivative of $f(y, p_1, \ldots, p_n)$ with respect to p_n. In fact, we have:

$$\begin{aligned} \frac{\partial f(y, p_1, \ldots, p_n)}{\partial p_n} = & \sum_{A \in \mathcal{B}_y(1,\ldots,n): n \in A} \prod_{i \in A: i \neq n} p_i \prod_{j \in A^c} (1 - p_j) \\ & - \sum_{A \in \mathcal{B}_y(1,\ldots,n): n \notin A} \prod_{i \in A} p_i \prod_{j \in A^c: j \neq n} (1 - p_j) \end{aligned}$$

$$= \sum_{A \in \mathcal{B}_{y-1}(1,\ldots,n-1)} \prod_{i \in A} p_i \prod_{j \in A^c} (1-p_j)$$
$$- \sum_{A \in \mathcal{B}_{y}(1,\ldots,n-1)} \prod_{i \in A} p_i \prod_{j \in A^c} (1-p_j).$$

Consider the quantity $H^{y-1} := \sum_{A \in \mathcal{B}_{y-1}(1,\ldots,n-1)} \prod_{i \in A} p_i \prod_{j \in A^c} (1-p_j)$. *The first term in the last equality follows from the fact that the index* n *indeed belongs to set* $\mathcal{B}_y(1,\ldots,n)$, *but is not used in any of the multiplication operations. This is equivalent to the selection of* $y-1$ *many elements from* $\{1,\ldots,n-1\}$. *Similarly, consider the quantity* $H^y := \sum_{A \in \mathcal{B}_{y}(1,\ldots,n-1)} \prod_{i \in A} p_i \prod_{j \in A^c} (1-p_j)$. *The second term in the last equality is due to the fact that the index* n *does not belong to set* $\mathcal{B}_y(1,\ldots,n)$, *and is not used in any of the multiplication operations. This is equivalent to the selection of* y *many elements from* $\{1,\ldots,n-1\}$. *Thus, the partial derivative of* $f(y,p_1,\ldots,p_n)$ *with respect to* p_n *is given by:*

$$\frac{\partial f(y,p_1,\ldots,p_n)}{\partial p_n} = \begin{cases} -H^0 & \text{if } y = 0, \\ H^{y-1} - H^y & \text{if } 1 \le y \le n-1, \\ H^{n-1} & \text{if } y = n. \end{cases}$$

Then, it is easy to obtain the partial derivative of $F(y,p_1,\ldots,p_n)$ *with respect to* p_n *as follows:*

$$\frac{\partial F(y,p_1,\ldots,p_n)}{\partial p_n} = \begin{cases} -H^0 & \text{if } y = 0, \\ -H^y & \text{if } 1 \le y \le n-1, \\ 0 & \text{if } y = n. \end{cases}$$

Since $p_n \in [0,1]$, *we clearly have* $\frac{\partial F(y,p_1,\ldots,p_n)}{\partial p_n} \le 0$ *for* $y = 0,\ldots,n$. *This proves the property of monotonicity of Poisson Binomial distribution with respect to* p_n.

Proof of Proposition 2.4

Consider any pair of maintenance decisions $v' = (w', z'), v'' = (w'', z'')$ with the following property:

$$(h,t') \le (h,t'') \text{ for } (h,t') \in \mathcal{I}(v'),\ (h,t'') \in \mathcal{I}(v'') \text{ and } h \in \mathcal{H}'.$$

Let us first consider the set of generators prone to failure. As before, we let $\hat{\zeta}_{\mathcal{G}}(w')$ and $\hat{\zeta}_{\mathcal{G}}(w'')$ be the Poisson Binomial random variables with success probabilities $\{p'_i = \mathbb{P}(\xi_i \le m_i(w'));\ i \in \mathcal{G}\}$ and $\{p''_i = \mathbb{P}(\xi_i \le m_i(w''));\ i \in \mathcal{G}\}$, respectively. Clearly,

the maintenance schedule under decision w'' is in a later period than the maintenance schedule under decision w', which implies that $m_i(w') \leq m_i(w'')$ for $i \in \mathcal{G}'$. Then, we have $p'_i \leq p''_i$. Secondly, we consider the set of transmission lines prone to failure. We let $\hat{\zeta}_{\mathcal{L}}(z')$ and $\hat{\zeta}_{\mathcal{L}}(z'')$ be the Poisson Binomial random variables with success probabilities $\{p'_{ij} = \mathbb{P}(\xi_{ij} \leq m_{ij}(z'));\ (i,j) \in \mathcal{L}\}$ and $\{p''_{ij} = \mathbb{P}(\xi_i \leq m_i(z''));\ i \in \mathcal{L}\}$, respectively. Similarly, we have $p'_{ij} \leq p''_{ij}$ for $(i,j) \in \mathcal{L}'$.

By Lemma A.1, we have $\mathbb{P}(\hat{\zeta}_{\mathcal{G}}(w') \leq \rho_{\mathcal{G}}) \geq \mathbb{P}(\hat{\zeta}_{\mathcal{G}}(w'') \leq \rho_{\mathcal{G}})$ and $\mathbb{P}(\hat{\zeta}_{\mathcal{L}}(z') \leq \rho_{\mathcal{L}}) \geq \mathbb{P}(\hat{\zeta}_{\mathcal{L}}(z'') \leq \rho_{\mathcal{L}})$. By using the independence of these random variables, we immediately have that $\mathcal{P}(v') \geq \mathcal{P}(v'')$.

APPENDIX B

Physical Quantities.

We present the physical parameters and constants used in this thesis.

We first note that each pipe $(i,j) \in \mathcal{P}'$ is characterized by its length L_{ij}, its diameter D_{ij} and its roughness k_{ij}. The length and diameter parameters are measured in meters, whereas roughness is a unitless parameter. Then, the resistance coefficient w_{ij} of pipe (i,j) can be computed as

$$w_{ij} = \frac{16\lambda_{ij} L_{ij} p_0 \rho_0 z_m T_m}{\pi^2 D_{ij}^5 z_0 T_0}.$$

Here, z_0 and z_m are the norm and mean compressibility factors; T_0 and T_m are the norm and mean gas temperature; ρ_0 is the norm density and p_0 is the norm gas pressure. The friction coefficient λ_{ij} is given by the Nikuradse's formula:

$$\lambda_{ij} = \left(2\log_{10}\left(\frac{D_{ij}}{k_{ij}}\right) + 1.138\right)^{-2}.$$

The compressibility factors can be approximately computed by the Papay's equation:

$$z_k := z_k(p_k, T_k) = 1 - 3.52(p_k/p_c)e^{-2.26T_k/T_c} + 0.274(p_k/p_c)^2 e^{-1.878T_k/T_c},$$

where p_c and T_c are the pseudocritical pressure and pseudocritical temperature, respectively. Thus, the norm compressibility factor is given by $z_0(p_0, T_0)$ whereas the mean compressibility factor is given by $z_m(p_m, T_m)$ with $p_m = (\max\{\underline{p}_i, \underline{p}_j\} + \min\{\overline{p}_i, \overline{p}_j\})/2$. Each resistor $(i,j) \in \mathcal{P}''$ is associated with a unitless drag factor $\zeta_{ij} > 0$. The resistance coefficient of resistor (i,j) is then computed as

$$w_{ij} = \frac{16\zeta_{ij} p_0 \rho_0 z_m T_m}{\pi^2 D_{ij}^4 z_0 T_0}.$$

For each compressor $(i,j) \in \mathcal{C}$, the consumption parameter κ'_{ij} is computed as

$$\kappa'_{ij} = \frac{1}{3.6\ 10^5 \kappa} \frac{\rho_0 R T_m z_m}{m \eta_{ad} \eta_{drive} H_c}.$$

Here, R is the universal gas constant; m is the molar mass of the gas; H_c is the lower calorific value; $\eta_{adiabatic}$ and η_{drive} are the adiabatic and driver efficiency, respectively. Also, the physical constant κ is calculated by $(\chi-1)/\chi$ where χ is the estimate for the isentropic exponent parameter.

In Table B.1, we present the constants used in the parameter calculations along with their units. The values for constants $\eta_{adiabatic}$ and η_{driver} are chosen as in Tabkhi, Pibouleau, Hernandez-Rodriguez, Azzaro-Pantel & Domenech (2010).

Notation	Definition	Value	Unit
T_0	norm gas temperature	283.15	K
T_m	mean gas temperature	273.15	K
ρ_0	norm gas density	0.785	kg/m^3
p_o	norm pressure	101325	Pa
p_c	pseudocritical pressure	459293	Pa
T_c	pseudocritical temperature	188.55	K
R	universal gas constant	8.3145	J/mol/K
m	molar mass of gas	0.01857	kg/mol
H_c	lower calorific value of gas	9.8	kwh/m^3
χ	isentropic exponent	1.296	1
$\eta_{adiabatic}$	adiabatic efficiency	0.90	1
η_{drive}	driver efficiency	0.35	1

Table B.1 Physical constants.

In our optimization model, we use constant cost coefficients. In particular, we choose $C_{ij}^{fc} = 0.1372$\$/kwh (EIA, 2020), $C_{ij}^{on} = 5618$\$ (Yucekaya, 2013) for each compressor $(i,j) \in \mathcal{C}$. For each store $j \in \mathcal{S}(i)$, $C_j^{wd} = 0.1311$\$/m^3. We also choose $\eta_j' = \eta_j'' = 0.90$ for each store j. The minimum-up and minimum-down time restrictions are as follows: $MU_{ij} = MD_{ij} = 2$ for each $(i,j) \in \mathcal{C} \cup \mathcal{V}$; $MU_{ij} = MD_{ij} = 1$ for each $(i,j) \in \mathcal{R}$ (see, e.g., Burlacu et al. (2019)). Also, we let $\underline{\delta}_{ij} = 5, \bar{\delta}_{ij} = 15$ and chose $\underline{r}_{ij} = 1.0895$ and $\bar{r}_{ij} = 1.6009$ as in Burlacu et al. (2019) for each $(i,j) \in \mathcal{C}$; $\underline{r}_{ij} = 1/1.0895$ and $\bar{r}_{ij} = 1/1.6009$ for each control valve $(i,j) \in \mathcal{V}$. In Table B.2, we finally present the units of the original variables in our optimization model by dropping their subscripts:

Notation	Definition	Unit
f	gas flow	m^3/s
l	fuel gas consumption	m^3/s
p	gas pressure	Pa
s	gas storage level	m^3
s'	gas injected	m^3/s
s''	gas withdrawn	m^3/s

Table B.2 Variables.